1-1-2013

Photochemical Electrocyclic Ring Closure and Leaving Group Expulsion from N-(9-oxothioxanthenyl)Benzothiophene Carboxamides

Majher I. Sarker
majher.sarker@marquette.edu

Tasnuva Shahrin
Marquette University, tasnuva.shahrin@marquette.edu

Mark G. Steinmetz
Marquette University, mark.steinmetz@marquette.edu

Qadir K. Timerghazin
Marquette University, qadir.timerghazin@marquette.edu

Accepted version. *Photochemical & Photobiological Sciences*, No. 2 (2013): 309-322. DOI.

RSC Publishing Photochemical & Photobiological Sciences

Photochemical electrocyclic ring closure and leaving group expulsion from N-(9-oxothioxanthenyl)benzothiophene carboxamides.

Journal:	*Photochemical & Photobiological Sciences*
Manuscript ID:	PP-ART-03-2012-025051.R2
Article Type:	Paper
Date Submitted by the Author:	n/a

Complete List of Authors:	Sarker, Majher; Marquette University, Chemistry Shahrin, Tasnuva; Marquette University, Chemistry Steinmetz, Mark; Marquette University, Chemistry Timerghazin, Qadir; Marquette University, Chemistry

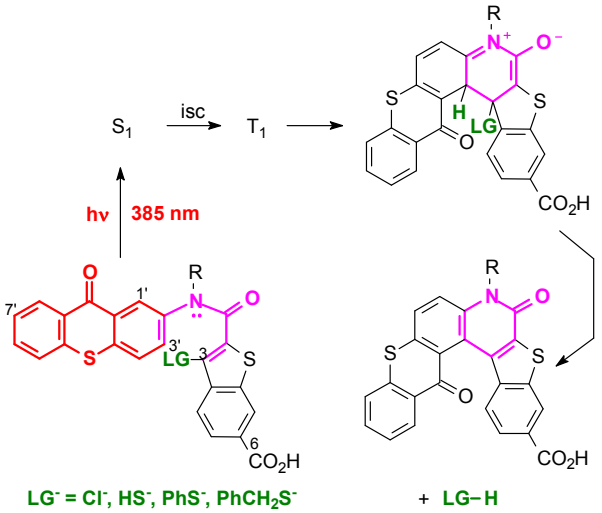

Water-soluble benzothiophene carboxamides with thioxanthone attached to the amide nitrogen undergo 385 nm photolytic elimination of Cl^-, PhS^-, HS^-, or $PhCH_2S^-$ from the C-3 position of the benzothiophene ring system.

Cite this: DOI: 10.1039/c0xx00000x

www.rsc.org/xxxxxx

ARTICLE TYPE

Photochemical electrocyclic ring closure and leaving group expulsion from N-(9-oxothioxanthenyl)benzothiophene carboxamides.

Majher I. Sarker, Tasnuva Shahrin, Mark G. Steinmetz*[a], and Qadir K. Timerghazin*[b]

Received (in XXX, XXX) Xth XXXXXXXXX 20XX, Accepted Xth XXXXXXXXX 20XX

DOI: 10.1039/b000000x

N-(9-oxothioxanthenyl)benzothiophene carboxamides bearing leaving groups (LG^- = Cl^-, PhS^-, HS^-, $PhCH_2S^-$) at the C-3 position of the benzothiophene ring system photochemically cyclize with nearly quantitative release of the leaving group, LG^-. The LG^- photoexpulsions can be conducted with 390 nm light or with a sunlamp. Solubility in 75% aqueous CH_3CN is achieved by introducing a carboxylate group at the C-6 position of the benzothiophene ring. The carboxylate and methyl ester derivatives regiospecifically cyclize at the more hindered C-1 position of the thioxanthone ring. Otherwise, the photocyclization favors the C-3 position of the thioxanthone. Quantum yields for reaction are 0.01-0.04, depending on LG^- basicity. Electronic structure calculations for the triplet excited state show that excitation transfer occurs from the thioxanthone to the benzothiophene ring. Subsequent cyclization in the triplet excited state is energetically favourable and initially generates the triplet excited state of the zwitterionic species. Expulsion of LG^- is thought to occur once this species converts to the closed shell ground state.

Introduction

Photochemically removable protecting groups that release biologically active molecules upon exposure to light (cage compounds) have been widely used in biological applications and physiological studies.[1,2] However, the cage compounds typically used have certain drawbacks, which may not always be obvious. In particular, UV light is most often used to effect the photochemical release of the biologically active molecule, but may cause cellular damage and mortality.[3] Cage compounds may undergo premature hydrolytic or even enzymatic release of the bioeffector in living cells.[1] Finally, the types of bioeffector leaving groups that can be photochemically released from the photoremovable protecting group are all too often limited to rather weak bases such as carboxylate groups and phosphate esters.

Our research attempts to address the above problems by expelling the bioeffector leaving groups via intermediates that have zwitterionic character. Intermediates **2** are generated upon photochemical electrocyclic ring closure reaction of derivatives of benzothiophene carboxanilides **1** (Scheme 1). Ring A subunit would represent a chromophore that absorbs light at long wavelengths that extend into the visible region.

The use of Scheme 1 approach to photochemically expel leaving groups from the C-3 position of the benzothiophene ring system approach was initially tested, experimentally, at short wavelengths in the UV with carboxanilides **5** (eq 1).[4] Carboxanilides **5** were found to release various leaving groups LG^- that vary in basicity in essentially quantitative yields. Quantum yields decreased with increasing basicity of the LG^- released over the range Φ = 0.23 – 0.07 (LG^- = Cl^-, $PhCH_2CO_2^-$, PhS^-, $PhCH_2S^-$, PhO^-). Although the photolysis wavelength was at 310 nm in the initial studies of **5**, the wavelength could be extended to 365 nm by incorporating a *p*-benzoyl group into the benzene ring of anilide **5**.

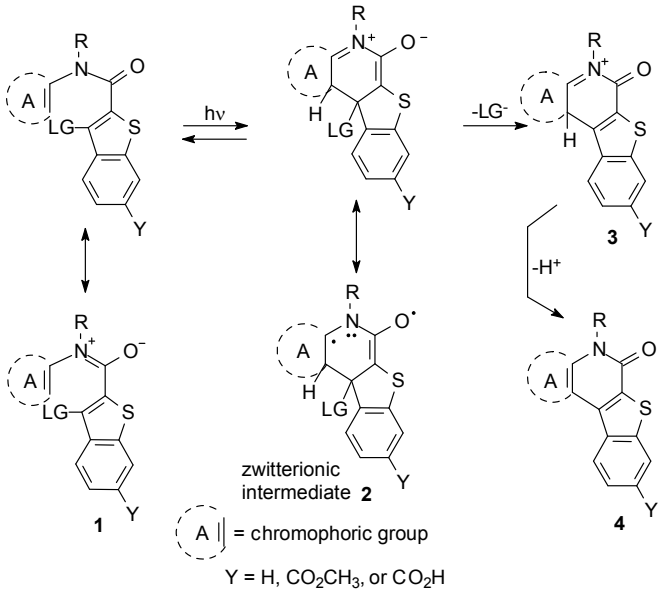

Scheme 1

Because of the potentially modular chromophore (ring A) and the ability of the putative zwitterionic intermediate to release relatively basic leaving groups such as thiolates[5,7] and

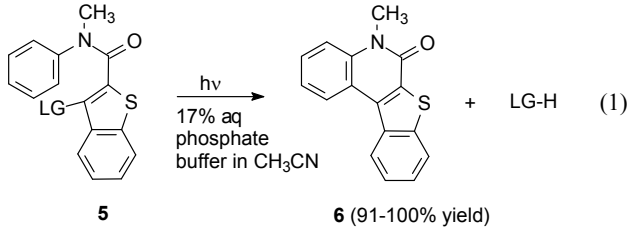

$LG^- = Cl^-, PhCH_2CO_2^-, PhS^-, PhCH_2S^-, PhO^-, HO^-$

phenolates[8], i.e., side-chain groups of cysteine and tyrosine residues in peptides and proteins, the photochemical electrocyclic ring closure approach to the generation of zwitterionic intermediates appeared to be promising. In this paper we extend the absorption maximum of the chromophoric group to 385 nm by use of the thioxanthone chromophore as ring A, as shown for benzothiophene carboxamides **7**-**10**. In addition, solubilities in aqueous buffered media are greatly improved by attaching a C-6 carboxylate group (Y = CO_2H) in to the benzothiophene ring system.

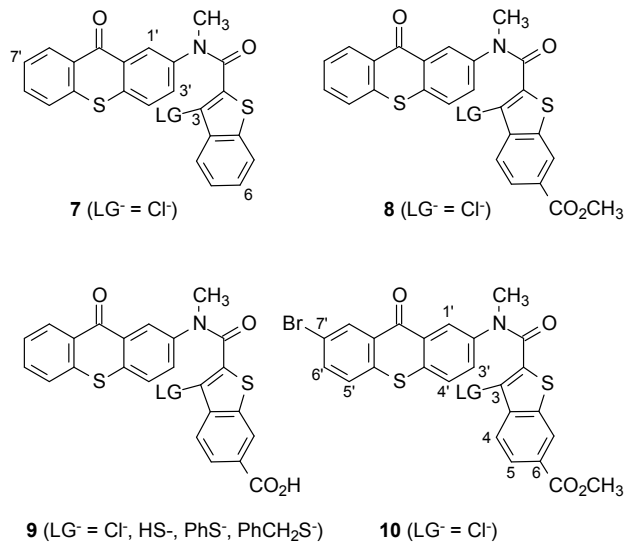

Fig. 1 Compounds photolyzed.

The leaving groups LG^- have been limited to chloride and various thiolates, including the recently discovered gasotransmitter H_2S[9] ($LG^- = HS^-$ at pH 7). These LG^- have been chosen to ascertain how quantum yields respond to change in leaving group basicities. Secondly, our focus on the release of thiols anticipates an ultimate goal of developing a photoremovable protecting group for cysteine residues in peptides such as glutathione. Leaving groups such as phenolate or carboxylate are outside the scope of this paper. Moreover, the benzothiophene C-6 carboxylate group greatly complicates their synthesis.

Results

Syntheses

The benzothiophene carboxamides **7**-**10** ($LG^- = Cl^-$) are synthesized by reacting 2-methylaminothioxanthones **13**[10] and **14** with acid chlorides **11**[11] or **12** (eq. 2). The 3-chloro group of **8** ($LG^- = Cl^-$) is then readily substituted by reaction with thiols[4] to

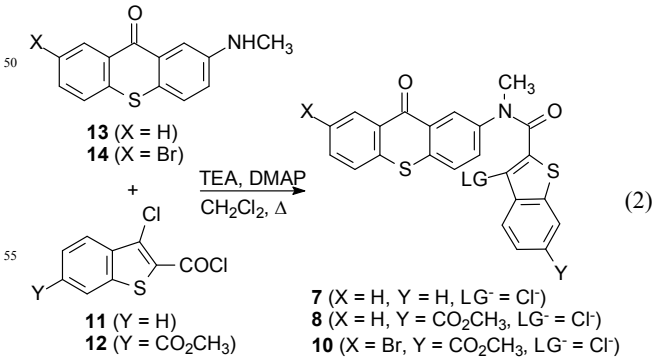

obtain **9** ($LG^- = HS^-, PhS^-, PhCH_2S^-$) (Scheme 2). The reaction to give acid **9** ($LG^- = PhS^-$) is accompanied by demethylation of the methyl ester, whereas to obtain the acid **9** ($LG^- = PhCH_2S^-, HS^-$),

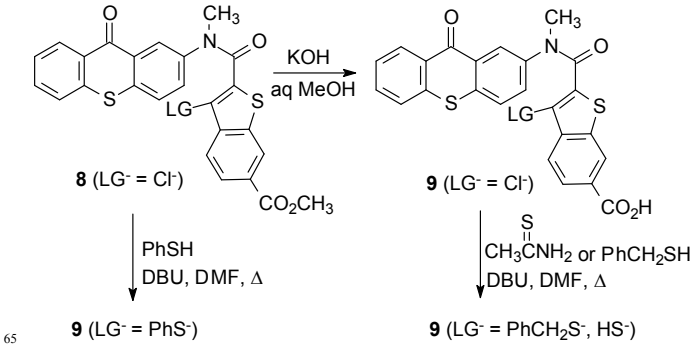

Scheme 2

The leaving group LG^- was limited to chloride and thiolates, including the recently discovered gasotransmitter H_2S[9] ($LG^- = HS^-$ at pH 7). These LG^- have been chosen to ascertain how quantum yields respond to change in leaving group basicities. Secondly, our focus on the release of thiols anticipates an ultimate goal of developing a photoremovable protecting group for cysteine residues in peptides such as glutathione. Leaving groups such as phenolate or carboxylate are outside the scope of this paper. Moreover, the benzothiophene C-6 carboxylate group greatly complicates their ester hydrolysis was performed prior to introducing the thiolate leaving group.

The benzothiophene carbonyl chloride **12** was synthesized from the corresponding cinnamic acid derivative **17** (Scheme 3), whereas the synthesis of benzothiophene **11** (eq. 2) was reported previously.[11] In the case of benzothiophene **12** the precursor, cinnamic acid **17**, was obtained by Knoevenagel condensation of 4-formyl methyl benzoate **16**.[12] Somewhat unusual reaction conditions were necessary for the esterification step affording **16**.

The syntheses of 2-methylaminothioxanthones **13** and **14** (eq 2 and Scheme 4) started with the corresponding known 2-nitro compounds **18**[10]and **19**[13], which were prepared by literature

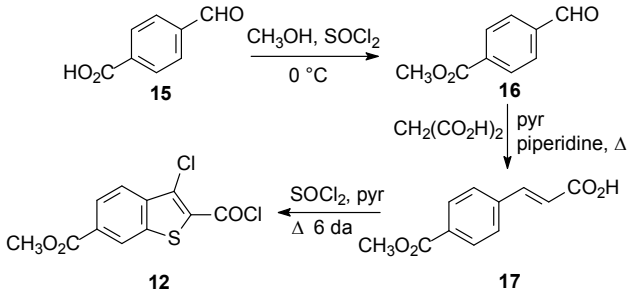

Scheme 3

methods. The 2-nitro substituent was reduced to the amines **20** and **21** by iron,[10] followed by acylation. The resultant carboxamides **22** and **23** were then alkylated to introduce the *N*-methyl substituents **24**, **25**. Subsequent base hydrolysis of the acetamides furnished the thioxanthone 2-methylamines **13** and **14**.

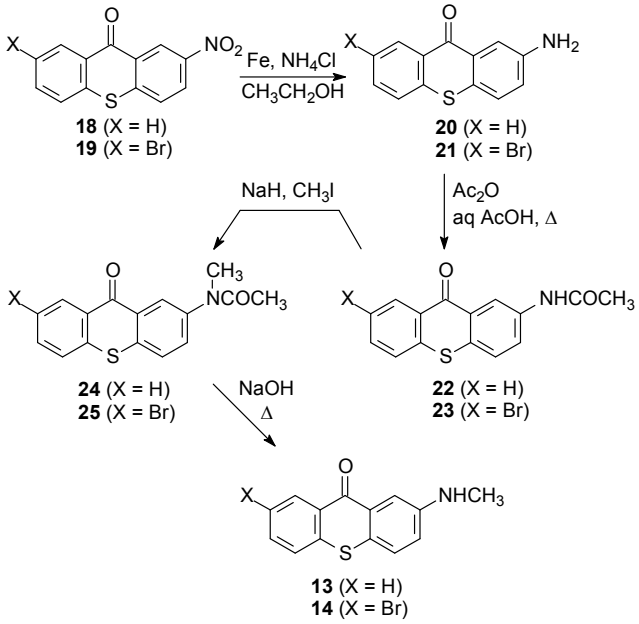

Scheme 4

Photochemistry

Ester **8** (LG^- = Cl^-) and acid **9** (LG^- = Cl^-) both exhibit absorption maxima at 385 nm in aqueous dioxane or acetonitrile (Figure 2). For the ester $\varepsilon = 5600\ M^{-1}\ cm^{-1}$, while the acid has $\varepsilon = 4200\ M^{-1}\ cm^{-1}$. For preparative photolyses Pyrex-filtered light from a Hanovia medium pressure mercury lamp was used. A sunlamp was also effective at photolysing all of the compounds in the study. Quantum yields were determined at 390 nm using a monochromator for wavelength selection utilizing a high pressure mercury lamp as the light source.

Preparative photolysis of 10^{-2} M ester **8** (LG^- = Cl^-) in N_2 saturated 19% H_2O containing 100 mM phosphate buffer (pH 7) in CH_3CN resulted in nearly quantitative expulsion of the chloride leaving group and formation of the single regioisomeric photoproduct **26**, as quantified by NMR integration against DMF as an internal standard (Scheme 5). Photoproduct **26** was identified by ^1H NMR spectroscopy and elemental analysis. The regiospecificity was further established, unambiguously, by 600 MHz ^1H NMR COSY, which clearly showed five vicinal

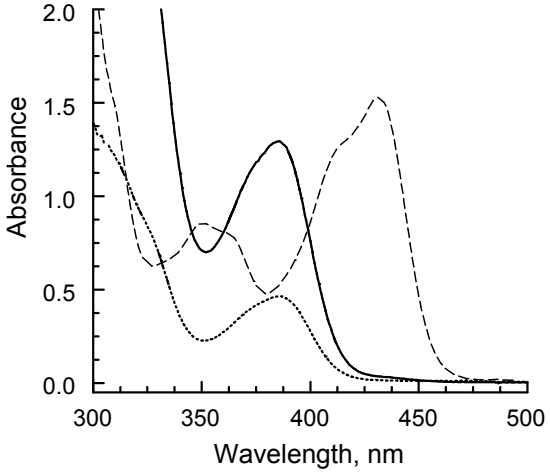

Fig. 2 Absorption spectra of 2.3 x 10^{-4} M ester **8** (LG^- = Cl^-) (——) in 17% aq phosphate buffer in dioxane, 1.1 x 10^{-4} M acid **9** (LG^- = Cl^-) (····) in 75% aq phosphate buffer in CH_3CN, and 1.5 x 10^{-4} M photoproduct ester **26** produced from ester **8** (LG^- = Cl^-) (– – – –).

couplings as cross peaks for protons in the three benzenoid rings. Regioisomer **28** would have shown only four vicinal couplings in the COSY spectrum. The solubility of **26** in all solvents was relatively low, which precluded obtaining a satisfactory ^{13}C NMR spectrum. The compound was obtainable only as a powder, despite repeated attempts to obtain crystals for structure determination using X-ray diffraction. The absorption spectrum

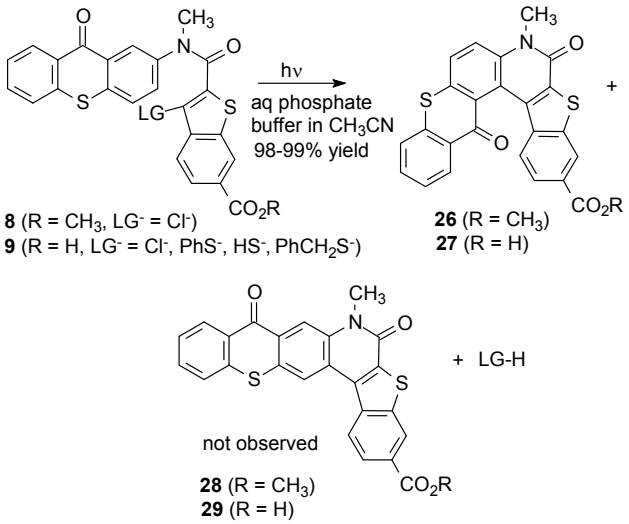

Scheme 5

of ester **26** showed a long wavelength maximum at 432 nm (ε 10300 M^{-1} cm^{-1}) in aq dioxane containing phosphate buffer (Figure 2).

Similarly, preparative photolysis of 10^{-2} M acid **9** (LG^- = Cl^-) in N_2 saturated 75% H_2O in CH_3CN containing 100 mM phosphate buffer (pH 7) gave the single regioisomeric photoproduct **27** in 98% yield by NMR integration, as above for **8** (LG^- = Cl^-). The regiospecificity was again established by 600 MHz ^{1}H NMR COSY. In addition, the ^{1}H NMR NOESY showed cross peaks establishing the close spatial proximity of a proton ortho to the thioxanthone carbonyl group and the C-4 and C-5 protons of the benzothiophene benzene ring. The acid photoproduct **27** did not have sufficient solubility in aqueous solvent to obtain the ^{13}C NMR spectrum, and since it was only obtainable as a powder, the X-ray structure also could not be determined. Photolysis of acid **9** (LG^- = PhS^-, HS^-, $PhCH_2S^-$) under the same conditions as **8** (LG^- = Cl^-) also gave photoproduct **27** in 98-100% yields upon expulsion of these thiolate leaving groups. For acid **9** (LG^- = $PhCH_2S^-$) the released benzyl thiol was quantified in photolyses of 4.5 x 10^{-3} M solutions of 35% D_2O in CD_3CN containing phosphate buffer (as above) contained in NMR tubes. Yields were 96% thiol and 99% of **27** at 100% conversion of reactant by ^{1}H NMR spectroscopy. Very similar results were found when DMSO-d_6 was the photolysis solvent.

The photolyses of ester **8** (LG^- = Cl^-) and acids **9** (LG^- = Cl^-, PhS^-, HS^-, $PhCH_2S^-$) were repeated with a 120 W sunlamp for 72 h under otherwise the same conditions described above for the Hanovia runs. In all cases the leaving groups were expelled essentially quantitatively to give exclusively product **26** or **27**.

The regiospecific formation of **26** or **27** in the preparative photolyses of ester **8** or acids **9** requires the presence of the ester and carboxylic acid substituents attached to the C-6 position of the benzothiophene ring system of the reactants. In contrast, photolyses of the unsubstituted benzothiophene ring system **7** (LG^- = Cl^-) in 16% water containing 100 mM phosphate buffer in CH_3CN gave both regioisomeric photoproducts **30** and **31** as a 42 : 58 mixture, respectively, in 100% yield according to 400 MHz ^{1}H NMR spectroscopy (Scheme 6). A pure sample of

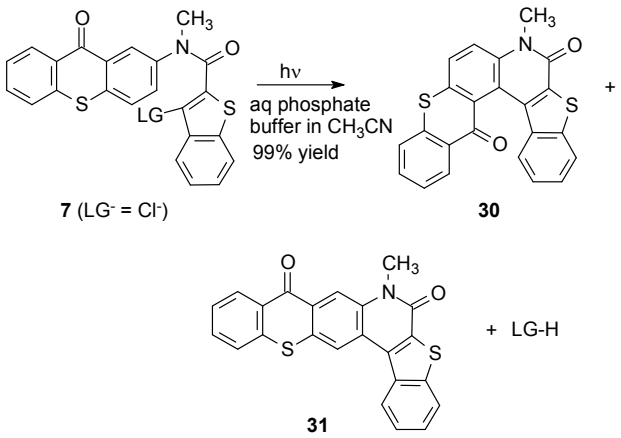

Scheme 6

regioisomer **31** crystallized from a DMSO solution of the mixture of **30** and **31**. A pure sample of **30** was precipitated upon addition of H_2O to the supernatant. The ^{1}H NMR spectrum of the pure sample of **31** was distinctly different from that of regioisomer **30**. The structure of **30** was assigned by comparing chemical shifts of protons of the *N*-methyl and the thioxanthone ring system to the corresponding protons of the pure regioisomeric acid **27** (see Supplementary Information) that was established by ^{1}H NMR COSY. Eventually, a crystalline sample of **30** was obtained from $CHCl_3$ as the solvent, and its structure was confirmed by X-ray crystallography.

The product quantum yield for 1.8 x 10^{-3} M ester **8** (LG^- = Cl^-) in N_2 saturated 19% H_2O in dioxane containing 100 mM buffer, photolyses was Φ = 0.039, according to NMR spectroscopy using DMF as standard. In addition, the reactant concentration was reduced to 1.0 x 10^{-4} M, and the quantum yield for photoproduct **26** was found to Φ = 0.037. In this latter case the photoproduct was quantified by absorption spectroscopy rather than by NMR spectroscopy. The similar Φ values found for the two reactant concentrations suggest that competitive absorption by photoproduct formed at the front face of the photolysis cell was not significant, possibly because the photolysis wavelength coincided with a minimum in photoproduct absorption (Figure 2).

Under similar conditions as with **8** (LG^- = Cl^-), the quantum yield for **7** (LG^- = Cl^-) was found to be Φ = 0.069 for the formation of **30** plus **31**, using NMR to quantify the products. The higher observed Φ than ester **8** may be because reactant **7** cyclizes at two sites ortho to the amide nitrogen (C-1 and C-3) of the thioxanthone ring, whereas cyclization of the ester **8** at C-3 is apparently inhibited.

With the more aqueous soluble carboxylic acid **9** the conditions were 2.0 x 10^{-3} M acid in 75% aq buffer in CH_3CN. In N_2 saturated aqueous buffer **27** was formed from acid **9** (LG^- = Cl^-) with Φ = 0.034. Quantum yields for the carboxylic acids decreased with increasing basicity of LG^- expelled. Thus, in N_2 saturated aqueous buffer and LG^- = PhS^-, Φ = 0.017, whereas for LG^- = $PhCH_2S^-$, Φ = 0.011. However, for LG^- = HS^-, Φ = 0.0079.

In air-saturated solution quantum yields for ester **8** (LG^- = Cl^-) decreased to Φ = 0.019. The significantly lower quantum yield in the presence of air would be consistent with quenching of a triplet excited state by dissolved O_2. Furthermore, quenching by 9.2-37 x 10^{-6} M piperylene as quencher Q gave a slope $k_q\tau$ = 7.03 x 10^4 M^{-1} for a Stern-Volmer plot Φ°/Φ vs. [Q] (see Supplementary Information). If it is assumed that k_q = ca. 10^{10} M^{-1} s^{-1}, then τ would be ca. 7 μs. This lifetime is comparable to 13.3 μs for the unsubstituted thioxanthone in polar protic solvent (methanol) or 6.7 μs in CH_3CN.[14]

To determine whether a "heavy atom effect" promoted intersystem crossing of the singlet excited state to the triplet excited state, work focused upon the C-7 bromide of thioxanthone ester **10** (LG^- = Cl^-). Preparative photolysis of ester **10** in N_2 saturated 19% H_2O in CH_3CN containing 100 mM phosphate buffer (pH 7), as above for ester **8** (LG^- = Cl^-), exclusively gave regioisomer **32** in 99% yield, and **33** was not observed by ^{1}H NMR spectroscopy of the photolysate (Scheme 7). Quantum yield determinations gave Φ = 0.053 for formation of **32**, which is 38% higher than Φ = 0.039 found for ester **8** (LG^-

= Cl^-).

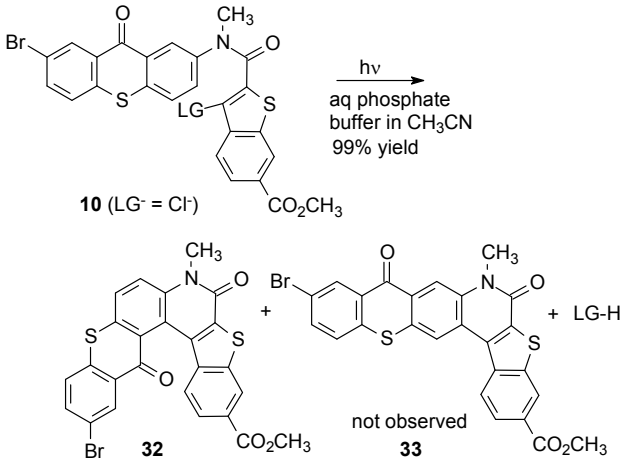

Scheme 7

Discussion

The photochemistry of **7-9** is similar to that reported previously for benzothiophene carboxanilides **5**.[4] The thioxanthones, however, have the advantage of being photoreactive at relatively long photolysis wavelengths, whereas **5** reacts upon irradiation deep in the UV (310 nm). Photolyses of **7-9** can be conducted at 390 nm or by use of a sunlamp. In both cases the direct photolyses result in expulsion of the various LG^- in nearly quantitative yields, regardless of basicity of the LG^-. As with **5**, the photochemical mechanism for **7-9** is thought to involve expulsion of a leaving group LG^- from a zwitterionic intermediate **2** (Scheme 1) that is formally produced via excited state $6e^-$ electrocyclic ring closure.

By comparison to **7-9**, most other commonly used photoremovable protecting groups have longest wavelength maxima at shorter wavelengths: *o*-nitrobenzyl λ_{max} 272 nm (ε 6,200),[15,16] nitroveratryl λ_{max} 330 nm (ε 5,000),[16] *p*-hydroxyphenacyl λ_{max} 282 nm (ε 14,000),[17] and desyl λ_{max} 323 nm (ε 400).[18] A long wavelength absorber is aminocoumarinylmethyl λ_{max} 402 nm (ε 18,600).[19] Likewise, certain brominated hydroxycoumarinylmethyl groups have wavelength maxima ranging from 325-397 nm (ε ca.1.2-2.0 x 10^4).[20] Hydroxyquinolinylmethyl protecting groups have maxima at wavelengths as long as 386 nm (ε 3,300).[21] However, the coumarinylmethyl[22] and hydroxyquinolinylmethyl[21] protecting groups only release weakly basic leaving groups. It should be noted that the above wavelength maxima do not represent the practical, usually longer wavelengths used for photorelease experiments.[23] In addition, certain cage compounds, including coumarinylmethyl[20] and hydroxyquinolinylmethyl[21] derivatives undergo uncaging upon 2-photon excitation in the IR region.[24]

Four aspects of the photochemistry of **7-9** and **10** will be discussed further, below. First, quantum yields decrease with increasing leaving group basicity. Secondly, the cyclization step producing the zwitterionic intermediate likely involves the triplet excited state. Quantum yields for **7-10** are generally much lower than for **5**, which photolyzes efficiently. Furthermore, the photocyclization products of **7-9** are formed regioselectively or regiospecifically.

For acid **9** the quantum yields for reaction decrease for the series LG^- = Cl^-, PhS^-, and $PhCH_2S^-$. This decrease follows the increasing basicities of these anions. As noted, the same trend in Φ was previously reported for **5**, although a wider variety of leaving groups was investigated in that case.[4] Nevertheless, as noted previously, the decrease in Φ with increasing LG^- basicities is thought to be consistent with the zwitterionic intermediate **2** as undergoing ring opening to regenerate reactant in competition with LG^- expulsion.

We note that for **9** (LG^- = HS^-), the expulsion of HS^- is inefficient in terms of Φ, but nevertheless occurs essentially in quantitative chemical yields. The low Φ could be due to quenching of the thioxanthone triplets by the benzothiophene SH moiety. Mercaptans are known quenchers of ketone triplet excited states, and bimolecular rate constants k_q are 10^7-10^8 M^{-1} s^{-1} for quenching of benzophenone triplets.[25] Such quenching has also been noted as being reversible.[25] Such reversibility would be necessary to account for the essentially quantitative yields of photoproduct **27** found upon photolysis of **9** (LG^- = HS^-). Given the high yields of **27**, we still consider **9** (LG^- = HS^-) to be of potential practical use in biological and physiological studies, because the conjugate acid, H_2S, which would be formed upon LG^- release at physiological pH, has been found to be involved in regulation of vascular tone and blood pressure, in addition to stimulating natriuresis and diuresis in the kidneys.[26] It has been noted that such studies of the various roles played by H_2S are hindered by the absence of the readily controllable method for its generation.[27]

In the case of ester **8** (LG^- = Cl^-) the photoreaction is quenched by both oxygen and piperylene. Such quenching is consistent with the involvement of the triplet excited state in the formation of the proposed zwitterionic intermediate **2**. The 38% higher quantum yield observed for the bromo ester **10** (Φ = 0.053) as compared to ester **8** (Φ = 0.039 may be due to the "heavy atom effect", which is expected to promote intersystem crossing and increase the triplet yield for the bromide. Unsubstituted thioxanthone has a triplet yield of 0.56 in polar, protic solvent (CH_3OH) and 0.85 in nonpolar hydrocarbon solvent (cyclohexane).[28]

Stern-Volmer quenching of the triplet excited state of **8** (LG^- = Cl^-) by piperylene yields a triplet excited state lifetime of ca. 7 μs, which is rather like and only somewhat shorter than a typical

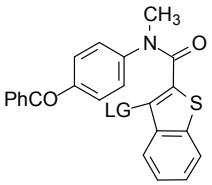

34 (LG^- = Cl^-)

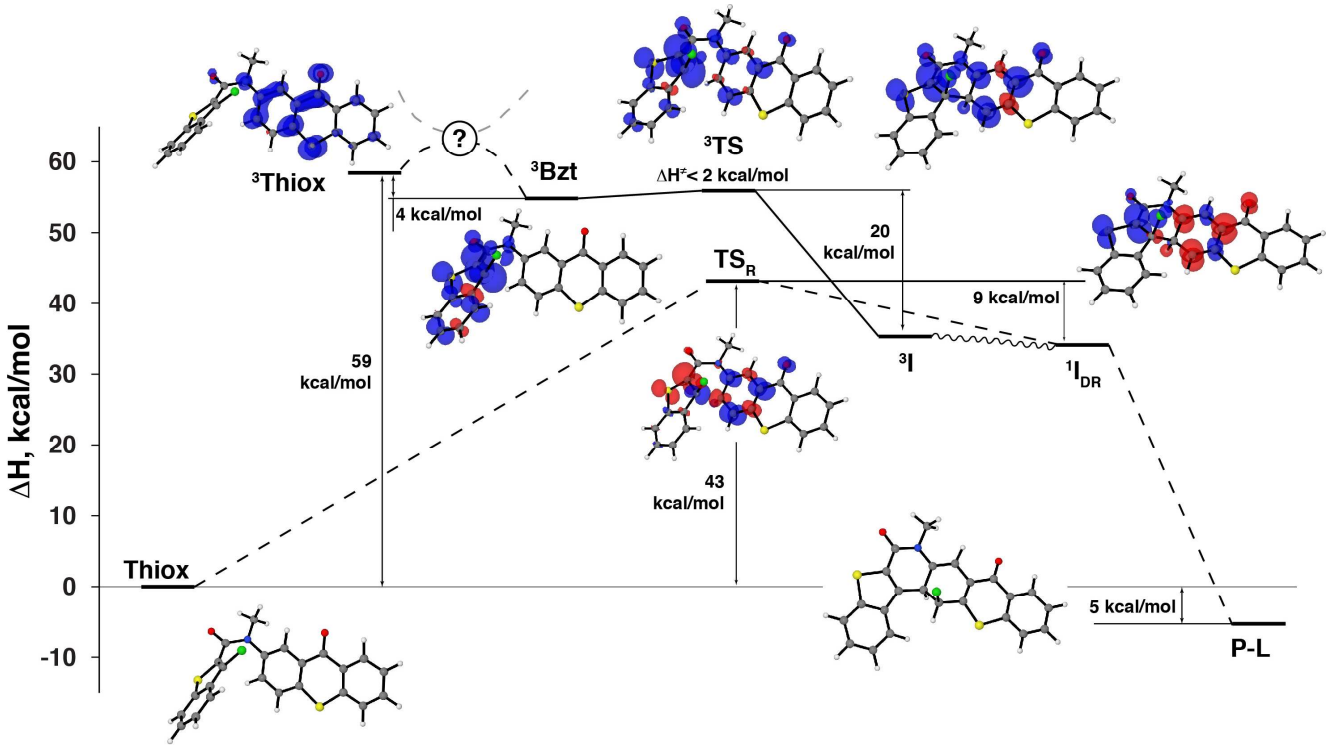

Fig. 3. Relative enthalpies of the stationary points on the ground-state singlet S_0 and lowest triplet T_1 surfaces relevant for formation of the linear ring closure product. Unpaired spin density isosurfaces are shown for open-shell species. The unsubstituted model is shown; relative enthalpies for methyl ester-substituted model are within 1 kcal mol^{-1}.All structures correspond to the lowest electronic state of a given multiplicity, as confirmed by wavefunction stability tests.

triplet excited of thioxanthone. The lifetime is consistent with a cyclization step that is not exceptionally rapid. This raises the possibility radiationless decay to the ground state could compete with the cyclization, which would account for relatively low quantum efficiency of Φ = 0.037-0.039 for **8** (LG^- = Cl^-) as compared to anilide **5** (LG^- = Cl^-, Φ = 0.23) or *p*-benzoyl derivative **34** (LG^- = Cl^-, Φ = 0.15). However, such comparisons are more direct for **7** (LG^- = Cl^-), which like **5** or **34**, has no carboxylate group at C-6 of the benzothiophene ring. Quantum yields for **7** (LG^- = Cl^-) are also rather low at 0.069.

The lower reactivity of thioxanthones vs. **5** or **34** may be due to the fact that E_T = 64 kcal mol^{-1} for thioxanthone,[28b] whereas E_T = 69 kcal mol^{-1} for unsubstituted benzothiophene.[29] The high quantum yield observed for **5** (LG^- = Cl^-) and the progressively lower quantum yields for **34** and the thioxanthones seems to imply that the triplet excited state should be localized on the benzothiophene moiety for the reaction to be efficient. For **5** the triplet excitation is likely localized mainly on the benzothiophene ring. For benzophenone (E_T = 69 kcal mol^{-1}) the triplet excited state is essentially equienergetic with the benzothiophene.. On the other hand, endothermic energy transfer would be needed to populate the benzothiophene triplet excited state upon initial generation of the thioxanthone (E_T = 64 kcal mol^{-1}) triplet excited state. Energetically less favorable energy transfer from chromophore triplet excited state to the benzothiophene moiety might account for the lower quanatum efficiencies of the thioxanthones relative to **5** and **34**.

We performed electronic structure calculations to gain some insight into the mechanism of the photochemical ring closure in an attempt to pinpoint the origins of the different regiospecificity for the carboxyl/methyl ester substituted derivatives **8** and **9**. To realistically model the entire photochemical reaction that involves transitions between different electronic states, one would require computationally expensive multi-reference methods and, probably, extensive non-adiabatic dynamics calculations. Here, we adopted a more limited approach and only examined some relevant stationary points on the lowest ground singlet S_0 and triplet T_1 electronic states using density functional theory (DFT) calculations at the PBE0/6-31G(d) level with solvent effects included using a polarizable continuum model.

The unsubstituted compound **7** and its methyl ester derivative **8** were considered in two conformations, L (Figure 3) and U (Figure 4), that correlate with the corresponding regioisomeric ring closure products, **30** for U and **31** for L in the case of **7**, and likewise to products **26** and **28** for U and L conformers in the case of ester **8**. For the starting molecules **7** and **8** these conformers are virtually isoenergetic in the ground state, with only with slight preference for the helical conformation U (< 0.5 kcal mol^{-1}). Thus, preexcitation conformational dynamics cannot

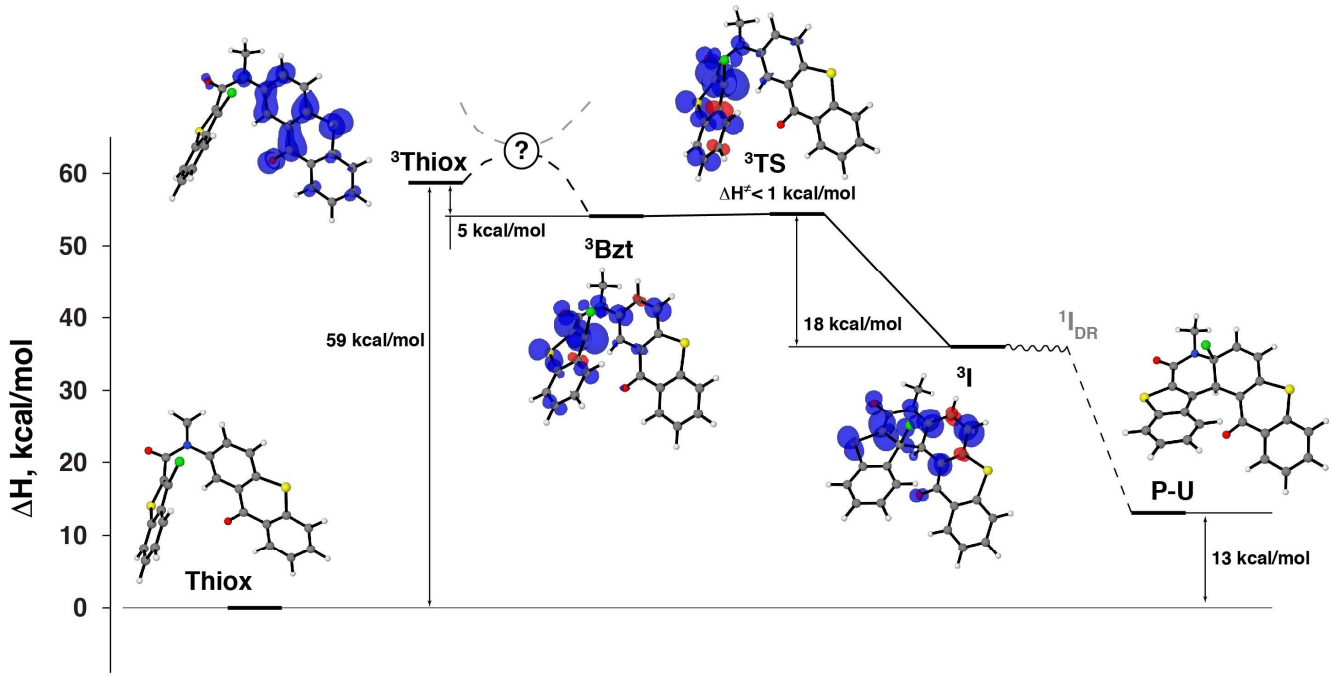

Fig. 4. Releative enthalpies of the stationary points on the ground-state singlet S_0 and lowest triplet T_1 surfaces relevant for the formation of the U-shaped helical ring closure product. Unpaired spin density isosurfaces are shown for open-shell species. The unsubstituted model is shown; the relative enthalpies for methyl ester-substituted model are within 1 kcal mol^{-1}. No local minimum corresponds to the $^1I_{DR}$ intermediate, since the geometry optimization directly converges to closed-shell product **P-U**.

account for the ring closure regiospecificity. Figures 3 and 4 depict the stationary points on the ground state singlet and lowest triplet excited state surfaces relevant for formation of the cyclized products of **7**. The relative enthalpies for ester compound **8** are within 1 kcal mol^{-1} and therefore, the Figures are not shown.

We used the ground-state structures for **7** and **8**, denoted as **Thiox**, as starting points to optimize the triplet-state geometries. Relaxed lowest triplet excited state structures **^{3}Thiox** are 59 kcal mol^{-1} higher in enthalpy compared to the S_0 state minima. The geometry changes in the **^{3}Thiox** excited state are relatively small compared with S_0, aside from expected bond length changes. However, further geometry search revealed another minima on the T_1 surface (**^{3}Bzt**) that is 4 kcal mol^{-1} lower relative to the S_0-like **^{3}Thiox** structures. The main geometric difference between **^{3}Bzt** and **^{3}Thiox** structures is the pyramidalization at the C-3 carbon atom in **^{3}Bzt**.

Unpaired spin density plots (Figures 3 and 4) show that in **^{3}Thiox**, which presumably forms from the S_1 state via intersystem crossing, the excitation is localized on the thioxanthone moiety. On the other hand, in the pyramidal **^{3}Bzt** intermediates the excitation is on the benzothiophene moiety. Thus, the **^{3}Thiox** to **^{3}Bzt** transformation changes the nature of the lowest adiabatic T_1 state and corresponds to excitation transfer between the two parts of the molecule. This transition likely proceeds via a crossing between two diabatic triplet states, corresponding to excited thioxanthone and benzothiophene, respectively. For this transition, C-3 atom pyramidalization appears to be the main reaction coordinate, aside from the solvent coordinate, which also may be important. Modelling of the **^{3}Thiox** to **^{3}Bzt** transition would require sophisticated multi-reference calculations; not surprisingly, our attempts to locate a transition state on the lowest adiabatic T_1 surface with DFT methods were not successful.

In **^{3}Bzt**, the pyramidalized C-3 atom is poised to attack the C-3' (L conformer) or the C-1' (U conformer) atoms of the thioxanthone moiety. We located transition state structures **^{3}TS** (Figures 3 and 4) for the ring closure reactions in the T_1 state, starting from the **^{3}Bzt** structures. For the L conformers, the barrier heights are ca. 1–2 kcal mol^{-1} for both **7** and **8**. For the U conformers the barrier is virtually non-existent, <1 kcal mol^{-1} for both **7** and **8**. The ring closure reaction leads to triplet intermediates **^{3}I** that are lower in energy than the initial **^{3}Bzt** structures by 20 and 18 kcal mol^{-1} for the L and U isomers, respectively, for both **7** and **8**.

Broken spin symmetry open-shell DFT calculations suggest that the singlet ground state lies just ca. 0.5 kcal mol^{-1} lower than **^{3}I** (for the equilibrium **^{3}I** geometry) and has a pronounced singlet diradical character ($S^2 \approx 1.0$). Thus, the triplet-to-singlet transition is highly probable once **^{3}I** is formed, or may even occur during the **^{3}Bzt** to **^{3}I** transformation. Geometry optimizations of the singlet diradical intermediates starting from the L-isomers of **^{3}I** lead to local minima **$^1I_{DR}$** (Figure 3), which are 1 kcal mol^{-1} lower than the corresponding **^{3}I** structures and have very similar geometries. Unpaired spin distributions in **^{3}I** and **$^1I_{DR}$** are very

similar, with the two unpaired electrons largely uncoupled and spatially separated, as evident from the spin distribution in $^1\mathbf{I}_{DR}$. The decoupling between the two unpaired electrons correlates very well with near-degeneracy between the singlet and triplet states for the intermediate **I**. For the U-isomers, however, geometry optimizations did not locate any minima corresponding to singlet diradical intermediates, $^1\mathbf{I}_{DR}$, as the open-shell character quickly collapses to become closed-shell during the optimization.

The optimized closed-shell singlet structures **P-U** are 23 kcal mol^{-1} lower than corresponding ^{3}**I** structures and significantly differ in geometry from ^{3}**I**, as the chlorine atom migrates to the C-2' position in structure **P-U**. We further optimized singlet diradicals $^1\mathbf{I}_{DR}$ with a collapsed closed-shell wavefunction. The closed shell species ultimately gives the closed-shell products **P-L** that are 40 kcal mol^{-1} lower in energy than ^{1}**I**. In the case of **P-L** the chlorine atom has migrated to the C-4' position.

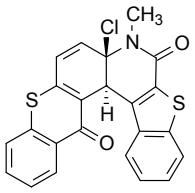

P-U

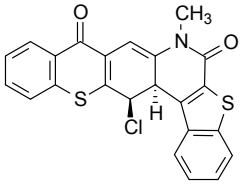

P-L

In the case of L isomer, we located an open-shell diradical transition state $\mathbf{TS}_R$ that corresponds to the ring reopening in $^1\mathbf{I}_{DR}$ leading to the **Thiox** reactant via a ~10 kcal mol^{-1} barrier (Figure 3). The diradical intermediates $^1\mathbf{I}_{DR}$ correspond to very shallow or, in the case of U isomer, non-existent minima on the potential energy surface. Thus, conversion of $^1\mathbf{I}_{DR}$ into products is a more likely process than the reverse ring-opening reaction. In the case of a poorer leaving group, $^1\mathbf{I}_{DR}$ can be more stable, which could increase the importance of the ring-opening reaction. Indeed, preliminary DFT calculations for LG$^-$ = HO$^-$ substituted models suggest a significantly more stable $^1\mathbf{I}_{DR}$ diradical. This agrees well with lower quantum yield previously observed for LG$^-$ that are more basic than LG$^-$ = Cl$^-$.

Our DFT calculations (Figures 3 and 4) did not find any practically significant differences between the **7** and **8**, since the enthalpies calculated, relative to the corresponding **Thiox** structures, never differed by more than 1 kcal mol^{-1}. Moreover, there is no substantial energetic difference between L and U conformers of **Thiox**, ^{3}**Thiox**, and ^{3}**Bzt**. For both L and U cases the barrier height for the ring closure of ^{3}**Bzt** is extremely low, although the ring closure is slightly more exothermic in the case of the L isomer (20 vs 18 kcal mol^{-1} for L and U, respectively). Further transformations of the ring closure intermediates do differ for L and U isomers, in that L ultimately gives the lower energy product **P-L**. This is only in agreement with the slight experimental preference for the L isomer product **31** of **7**, but is contrary to the regiospecific formation of **26** from **8**.

The photoproducts P-L and P-U are not experimentally observed, but they are the calculated products when solvent effects are implicitly included using a polarizable continuum model. Inclusion of discrete water molecules would very likely result in dissociation of the chloride leaving group to give the experimentally observed products involving loss of HCl. Experimentally, we previously observed a product that would be analogous to **P-U** or **P-L**. For example, photolysis of **35** gave **36** in CH_3CN under nonaqeous conditions, while **37** was the product in aq CH_3CN (Scheme 8).[28]

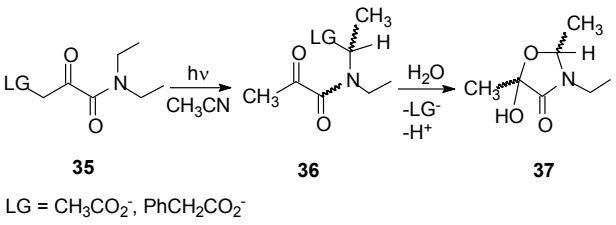

35 **36** **37**

LG = $CH_3CO_2^-$, $PhCH_2CO_2^-$

Scheme 8

When water was added to a solution of **36** in CH_3CN, **36** underwent solvolysis to give **37**. Our previous study also presented flash photolytic kinetic data in support of a mechanism for formation of **37** involving dissociation of the leaving group

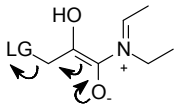

38

from zwitterionic intermediate **38**.[28] Our view has been that, upon release of the leaving group from **38**, the resultant imminium ion undergoes internal return in the ion pair to form **36**, while hemiacetal **37** results from capture of the imminium ion by the solvent under aqueous conditions.[30,31] Products **P-U** and **P-L** are considered to be closely related to **37**, and experimentally, one would also expect them to be quite labile with respect to solvolytic loss of HCl, if they were to be formed.

Calculated enthalpic profiles (Figures 3 and 4) suggest that once the pyramidal intermediates ^{3}**Bzt** are formed, they immediately undergo irreversible ring closure when LG$^-$ = Cl$^-$. Thus, the regiospecificity is likely determined at this or preceding reaction steps. Since L and U conformers are nearly isoenergetic for ^{3}**Thiox** and ^{3}**Bzt** (in fact, the U conformer of ^{3}**Bzt** is 1 kcal mol^{-1} lower than the L conformer), the unusual regiospecificity of **8** may have its origins in the dynamics of the excitation transfer between the two aromatic systems, ^{3}**Thiox** to ^{3}**Bzt**. Careful multi-reference modeling of this rate-limiting step, including calculations of the coupling between the diabatic triplet states involved, are required to test this hypothesis.

Conclusions

Thioxanthones bearing a benzothiophene carboxamide group at the C-2 position are capable of expelling leaving groups such as Cl$^-$, PhS$^-$, HS$^-$ and $PhCH_2S^-$ that are originally present at the C-3 position of the benzothiophene ring. The leaving group expulsions can be achieved using 390 nm light or a sunlamp in essentially quantitative yields. Moreover, the inclusion of a carboxylate group at the C-6 position of the benzothiophene ring system greatly improves solubilities in aqueous media. The photorelease of the leaving groups proceeds with quantum yields of 0.01-0.04, depending on leaving basicity. The carboxylate-substituted benzothiophenes photocyclize regiospecifically. The

preference is for photoelectrocyclization to the C-1 position of the thioxanthone ring to give a helical photoproduct. C-3 photocyclization is slightly preferred to C-1 photocyclization, when the benzothiophene ring lacks the C-6 carboxylate group. The photocyclizations occur in the triplet excited state according to quenching experiments with known triplet excited state quenchers. DFT calculations show that the triplet excited state cyclization is energetically favourable and produces a triplet excited state. Intersystem crossing of this species produces a singlet diradical, which in water is expected to collapse to the corresponding closed shell species (zwitterion) with C_3-Cl bond breaking to form product.

Experimental

Preparation of 3-chloro-benzo[b]thiophene-2-carboxylic acid methyl-(9-oxo-9H-thioxanthen-2-yl) amide[4] (7) (LG^- = Cl^-). To 1.2 g (5.0 mmol) of 2-methylaminothioxanthen-9-one (**13**)[10] and 15 mL of triethylamine in 30 mL of anhyd CH_2Cl_2 was added 1.4 g (6.1 mmol) of 3-chlorobenzo[b]thiophene-2-carbonyl chloride (11)[11] dissolved in 10 mL of anhyd CH_2Cl_2 at 5-8 °C in an ice bath. A catalytic amount of DMAP was added. The reaction mixture was warmed to room temperature and stirred for 48 h under N_2. The reaction mixture was filtered to remove triethylamine hydrochloride, the filtrate was washed three times with aq saturated $NaHCO_3$, H_2O, three times with aq. 2N HCl to remove unreacted amines, H_2O, brine, dried over Na_2SO_4, and concentrated in vacuo to give a dark solid containing amide **7** (LG^- = Cl^-). The solid was dissolved in benzene and refluxed with Norite for 2 h, followed by vacuum filtration through Celite to remove colored impurities. The filtrate was concentrated in vacuo and crystallized from benzene to obtain 1.8 g (81% yield) of red crystals, mp 168-170 °C. Found: C, 63.14; H, 3.31; N, 3.07%; calcd for $C_{23}H_{14}NO_2S_2Cl$: C, 63.38; H, 3.21; N, 3.21%; ^{1}H-NMR (400 MHz, $CDCl_3$): 3.60 (3H, s), 7.29-7.74 (9H, m), 8.48-8.62 (2H, m); ^{13}C-NMR (100 MHz, DMSO-d_6): 38.2, 119.3, 122.5, 123.9, 126.4, 127.0, 127.2, 127.5, 127.6, 128.2, 128.3, 129.2, 129.6, 131.8, 131.9, 133.8, 135.0, 135.9, 136.8, 137.6, 141.7, 162.2, 178.7.

Preparation of 3-chloro-2-[methyl-(9-oxo-9H-thioxanthen-2-yl)-carbamoyl]-benzo[b]thiophene-6-carboxylic acid methyl ester (8) (LG^- = Cl^-). To 1.2 g (5.0 mmol) of 2-methylaminothioxanthen-9-one (**13**)[10] and 15 mL of triethylamine in 20 mL of anhyd CH_2Cl_2 was added 1.7 g (5.9 mmol) of 3-chloro-2-(chlorocarbonyl)benzo[b]thiophene-6-carboxylic acid methyl ester (**12**) dissolved in 15 mL of anhyd CH_2Cl_2 at 5-8 °C in an ice bath. A catalytic amount of DMAP was added. The reaction mixture was warmed at room temperature and stirred for 48 h under N_2. The reaction mixture was filtered to remove triethylamine hydrochloride and the filtrate was washed three times with aq saturated $NaHCO_3$, H_2O, three times with aq. 2N HCl to remove unreacted amines, H_2O, brine, dried over Na_2SO_4, and concentrated in vacuo to give crude product **8**. The crude product was chromatographed on silica gel, eluting with 30% ethyl acetate in hexane to give 1.6 g (65% yield) of **8** (LG^- = Cl^-), mp 192-193 °C, as a yellow powder. Found: C, 61.05; H, 3.28; N, 2.78%; calcd for $C_{25}H_{16}NO_4S_2Cl$: C, 60.79; H, 3.24; N, 2.84%; ^{1}H-NMR (400 MHz, $CDCl_3$): 3.61 (3H, s), 3.91 (3H, s), 7.39-7.56 (4H, m), 7.61 (1H, t, J = 8.7 Hz), 7.73 (1H, d, J = 8.7 Hz), 8.01 (1H, d, J = 8.7 Hz), 8.39 (1H, s), 8.52 (1H, s), 8.57 (1H, d, J = 8.3 Hz); ^{13}C-NMR (100 MHz, $CDCl_3$): 38.3, 52.6, 120.7, 122.7, 124.9, 126.2, 126.8, 127.2, 127.3, 128.5, 128.7, 129.9, 130.0, 130.7, 132.8, 134.3, 136.6, 136.9, 137.5, 138.7, 141.1, 162.5, 166.5, 179.2.

Preparation of 3-chloro-2-[methyl-(9-oxo-9H-thioxanthen-2-yl)-carbamoyl]-benzo[b]thiophene-6-carboxylic acid (9) (LG^- = Cl^-). To 1.0 g (2.1 mmol) of ester **8** (LG^- = Cl^-) in 45 mL MeOH and 15 mL H_2O was added 0.11 g (0.93 equiv) of KOH. The mixture was refluxed for 4 h. After cooling to room temperature, 50 mL of H_2O was added, the solution was washed with ethyl acetate to remove any unreacted ester, and the aq. phase was acidified with conc HCl to pH 2 to give a precipitate. The aqueous suspended precipitate dissolved upon addition of ethyl acetate. The ethyl acetate extract was washed with brine, dried over Na_2SO_4, and concentrated in vacuo to obtain 0.61 g (61% yield) of acid **9** (LG^- = Cl^-) as a yellow powder, mp 286-287 °C. Found: C, 59.95; H, 3.04; N, 2.93%; calcd for $C_{24}H_{14}NO_4S_2Cl$: C, 60.06; H, 2.92; N, 2.92%; ^{1}H-NMR (400 MHz, DMSO-d_6): 3.50 (3H, s), 7.39-7.81 (6H, m), 7.88 (1H, d, J = 8.5 Hz), 8.30 (1H, d, J = 7.8 Hz), 8.34 (1H, s), 8.58 (1H, s), 13.16 (1H, br); ^{13}C-NMR (100 MHz, DMSO-d_6): 38.1, 118.9, 122.4, 125.7, 126.6, 127.1, 127.3, 127.9, 128.1, 129.0, 129.4, 129.5, 131.6, 133.4, 135.3, 135.8, 136.6, 137.4, 137.8, 141.3, 161.6, 167.1, 178.5.

Preparation of 2-[methyl-(9-oxo-9H-thioxanthen-2-yl)-carbamoyl]-3-phenylsulfanyl-benzo[b]thiophene-6-carboxylic acid (9) (LG^- = PhS^-)[4]. To a solution of 1.03 g (2.1 mmol) of ester **8** (LG^- = Cl^-) in 10 mL DMF was added 0.43 mL (0.46 g, 4.2 mmol) of thiophenol, followed by 0.63 mL, (0.64 g, 4.2 mmol) of DBU. The reaction mixture was stirred for 72 h at 80 °C under N_2 and then 50 mL of ethyl acetate was added. The ethyl acetate solution was washed with aq 1N HCl (250 mL) to remove excess of DBU and then washed three times with aq 1N NaOH (100 mL). The combined aqueous base solution was acidified with conc. HCl (pH = 2). The resultant light yellow precipitate was collected by filtration and crystallized from MeOH, followed by drying under vacuum, to obtain 0.90 g (78 % yield) of acid **9** (LG^- = PhS^-) as a yellow powder, mp 278-279 °C. Found: C, 64.94; H, 3.44; N, 2.48%; calcd for $C_{30}H_{19}NO_4S_3$: C, 65.1; H, 3.44; N, 2.53; ^{1}H-NMR (400 MHz, DMSO-d_6) 3.48 (3H, s), 6.63-7.12 (5H, m), 7.29-8.21 (7H, m), 8.21-8.41 (2H, m), 8.66 (1H, s), 13.1 (1H, s); ^{13}C-NMR (100MHz, DMSO-d_6): 38.1, 121.5, 123.8, 126.0, 126.6, 126.7, 127.3, 127.4, 127.7, 128.2, 128.5, 129.2, 129.4, 129.6, 129.7, 132.0, 133.8, 134.8, 135.9, 136.9, 139.3, 141.1, 141.5, 146.5, 162.9, 167.4, 178.6.

Preparation of 3-benzylsulfanyl-2-[methyl-(9-oxo-9H-thioxanthen-2-yl)-carbamoyl]-benzo[b]thiophene-6-carboxylic acid (9) (LG^- = $PhCH_2S^-$)[4]. To a solution of 1.0 g (2.1 mmol) of acid **9** (LG^- = Cl^-) in 10 mL DMF was added 0.75 mL (0.78 g, 6.3 mmol) of benzyl mercaptan followed by 1.2 mL (1.3 g, 8.4 mmol) of DBU. The reaction mixture was stirred for 48 h at 80 °C under N_2. The volatiles including DBU and benzyl mercaptan were evaporated at 80 °C under vacuum for 6 h without air contact. The residue was dissolved in $CHCl_3$, filtered, and the filtrate was washed three times with H_2O, brine and concentrated in vacuo to obtain crude acid **9** (LG^- = $PhCH_2S^-$) as

light yellow solid. The crude acid was dissolved in 17% H_2O in CH_3CN containing 100 mM phosphate buffer at pH 7 and filtered. The filtrate was acidified with conc. HCl, to obtain a precipitate, which was collected by filtration. Repeating this purification procedure gave 0.83 g (70 % yield) of acid **9** (LG^- = $PhCH_2S^-$) as a light yellow powder, mp 151-152 °C. Found: C, 65.60; H, 3.75; N, 2.49%; calcd for $C_{31}H_{21}NO_4S_3$: C, 65.61; H, 3.70%; N, 2.47%; ^{1}H-NMR (400 MHz, $CDCl_3$): 3.57 (3H, s), 4.03 (2H, s), 7.04-7.67 (6H, m), 7.86 (1H, s), 8.41 (1H, s), 8.51-8.59 (2H, m); ^{13}C-NMR (100 MHz, $CDCl_3$): 38.4, 41.2, 124.0, 125.5, 126.0, 126.2, 126.7, 126.8, 127.1, 127.5, 128.6, 128.8, 129.2, 129.9, 130.1, 131.0, 132.8, 136.5, 137.0, 137.6, 138.6, 141.3, 143.7, 145.3, 163.9, 171.2.179.4.

Preparation of 3-mercapto-2-[methyl-(9-oxo-9H-thioxanthen-2-yl)-carbamoyl]-benzo[b]thiophene-6-carboxylic acid (9) (LG^- = HS^-). To a solution of 0.29 g (0.61 mmol) of acid **9** (LG^- = Cl^-) in 10 mL DMF was added 0.14 g (1.8 mmol) of thioacetamide followed by 0..27 mL (0.27 g, 1.8 mmol) of DBU. The reaction mixture was stirred for 72 h at 100 °C under N_2. To the reaction mixture was added 50 mL ethyl acetate and 100 mL of H_2O. The aq. layer was separated and extracted with ethyl acetate and then acidified with conc. HCl (pH = 2) to obtain 0.15 g of a precipitate upon filtration. Most of the light yellow precipitate was then dissolved in 15 mg of KOH in 50 mL of H_2O and filtered. The filtrate was acidified with 1 N HCl and the precipitate was obtained by filtration. The precipitate was dried under vacuum and crystallized from ethyl acetate to give 0.12 g (42% yield) of NMR pure compound (**9**) (LG^- = HS^-), mp 210-212 °C. Found: C, 60.61; H, 3.48; N, 2.69%; calcd for $C_{24}H_{15}NO_4S_3$: C, 60.38; H, 3.14; N, 2.94%; ^{1}H-NMR (400 MHz, DMSO-d_6): 3.20 (3H, s), 7.24-7.51 (3H, m), 7.55-7.71 (4H, m), 8.24-8.31 (2H, m,), 8.50 (1H, s); ^{13}C-NMR (100 MHz, DMSO-d_6): 38.1, 123.4, 124.8, 125.5, 125.9, 126.6, 126.9, 127.3, 127.7, 128.3, 128.9, 129.1, 129.5, 131.4, 133.5, 135.5, 136.6, 138.7, 141.0, 141.3, 146.5, 162.0, 167.0, 178.5.

Preparation of 2-[(7-bromo-9-oxo-9H-thioxanthen-2-yl)-methyl-carbamoyl]-3-chloro-benzo[b]thiophene-6-carboxylic acid methyl ester (10) (LG^- = Cl^-). To 0.51 g (1.6 mmol) of 2-bromo-7-methylamino-thioxanthen-9-one (**14**) and 10 mL of triethylamine in 15 mL of anhyd CH_2Cl_2 was added 0.61 g (2.1 mmol) of 3-chloro-2-chlorocarbonyl-benzo[b]thiophene-6-carboxylic acid methyl ester (**12**) dissolved in 10 mL of anhyd CH_2Cl_2 at 5-8 °C in an ice bath. A catalytic amount of DMAP was added. The reaction mixture was warmed at room temperature and stirred for 48 h under N_2. The reaction mixture was filtered to remove triethylamine hydrochloride salt, the filtrate was washed three times with aq saturated $NaHCO_3$, H_2O, three times with aq. 2N HCl to remove unreacted amines, H_2O, brine, dried over Na_2SO_4, and concentrated in vacuo to give crude ester **10**. The crude ester **10** was chromatographed on silica gel, eluting with 20% ethyl acetate in hexane to give 0.55 g (60% yield) of NMR pure **10** (LG^- = Cl^-) as a brown powder, mp 237-239 °C. Found: C, 52.09; H, 2.64; N, 2.47%; calcd for $C_{25}H_{15}NO4S_2ClBr$: C, 52.40; H, 2.62; N, 2.44%; ^{1}H-NMR (400 MHz, $CDCl_3$): 3.61 (3H, s), 3.92 (3H, s), 7.35-7.54 (3H, m), 7.66-7.80 (2H, m), 8.02 (1H, d, J = 8.2 Hz), 8.40 (1H, s), 8.51 (1H, s), 8.69 (1H, s); ^{13}C- NMR (100 MHz, $CDCl_3$): 38.3, 52.6, 120.8, 120.9, 122.8, 124.9, 126.3, 127.3, 127.4, 127.8, 128.6, 129.6, 130.0, 131.0, 132.7, 134.1, 135.8, 136.1, 137.6, 138.7, 141.4, 162.5, 166.5, 178.1.

Preparation of 3-chloro-2-chlorocarbonyl-benzo[b]thiophene-6-carboxylic acid methyl ester (12). A stirred solution of 10.0 g (0.048 mol) of (*E*)-4-(methoxycarbonyl)cinnamic acid (**17**)[12] and 0.8 mL pyridine in 52 mL (0.72 mol) of thionyl chloride was refluxed for 6 days. After cooling at room temperature, 100 mL of 2N HCl was added until pH 2 was obtained and the mixture was filtered. The solid crude acid was dried under vacuum. To the crude acid in 50 mL benzene was added, dropwise, 5.7 g (0.048 mol, 3.5 mL) of thionyl chloride under N_2. The reaction mixture was refluxed overnight and then concentrated in vacuo to give 6.9 g (51% yield) of acid chloride **12** as a colorless powder, mp 259-260 °C. ^{1}H-NMR (400 MHz, DMSO-d_6): 3.87 (3H, s), 7.91 (1H, d, J = 8.7 Hz), 8.01 (1H, d, J = 8.7 Hz), 8.53 (1H, s).

Preparation of 2-methylaminothioxanthen-9-one (**13**). A mixture of 0.99 g (3.5 mmol) of amide **24** and 100 mL of aqueous 2 M NaOH was refluxed for 12 h. Upon cooling the reaction mixture was acidified with concentrated HCl to pH = 1 and then extracted with CH_2Cl_2. The extract was dried over Na_2SO_4 and concentrated in vacuo to give 0.47 g (56% yield) of amino ketone **13** as a yellow powder**,** mp 172-175 °C. ^{1}H-NMR (400 MHz, $CDCl_3$): 2.95 (3H, s), 3.98 (1H, br), 6.98 (1H, d, J = 8.7 Hz), 7.36 -7.48 (2H, m), 7.53 -7.60 (2H, m), 7.77 (1H, s), 8.62 (1H, d, J = 8.1 Hz).

Preparation of 2-bromo-7-methylaminothioxanthen-9-one (**14**). A mixture of 1.13 g (3.1 mmol) of amide **25** and 100 mL of aqueous 2 M NaOH was refluxed for 12 h. Upon cooling the reaction mixture was acidified with concentrated HCl to pH = 1 and then extracted with CH_2Cl_2. The extract was dried over Na_2SO_4, and concentrated in vacuo to give 0.36 g (36% yield) of amino ketone **14** as red powder**,** mp 198-200 °C. ^{1}H-NMR (400 MHz, $CDCl_3$): 2.95 (3H, s), 4.02 (1H, br), 6.98 (1H, d, J = 8.6 Hz), 7.38 (1H, d, J = 8.6 Hz), 7.43 (1H, d, J = 8.6 Hz), 7.66 (1H, d, J = 8.6 Hz), 7.73 (1H, s), 8.74 (1H, s).

Preparation of 2-amino-7-bromo-thioxanthen-9-one (**21**)[10]. A mixture of 1.7 g (5.0 mmol) of 2-bromo-7-nitrothioxanthen-9-one (**19**)[13], 1.6 g (31 mmol) ammonium chloride, and 0.90 g (16 mmol) iron in 60 mL water and 200 mL ethanol was refluxed overnight. After hot vacuum filtration through silica gel, the silica gel was washed with 30 mL and combined with the filtrate. The combined filtrate was concentrated in vacuo. To the residue was added 150 mL chloroform. The chloroform solution was dried over anhydrous sodium sulfate and concentrated in vacuo to give 1.0 g (66% yield) of NMR pure **21** as a brown powder, mp 201-203 °C. ^{1}H-NMR (400 MHz, $CDCl_3$): 3.96 (2H, br), 7.04 (1H, d, J = 8.9 Hz), 7.39 (1H, d, J = 8.9 Hz), 7.43 (1H, d, J = 8.9 Hz), 7.66 (1H, d, J = 8.3 Hz), 7.86 (1H, s), 8.72 (1H, s).

Preparation of N-(7-bromo-9-oxo-9H-thioxanthen-2-yl)-acetamide (**23**). A mixture of 1.0 g (3.3 mmol) amino ketone **21**, 50 mL glacial acetic acid, and 11.6 g (114 mmol) of acetic anhydride was stirred for overnight at room temperature. After adding 100 mL water with stirring, the resultant precipitate was filtered, washed with four times with 50 mL H_2O, and 10 mL of MeOH. The precipitate was washed with $CHCl_3$ and dried under vacuum to give 1.1 g (95% yield) of NMR pure acetamide derivative **23** as brown powder, mp 219-222 °C. ^{1}H-NMR (400

MHz, DMSO-d_6): 2.08 (3H, s), 7.78 (1H, d, J = 8.6 Hz), 7.81 (1H, d, J = 8.6 Hz), 7.90 (1H, d, J = 9.4 Hz), 8.01 (1H, d, J = 9.4 Hz), 8.48 (1H, s), 8.67 (1H, s), 10.34 (1H, s).

Preparation of N-methyl-N-(9-oxo-9H-thioxanthen-2-yl)-acetamide (**24**). To a stirred solution of 1.2 g (4.5 mmol) of N-(9-oxo-9H-thioxanthen-2-yl)-acetamide[10] **22** in 20 mL of THF was added 0.23 g (5.8 mmol) of NaH (60%) under N_2. The mixture was stirred for 15 min followed by dropwise addition of 0.96 g (6.8 mmol) of methyl iodide. The reaction mixture was stirred at room temperature for 48 h and then concentrated in vacuo to obtain a crude solid residue. To the residue was added $CHCl_3$, followed by filtration and concentration of the filtrate in vacuo to obtain 1.1 g (80 % yield) of methyl amide **24** as a yellow powder, mp 246-248 °C. ^{1}H-NMR (400 MHz, $CDCl_3$): 1.92 (3H, s), 3.33 (3H, s), 7.41-7.74 (5H, m), 8.44 (1H, s), 8.62 (1H, d, J = 8.5 Hz).

Preparation of N-(7-bromo-9-oxo-9H-thioxanthen-2-yl)-N-methyl-acetamide (**25**). To a stirred solution of 1.1 g (3.2 mmol) acetamide **23** in 20 mL of THF was added 0.17 g (4.2 mmol) of NaH (60%) under N_2. The mixture was stirred for 15 min followed by the dropwise addition of 0.70 g (4.9 mmol) of methyl iodide. The reaction mixture was stirred at room temperature for 48 h and then concentrated in vacuo to obtain a solid residue. To the residue was added $CHCl_3$, followed by filtration and concentration of the filtrate in vacuo to obtain 1.1 g (97 % yield) of methyl amide (**25**) as a yellow solid, mp 240-241 °C. ^{1}H-NMR (400 MHz, $CDCl_3$): 1.93 (3H, s), 3.34 (3H, s), 7.46-7.54 (2H, m), 7.66 (1H, d, J = 8.7 Hz), 7.76 (1H, d, J = 8.7 Hz), 8.45 (1H, s), 8.75 (1H, s).

Preparation of 6-methylcarboxylate-[1]benzothiopheno[2,3-c]benzo[a]anthracene-4-methyl-4*H*-7-thia-4-aza-3,12-dione (26) by photolysis of 8 (LG^- = Cl^-). A 0.010 M solution of **8** (LG^- = Cl^-) in N_2 saturated 17% H_2O in CH_3CN containing 100 mM phosphate buffer at pH 7 was irradiated with a 450 W Hanovia medium pressure mercury lamp with a Pyrex filter for 90 min. The photoproduct was isolated by filtration. The photoproduct was washed with H_2O and a small amount of $CHCl_3$ and dried under vacuum. The product was a yellow powder, mp >300 °C. Found: C, 65.39; H, 3.40; N, 3.11%; calcd for $C_{25}H_{15}NO_4S_2$: C, 65.65; H, 3.28; N, 3.06%; ^{1}H-NMR (400 MHz, DMSO-d_6): 3.89 (3H, s), 3.91 (3H, s), 7.71 (1H, d, J = 8.7 Hz), 7.72 (1H, t, J = 7.0 Hz), 7.85 (1H, d, J = 8.1 Hz), 7.86 (1H, t, J = 7.0 Hz), 7.97 (1H, d, J = 8.1 Hz), 8.08 (1H, d, J = 8.7 Hz), 8.13 (1H, d, J = 7.8 Hz), 8.16 (1H, d, J = 8.7 Hz), 8.85 (1H, s); The ^{13}C-NMR could not be obtained due to low solubility in d_6-DMSO. A COSY spectrum in d_6-DMSO was obtained (see Supporting Information).

Preparation of [1]benzothiopheno-6-carboxylic acid [2,3-c]benzo[a]anthracene-10-bromo-4-methyl-4*H*-7-thia-4-aza-3,12-dione (27) by photolysis of 9 (LG^- = Cl^-). A 0.010 M solution of **13** (LG^- = Cl^-) in N_2 saturated 75% H_2O in CH_3CN containing 100 mM phosphate buffer at pH 7 was irradiated with a 450 W Hanovia medium pressure mercury lamp with Pyrex filter for 90 min. The photolysate was acidified to pH 2 with conc. HCl to precipitate the photoproduct carboxylic acid **27**. The photoproduct was obtained by filtration, washing with H_2O, and drying under vacuum, as a yellow powder, mp >300 °C. Found: C, 64.66; H, 3.03; N, 3.10; calcd for $C_{24}H_{13}NO_4S_2$: C, 65.01; H, 2.93; N, 3.16%; ^{1}H-NMR (400 MHz, DMSO-d_6): 3.87 (3H, s), 7.66 (1H, d, J = 8.6 Hz), 7.71 (1H, t, J = 7.9 Hz), 7.82 (1H, d, J = 9.2 Hz), 7.84 (1H, t, J = 7.9 Hz), 7.95 (1H, d, J = 7.9 Hz), 8.06 (1H, d, J = 9.2 Hz), 8.12 (1H, d, J = 9.2 Hz), 8.14 (1H, d, J = 9.2 Hz), 8.77 (1H, s); ^{1}H NMR COSY and ^{1}H NMR NOESY were obtained (see Supporting Information); ^{13}C-NMR (100 MHz, DMSO-d_6) was not obtained due to low solubility.

Preparation of [1]benzothieno[2,3-c]benzo[a]anthracene-4-methyl-4*H*-7-thia-4-aza-3,12-dione (30) and its regioisomer 31 by photolysis of 7 (LG^- = Cl^-). A 0.010 M solution of **7** (LG^- = Cl^-) in N_2 saturated 17% H_2O in CH_3CN containing 100 mM phosphate buffer at pH 7 was irradiated with a 450 W Hanovia medium pressure mercury lamp with a Pyrex filter for 90 min. The photoproduct was isolated by filtration as a mixture of two isomers, **30**, **31**. The mixture of product isomers was dissolved in hot DMSO. Solid photoproduct isomer **31** was obtained upon cooling of the hot DMSO and filtration. Photoproduct isomer **31** was washed with water and methanol and dried under vacuum to obtain **31** as floppy powder, mp > 300 °C. Solid photoproduct isomer **30** was obtained upon addition of water to the above DMSO filtrate by filtration, after washing with water and methanol**.** The photoproduct isomer **30** was crystallized from $CHCl_3$ to give a yellow crystalline solid, mp 271-273 °C.

The photoproduct isomer **30** was characterized. Found: C, 68.88; H, 3.46; N, 3.35%; calcd for $C_{23}H_{13}NO_2S_2$: C, 69.17; H, 3.26; N, 3.51%; ^{1}H-NMR (400 MHz, DMSO-d_6): 3.87 (3H, s), 7.33 (1H, t, J = 7.8 Hz), 7.54 (1H, t, J = 8.0 Hz), 7.57 (1H, d, J = 8.7 Hz), 7.67 (1H, t, J = 8.1 Hz), 7.84 (1H, t, J = 8.1 Hz), 7.95 (1H, d, J = 8.1 Hz), 8.01 (1H, d, J = 9.4 Hz), 8.09 (1H, d, J = 6.7 Hz), 8.12 (1H, d, J = 8.1 Hz), 8.19 (1H, d, J = 8.1 Hz); ^{13}C-NMR (100 MHz, DMSO-d_6): 30.7, 115.9, 121.8, 124.2, 124.5, 125.8, 126.6, 127.2, 127.7, 127.8, 128.0, 129.4, 131.7, 132.5, 133.2, 133.9, 135.8, 136.2, 136.4, 138.7, 140.9, 157.8, 181.8.

The photoproduct isomer **31** was characterized. Found: C, 69.19; H, 3.36; N, 3.59%; calcd for $C_{23}H_{13}NO_2S_2$: C, 69.17; H, 3.26; N, 3.51%; ^{1}H-NMR (400 MHz, DMSO-d_6): 3.78 (3H, s), 7.46 (1H, t, J = 7.1), 7.55-7.69 (4H, m), 8.13 (1H, d, J = 7.1 Hz), 8.34 (1H, d, J = 8.4 Hz), 8.38 (1H, s), 8.79 (1H, s), 8.85 (1H, d, J = 4.5 Hz); The ^{13}C-NMR (100 MHz, DMSO-d_6) could not be obtained due to low solubility.

Preparation of 6-methylcarboxylate-[1]benzothiopheno[2,3-c]benzo[a]anthracene-10-bromo-4-methyl-4*H*-7-thia-4-aza-3,12-dione (32) by photolysis of (10) (LG^- = Cl^-). A 25 mL solution comprised of 0.010 M of **10** (LG^- = Cl^-) in N_2 saturated 20% H_2O in CH_3CN containing 100 mM phosphate buffer at pH 7 was irradiated with a 450 W Hanovia medium pressure mercury lamp with Pyrex filter for 60 min. The photoproduct was isolated by filtration and washed with H_2O, washed with a small amount of $CHCl_3$, and dried under vacuum. Photoproduct **32** was a yellow powder, mp >300 °C. Found: C, 55.69; H, 2.72; N, 2.53%; calcd for $C_{25}H_{14}NO_4S_2Br$: C, 55.97; H, 2.61; N, 2.61%; ^{1}H-NMR (400 MHz, DMSO-d_6): 3.87 (3H, s), 3.92 (3H, s), 7.66 (1H, d, J = 8.7 Hz), 7.83 (1H, d, J = 8.7 Hz), 7.93 (1H, d, J = 8.7 Hz), 7.99 (1H, d, J = 8.7 Hz), 8.05 (1H, d, J = 8.7 Hz), 8.14 (1H, s), 8.16 (1H, d, J = 8.7 Hz), 8.80 (1H, s); The ^{13}C-NMR (100 MHz, DMSO-d_6) could not be obtained due to low solubility.

General procedure for product quantum yield

determinations. A semi-micro optical bench was used for quantum yield determinations, similar to the apparatus described by Zimmerman.[32] Light from a 200 W high-pressure mercury lamp was passed through an Oriel monochromator, which was set to 390 nm wavelengths. The light was collimated through a lens. A fraction of the light was diverted 90° by a beam splitter to a 10 x 3.6 cm side quartz cylindrical cell containing an actinometer. The photolysate was contained in a 10 x 1.8 cm quartz cylindrical cell of 25 mL volume. The concentrations of the reactants were 0.0018-0.0030 M. All quantum yields reported herein were the average of two or more independent runs. Behind the photolysate was mounted a quartz cylindrical cell containing 25 mL of actinometer. Light output was monitored by ferrioxalate actinometery using the splitting ratio technique.

For **7** ($LG^- = Cl^-$), **8** ($LG^- = Cl^-$), and **10** ($LG^- = Cl^-$) 50 mL of water was added to the photolysate, and the diluted photolysate was extracted four times with 30 mL of CH_2Cl_2. The combined extracts were washed twice with 30 mL water, brine, and concentrated in vacuo. The residue was dissolved in d_6-DMSO. DMF was added as a standard for NMR analyses (vide infra). However, for **7** ($LG^- = Cl^-$) the NMR solvent was $CDCl_3$ and the NMR standard was DMSO.

For **9** ($LG^- = Cl^-$, PhS^-, HS^-, $PhCH_2S^-$) the photolysate was adjusted to pH 2 by addition of 3 N HCl. The resultant precipitate was collected by suction filtration and washed with 50 mL water. The precipitate was transferred to a flask, and any untransferred precipitate was dissolved in DMSO and combined with the transferred precipitate. The DMSO was evaporated to dryness under vacuum and DMSO-d_6 was added along with DMF as a standard for NMR analysis.

Products were analyzed by ^{1}H NMR spectroscopy using DMF or DMSO as the internal standard and conversions were 12-16%. At the concentrations used most of the incident light would have been absorbed near the front face of the photolysis cell, raising the concern that the photoproducts formed during the photolyses could competitively absorb the incident light, reducing the light absorbed by the reactants. This internal filter effect would depress the observed Φ values below the actual values. In the case of **8** ($LG^- = Cl^-$) the Φ was thus redetermined at an 18-fold lower concentration of 1.0×10^{-4} M of reactant and found to be within experimental error of the value obtained at higher concentration at 14% conversions for duplicate runs. Due to the very low concentrations of the photoproduct **26** formed, it had to be quantified by absorption spectroscopy of the exposed photolysates without any workup. The product absorption at 432 nm was deconvoluted from the tailing absorption of reactant using Origin 8.6 software (OriginLab). After deconvolution, concentrations were obtained from a calibration curve constructed from known mixtures of reactant and product.

Computational methods. Density Functional Theory (DFT) calculations were performed using hybrid version of Perdew, Burke, and Ernzerhof density functional PBE0[33] in combination with a standard double-zeta quality 6-31G(d) basis set.[34] Solvent (water) effects were included using integral equation formalism polarizable continuum model (IEFPCM).[35-37] All calculated structures were tested for wavefunction stability. Geometry optimizations were performed without any geometric restraints followed by harmonic vibrational frequency calculations, and the nature of the transition structures found was verified by following the reaction path using intrinsic reaction coordinate (IRC).[38] Enthalpies and Gibbs free energies were calculated from these frequencies without applying any scaling factors. Only the enthalpies are shown in Figures 3 and 4 (vide supra). All calculations were performed with Gaussian 09 package.[39]

Acknowledgements

The authors thank Dr. Sheng Cai for assistance with the NMR COSY and NOESY experiments and Dr. Sergey Lindemann for the X-ray diffraction studies. This work was supported by the National Science Foundation (MGS, CHE 1055339).

Notes and references

[a] *Department of Chemistry, Marquette University, P.O. Box 1881, Milwaukee, Wisconsin, 53201-1881, USA. Fax: (+1) 414 288 7066; Tel: (+1) 414 288 3535; E-mail:mark.steinmetz@marquette.edu.* [b]*Department of Chemistry, Marquette University, P.O. Box 1881, Milwaukee, Wisconsin, 53201-1881, USA. Fax: (+1) 414-288-7066; Tel: (+1) 414-288-5779; E-mail:qadir.timerghazin@marquette.edu.*

† Electronic Supplementary Information (ESI) available: ^{1}H NMR COSY for **26**, and **27**. 1H NMR NOESY for **27**. X-diffraction data for **30**. Comparison ^{1}H NMR between **27** and **30**. ^{1}H NMR for a mixture of **30** and **31**. ^{1}H NMR and ^{13}C NMR spectra of all synthesized compound. Stern-Volmer quenching **8** ($LG^- = Cl^-$) by piperylene. Computed structures in Figures 3 and 4. See DOI: 10.1039/b000000x/

1 H.-M. Lee, D.R. Larson and D.S. Lawrence, Illuminating the chemistry of life: design, synthesis, and applications of "caged" and related photoresponsive compounds, *ACS Chem. Biol.* 2009, **4**, 409-427 and references cited therein.

2 G. Mayer and A. Heckel, Biologically active Molecules with a light switch, *Angew. Chem. Int. Ed.* 2006, **45**, 4900-4921.

3 D. Warther, S. Gug, A. Specht, F. Bolze, J.-F. Nicoud, A. Mourot, M. Goeldner, Two-photon uncaging: new prospects in neuroscience and cellular biology, *Biorg. Med. Chem.* 2010, **18**, 7753-7758.

4 M. Sarker, T. Shahrin and M.G. Steinmetz, Photochemical eliminations involving zwitterionic intermediates generated via electrocyclic ring closure of benzothiophene carboxanilides, *Org. Lett.* 2011, **13**, 872-875.

5 (a) The nitrobenzyl group has been used as a photoremovable protecting group for sulfhydryl groups.[5b,c] It should be noted that the expected byproduct upon photochemical release of thiol is a nitrosoarene, and in general, nitrosoarenes undergo chemical reduction by thiols.[6] (b) C.-Y. Chang, T. T. Fernandez, R. Panchal and H. Bayley, Caged catalytic subunit of cAMP-dependent protein kinase, *J. Am. Chem. Soc.* 1998, **120**, 7661-7662. (c) H. Bayley, C.-Y. Chang, W.T. Miller, B. Niblack and P. Pan, Caged peptides and proteins by targeted chemical modification, in *Methods in Enzymology*, 1998, **291**, 117-135.

6 S. Montanari, C. Paradisi and G. Scorrano, Pathways of nitrosobenzene reduction by thiols in alcoholic media, *J. Org. Chem.* 1999, **64**, 3422-3428.

7 A. Specht, S. Loudwig, L. Peng and M. Goeldner, *p*-Hydroxyphenacyl bromide as a photoremovable thiol label: a potential phototrigger for thiol-containing biomolecules, *Tetrahedron Lett.* 2002, **43**, 8947-8950.

8 J.W. Walker, S.H. Gilbert, R.M. Drummond, M. Yamada, R. Sreekumar, R.E. Carraway, M. Ikebe and F. S. Fay, Signaling pathways underlying eosinophil cell motility revealed by using caged peptides", *Proc. Natl. Acad. Sci USA*, 1998, **95**, 1568-1573.

9 (a) H. Kimura, Hydrogen sulfide: its production, release, and functions, *Amino Acids*, 2011, **41**, 113-121. (b) M.M. Gadalla and S.H. Snyder, Hydrogen sulfide as a gasotransmitter, *J. Neurochem.* 2010, **113**, 14-26.

10 J. K. Moon, J. W. Park, W. S. Lee, Y. J. Kang, H. A. Chung, M. S. Shin, and Y. J. Yoon, Synthesis of Some 2-Substituted-thioxanthones, *J. Heterocyclic Chem.* 1999, **36**, 793-798.

11 W. B. Wright and H. J. Brabander, The Preparation of 3-Chlorobenzo[b] thiophene Derivatives from Cinnamic Acids, *J. Heterocyclic Chem*. 1971, **8**, 711-714.

12 Z. Pechlivanidis, H. Hopf and L. Ernst, Paracyclophanes: Extending the Bridges. Synthesis, *Eur. J. Org. Chem.* 2009, 223-237.

13 R. A. Delden, J.H. Hurenkamp and B.L. Feringa, Photochemical and Thermal Isomerization Processes of a Chiral Auxiliary Based Donor – Acceptor Substituted Chiroptical Molecular Switch: Convergent Synthesis, Improved Resolution and Switching Properties, *Chem. Eur. J*. 2003, **9**, 2845-2853.

14 M. G. Neumann, M. H. Gehlen, M. V. Encinas, N. S. Allen, T. Corrales, C. Peinado and F. Catalina, Photophysics and Photoreactivity of Substituted Thioxanthones, *J. Chem. Soc., Faraday Transactions,* 1997, **93**, 1517-1521.

15 Y. Ilichev, M.A. Schworer and J. Wirz, Photochemical reaction mechanisms of 2-nitrobenzyl compounds: methyl ethers and caged ATP, *J. Am. Chem. Soc.* 2004, **126**, 4581-4595.

16 J. W. Walker, H. Martin, F.R. Schmitt, and R.J. Barsotti, Rapid release of an α-adrenergic receptor ligand from photolabile analogues, *Biochemistry*, 1993, **32**, 1338-1345.

17 K. Stensrud, J. Noh, K. Kandler, J. Wirz, D. Heger, and R.S. Givens, Competing pathways in the photo-Favorskii rearrangement and release of esters: studies on fluorinated *p*-hydroxyphenacyl-caged GABA and glutamate phototriggers, *J. Org. Chem.* 2009, **74**, 5219-5227.

18 R.S. Givens, J.F.W. Weber, A.H. Jung and C.-H. Park, New photoprotecting groups: desyl and *p*-hydroxyphenacyl phosphate and carboxylate esters, *Methods in Enzymology*, 1998, **120**, 1-29.

19 V. Hagen, J. Bendig, S. Frings, T. Eckardt, S. Helm, D. Reuter and U.B. Kaupp, Highly efficient and ultrafast phototriggers for cAMP and cGMP by using long-wavelength UV/Vis-activation, *Angew. Chem. Int. Ed.* 2001, **40**, 1045-1048.

20 T. Furuta, S. S.-H. Wang, J.L. Dantzker, T.M. Dore, W.J. Bybee, E.M. Callaway, W. Denk and R.Y. Tsien, *Proc. Natl. Acad. Sci, USA*, 1999, **96**, 1193-1200.

21 M.J. Davis, C.H. Kragor, K.G. Reddie, H.C. Wilson, Y.Zue and T.M. Dore, Substituent effects on the sensitivity of a quinoline photoremovable protecting group to one- and two-photon excitation, *J. Org. Chem.* 2009, **74**, 1721-1729.

22 (a) A. V. Pinheiro, A.J. Parola, P.V. Baptista, and J.C. Lima, pH Effect on the photochemistry of 4-methylcoumarin phosphate esters: caged-phosphate case study. *J. Phys. Chem. A.* 2010, **114**, 12795-12803. (b) R. Schmidt, D. Geissler, V. Hagen, and J. Bendig, Mechanism of photocleavage of (coumarin-4-yl)methyl esters, *J. Chem. Phys.* 2007, **111**, 5768-5774.

23 V. San Miguel, C.G. Bochet, and A. del Campo, Wavelength-selective caged surfaces: how many functional levels are possible? *J. Am. Chem. Soc.* 2011, **133**, 5380-5388.

24 For a review of two-photon uncaging, see H. Kasai, M. Matsuzaki, and G.C.R. Ellis-Davies, Two-Photon Uncaging Microscopy, in *Imaging in Neuroscience and Development*, ed. R. Yuste and A. Konnerth, Cold Spring Harbor, New York, 2005, pp 275-383.

25 (a) With arylthiols efficient quenching[23a] of benzophenone by hydrogen transfer results in thiyl and ketyl radicals,[23b] which regenerate starting materials by disproportionation more rapidly than homocoupling to pinacol and disulfide.[23a-d] With mesitylmercaptan and benzophenone a quantum yield of 0.1 has been reported for disulfide formation.[23c] We did not observe disulfide or pinacol products in our study. A computational study indicates that such disporportionation will be facile.[23d] An alternate mechanism for quenching is electron transfer and rapid back electron transfer, which may be more important for alkylthiols than arylthiols[23b] (a) J. B. Guttenplan and S.G. Cohen, Quenching and reduction of photoexcited benzophenone by thioethers and mercaptans, *J. Org. Chem.* 1973, **38**, 2001-2007. (b) S. Inbar, H. Linschitz, and S. G. Cohen, Quenching and radical formation in the reaction of photoexcited benzophenone with thiols and thioethers (sulfides). Nanosecond flash studies. *J. Am. Chem. Soc.* 1982, **104**, 1679-1682. (c) S.G. Cohen, A.W. Rose, P.G. Stone, A. Ehret, Competitive processes in retardation by mercaptans of photoreduction by alcohols, *J. Am. Chem. Soc.* 1979, **101**, 1827-1832. (d) H. Cardy, E. Poquet, M. Chaillet, and J. Ollivier, Ab intio CI study of hydrogen abstraction from hydrogen and methyl sulphide by ketone triplet excited state, *Chem. Phys.* 1993, 79-90.

26 J. Beltowski, Hypoxia in the renal medulla: implications for H_2S signaling, *J. Pharmacol. Exp. Therapeutics*, 2010, **334**, 358-363.

27 H. Zhao, H. Wang and M. Xian, Cysteine-activated hydrogen sulfide (H_2S) donors, *J. Am. Chem. Soc.* 2011, **133**, 15-17.

28 (a) O. Rubio-Pons, L. Serrano-Andres, D. Burget and P. Jacques, A butterfly like motion as a clue to the photophysics of thioxanthone. *J. Photochem. Photobiol. A: Chem.* 2006, **179**, 298-304. (b) X. Allonas, C. Ley, C. Bibaut, P. Jacques and J.P. Fouassier, Investigation of the triplet quantum yield of thioxanthone by time-resolved thermal lens spectroscopy: solvent and population lens effects, *Chem. Phys. Lett.* 2000, **322**, 483-490.

29 (a) J. Seixas de Melo, L.M. Rodrigues, C. Serpa, L.G. Arnaut, I.C.F.R. Ferreira and M.-J. R. P. Queiroz, Photochemistry and Photophysics of Thienocarbazoles, *Photochem. Photobiol.* 2003, **77**, 121-128. (b) B. Wex, B. R. Kaafarani, E. O. Danilov and D. C. Neckers, Altering the emission behavior with the turn of a thiophene ring: the photophysics of condensed ring systems of alternating benzenes and thiophenes, *J. Phys. Chem. A.* 2006, **110**, 13754-13758.

30 C. Ma, M.G. Steinmetz, E.J. Kopatz, and R. Rathore, Photochemical cleavage and release of carboxylic acids from α–keto amides, *J. Org. Chem.* 2005, **70**, 4431-4442.

31 C. Ma, Y. Chen, and M.G. Steinmetz, Photochemical cleavage and release of para-substituted phenols from α–keto amides. *J. Org. Chem.* 2006, **71**, 4206-4215.

32 H. E. Zimmerman, Apparatus for quantitative and preparative photolysis. The Wisconsin black box, *Mol. Photochem*., 1971, **3**, 281-92.

33 J. P. Perdew, K. Burke, and M. Ernzerhof, Generalized gradient approximation made simple, *Phys. Rev. Lett.* 1996, **77**, 3865-3868 .

34 W.J. Hehre, L. Radom, P.v.R. Schleyer, J.A. Pople, Ab Initio Molecular Orbital Theory, John Wiley and Sons, New York, 1985

35 G. Scalmani and M. J. Frisch, Continuous surface charge polarizable continuum models of solvation. I. General formalism, *J. Chem. Phys*., 2010, **132**, 114110

36 J. Tomasi, B. Mennucci, and R. Cammi, Quantum mechanical continuum solvation models, *Chem. Rev.*, 2005, **105**, 2999

37 J. Tomasi, B. Mennucci, and E. Cancès, The IEF version of the PCM solvation method: An overview of a new method addressed to study molecular solutes at the QM ab initio level, *J. Mol. Struct. (Theochem)*, 1999, **464**, 211

38 K. Fukui, The path of chemical reactions-the IRC approach, *Acc. Chem. Res.* 1981, **14**, 363–368.

39 M. J. Frisch, G. W. Trucks, H. B. Schlegel, G. E. Scuseria, M. A. Robb, J. R. Cheeseman, G. Scalmani, V. Barone, B. Mennucci, G. A. Petersson, H. Nakatsuji, M. Caricato, X. Li, H. P. Hratchian, A. F. Izmaylov, J. Bloino, G. Zheng, J. L. Sonnenberg, M. Hada, M. Ehara, K. Toyota, R. Fukuda, J. Hasegawa, M. Ishida, T. Nakajima, Y. Honda, O. Kitao, H. Nakai, T. Vreven, J. A. Montgomery, Jr., J. E. Peralta, F. Ogliaro, M. Bearpark, J. J. Heyd, E. Brothers, K. N. Kudin, V. N. Staroverov, R. Kobayashi, J. Normand, K. Raghavachari, A. Rendell, J. C. Burant, S. S. Iyengar, J. Tomasi, M. Cossi, N. Rega, J. M. Millam, M. Klene, J. E. Knox, J. B. Cross, V. Bakken, C. Adamo, J. Jaramillo, R. Gomperts, R. E. Stratmann, O. Yazyev, A. J. Austin, R. Cammi, C. Pomelli, J. W. Ochterski, R. L. Martin, K. Morokuma, V. G. Zakrzewski, G. A. Voth, P. Salvador, J. J. Dannenberg, S. Dapprich, A. D. Daniels, O. Farkas, J. B. Foresman, J. V. Ortiz, J. Cioslowski and D. J. Fox, *Gaussian 09, Revision B.01*, Gaussian, Inc., Wallingford CT, 2009

Supporting Information

Photochemical Electrocyclic Ring Closure and Leaving Group Expulsion from *N*-(9-oxothioxanthenyl)benzothiophene Carboxamides.

Majher Sarker, Tasnuva Shahrin, Mark G. Steinmetz, and Qadir Timerghazin**

Department of Chemistry, Marquette University, Milwaukee, Wisconsin 532011881

Mark.steinmetz@marquette.edu, Qadir.timerghazin@marquette.edu

Table of Contents

List of NMR Spectra

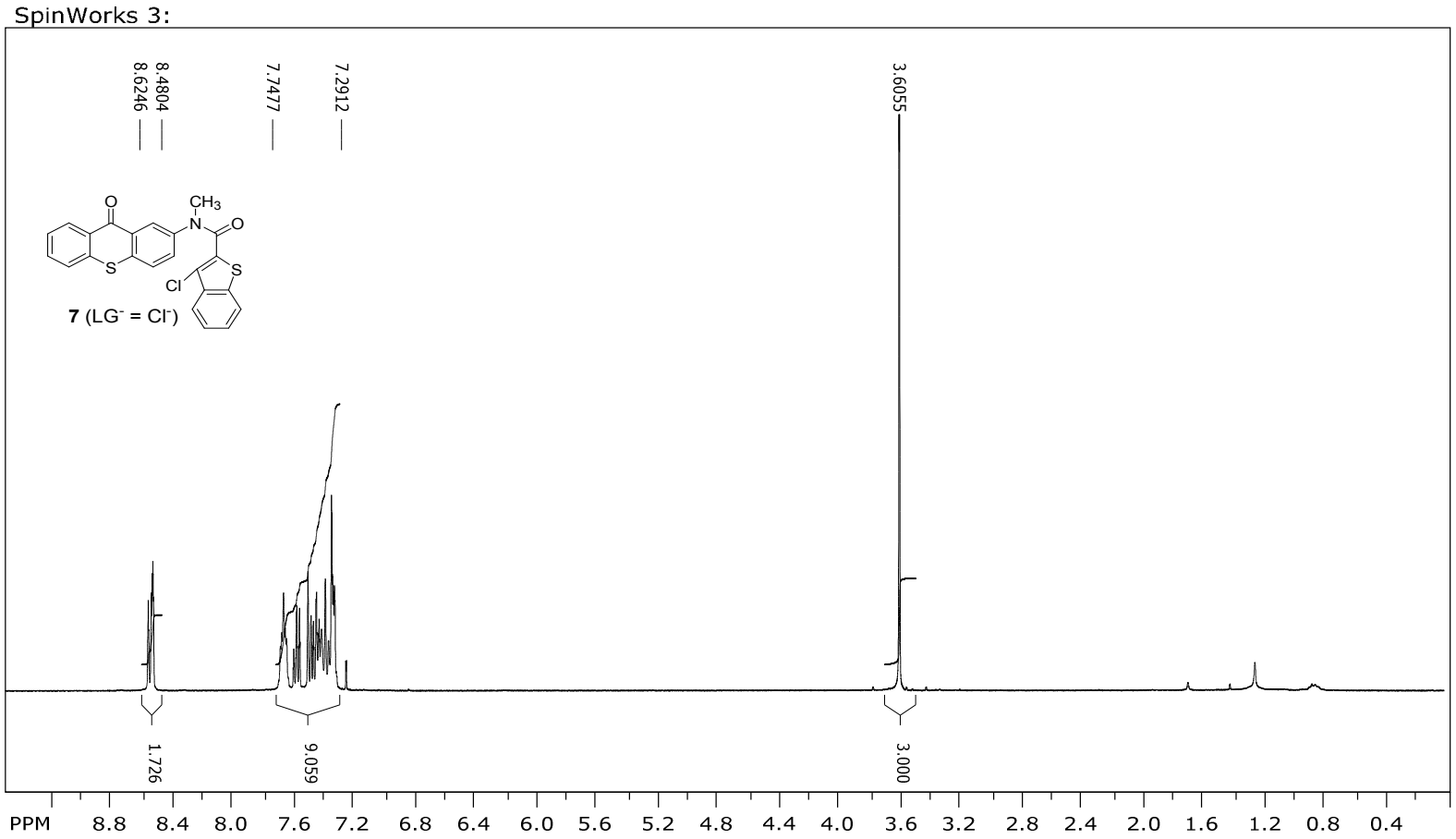

Figure 1. ^{1}H NMR spectrum of 3-Chloro-benzo[b]thiophene-2-carboxylic acid methyl-(9-oxo-9H-thioxanthen-2-yl)-amide[1] (**7**) ($LG^{-} = Cl^{-}$) in $CDCl_3$

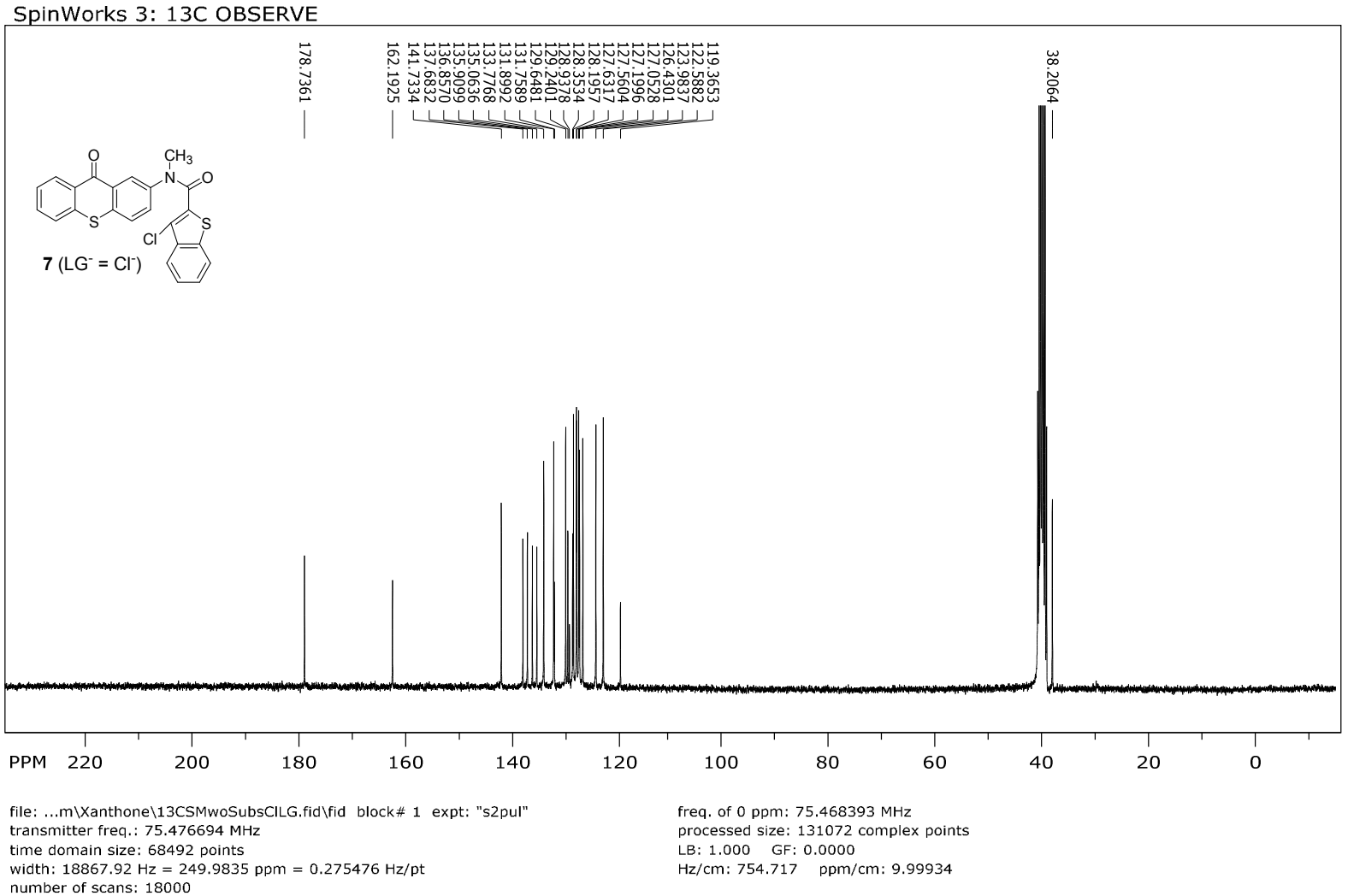

Figure 2. ^{13}C NMR spectrum of 3-Chloro-benzo[b]thiophene-2-carboxylic acid methyl-(9-oxo-9H-thioxanthen-2-yl)-amide[1] (**7**) ($LG^- = Cl^-$) DMSO-d_6

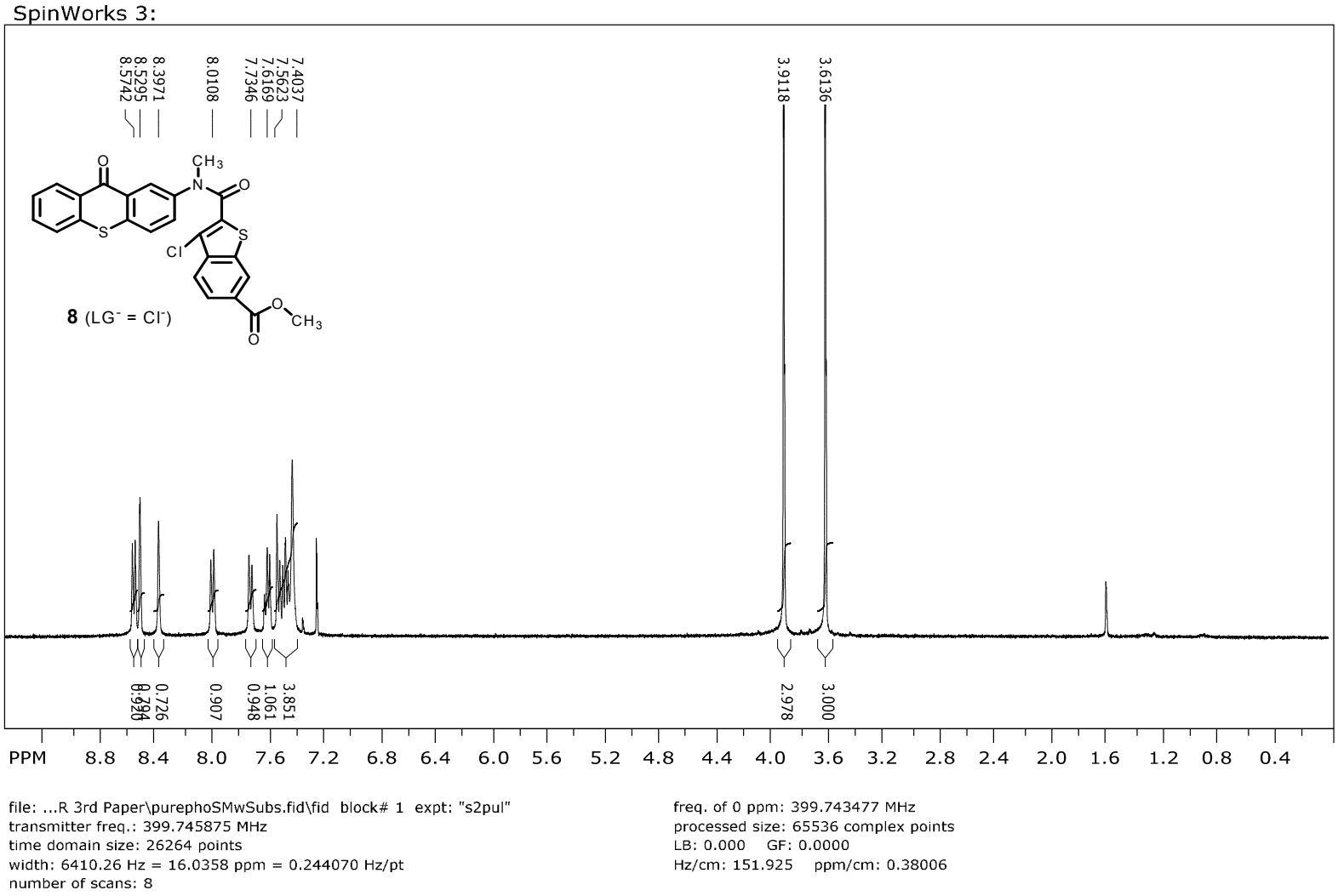

Figure 3, ^{1}H NMR spectrum of 3-Chloro-2-[methyl-(9-oxo-9H-thioxanthen-2-yl)-carbamoyl]-benzo[b]thiophene-6-carboxylic acid methyl ester (**8**) ($LG^{-} = Cl^{-}$) in $CDCl_3$

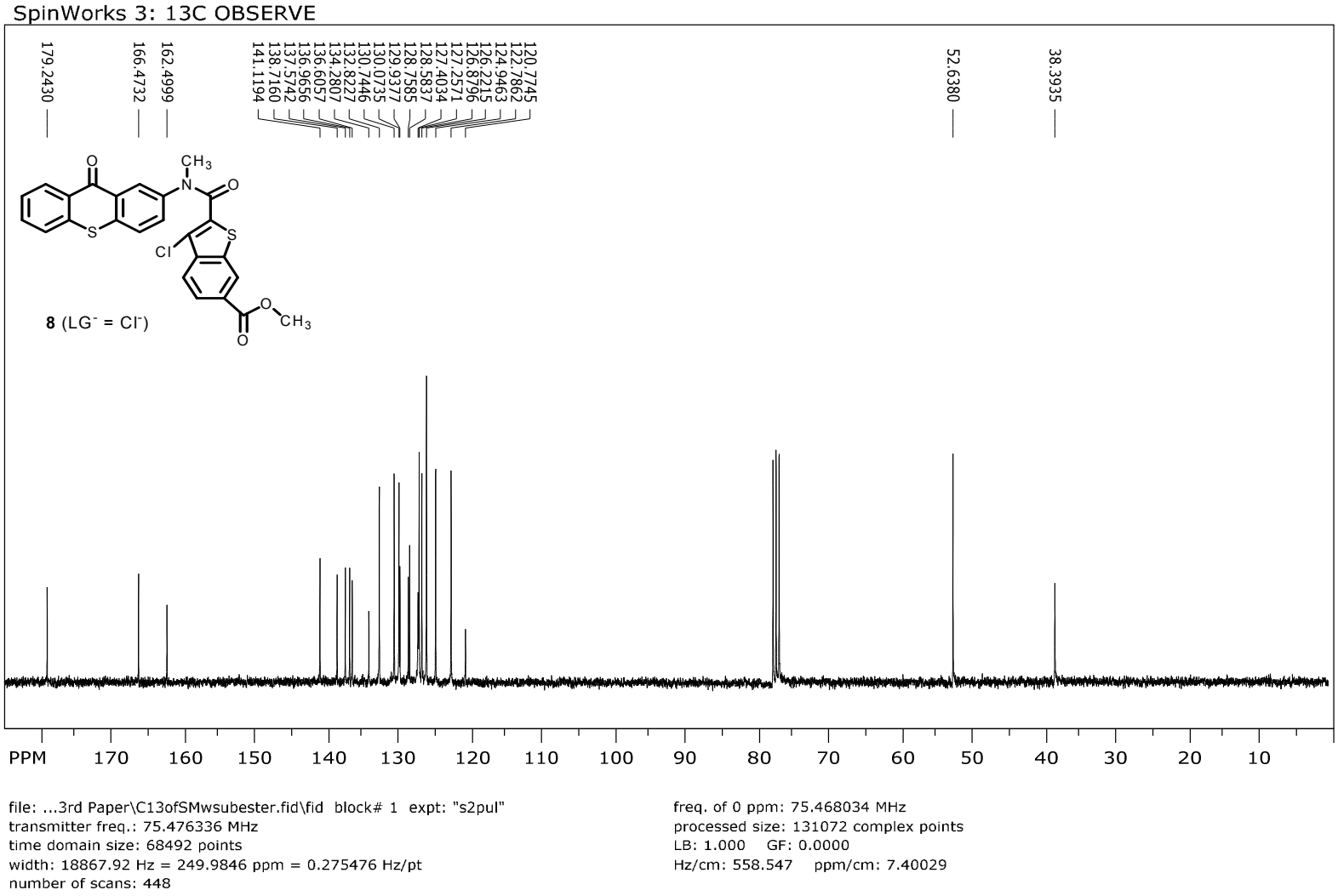

Figure 4, ^{13}C NMR spectrum of 3-Chloro-2-[methyl-(9-oxo-9H-thioxanthen-2-yl)-carbamoyl]-benzo[b]thiophene-6-carboxylic acid methyl ester (**8**) ($LG^- = Cl^-$) in $CDCl_3$

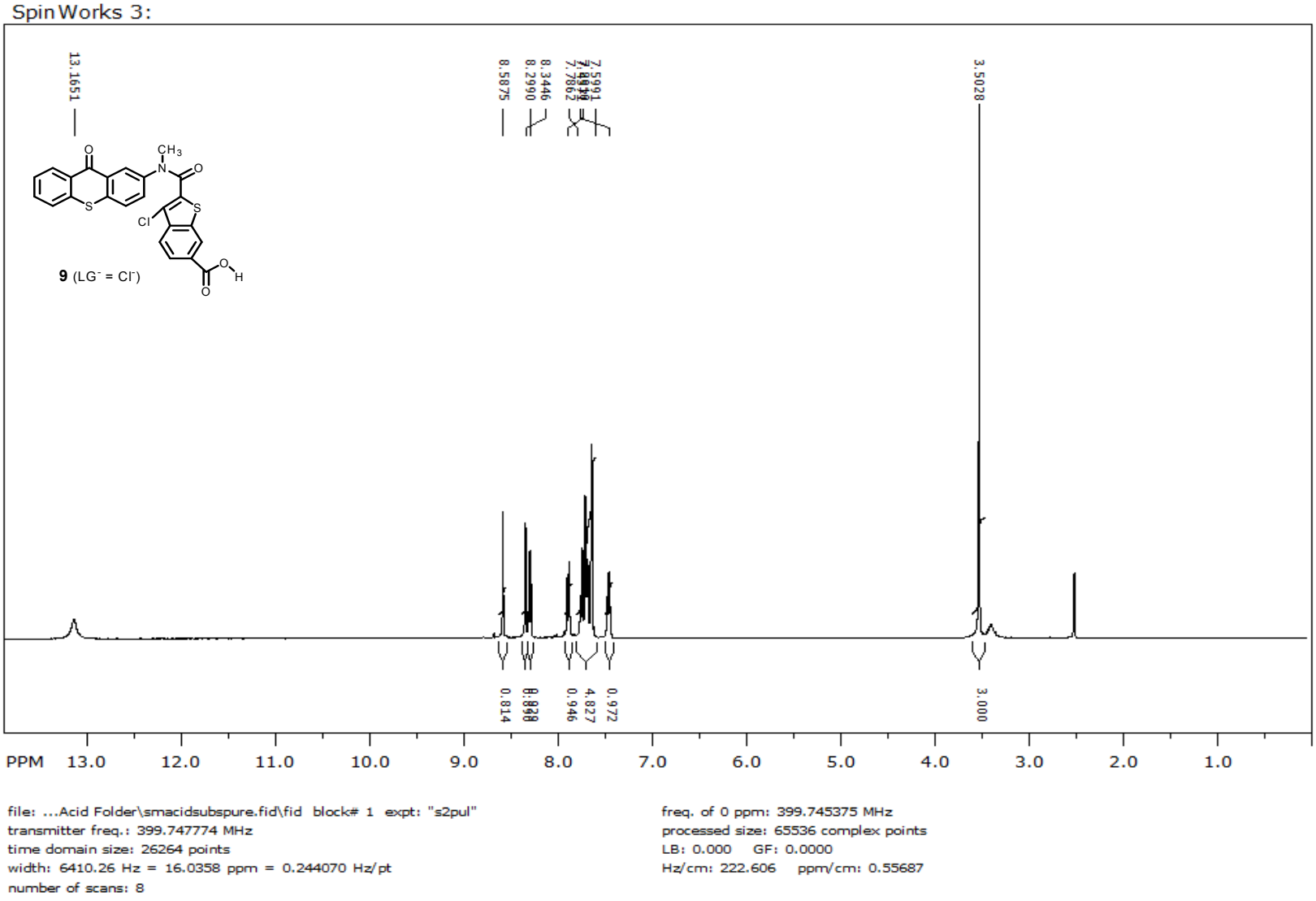

Figure 5, ^{1}H NMR spectrum of 3-Chloro-2-[methyl-(9-oxo-9H-thioxanthen-2-yl)-carbamoyl]-benzo[b]thiophene-6-carboxylic acid (**9**) ($LG^{-} = Cl^{-}$) in DMSO-d_6

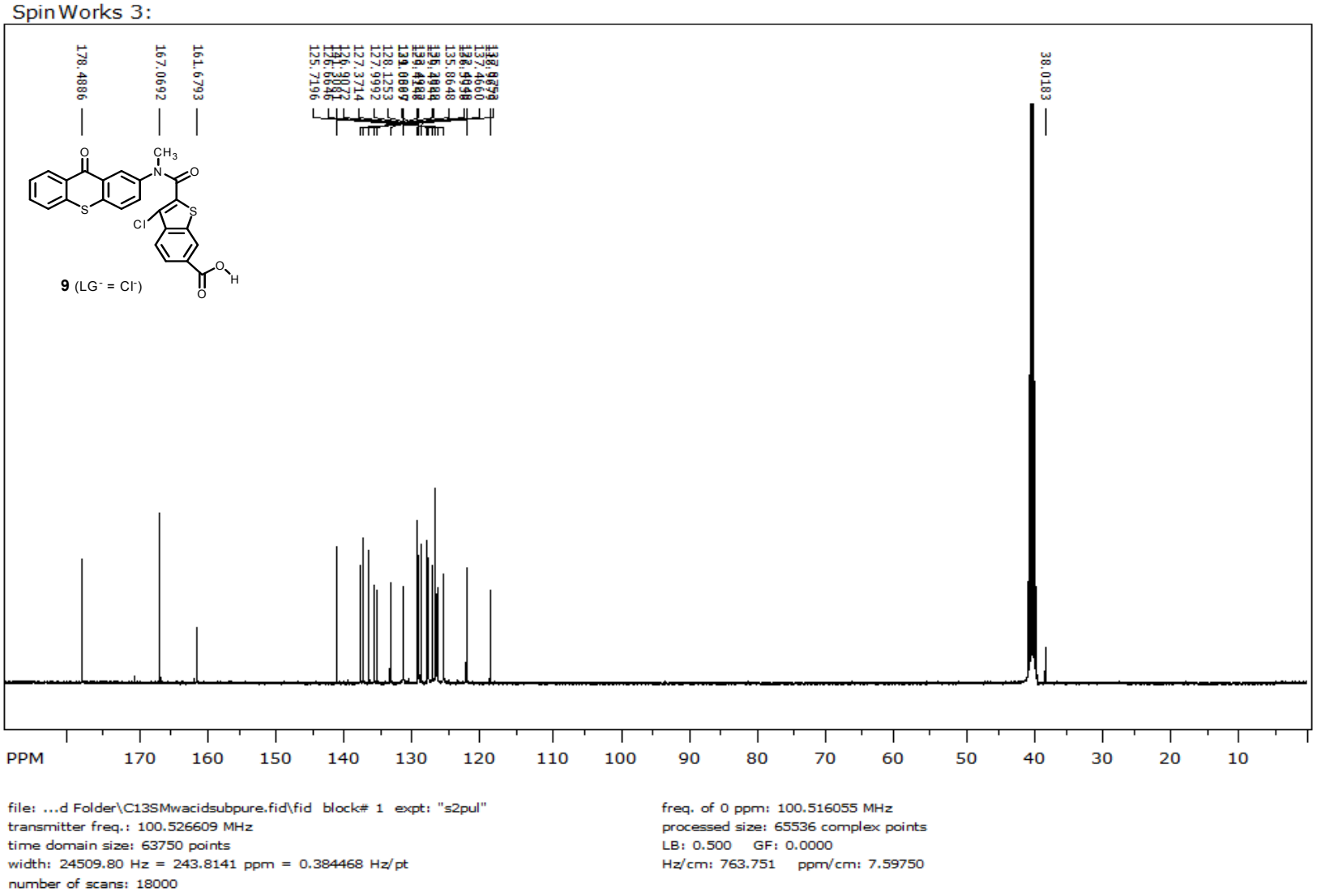

Figure 6, ^{13}C NMR spectrum of 3-Chloro-2-[methyl-(9-oxo-9H-thioxanthen-2-yl)-carbamoyl]-benzo[b]thiophene-6-carboxylic acid (**9**) ($LG^- = Cl^-$) in DMSO-d_6

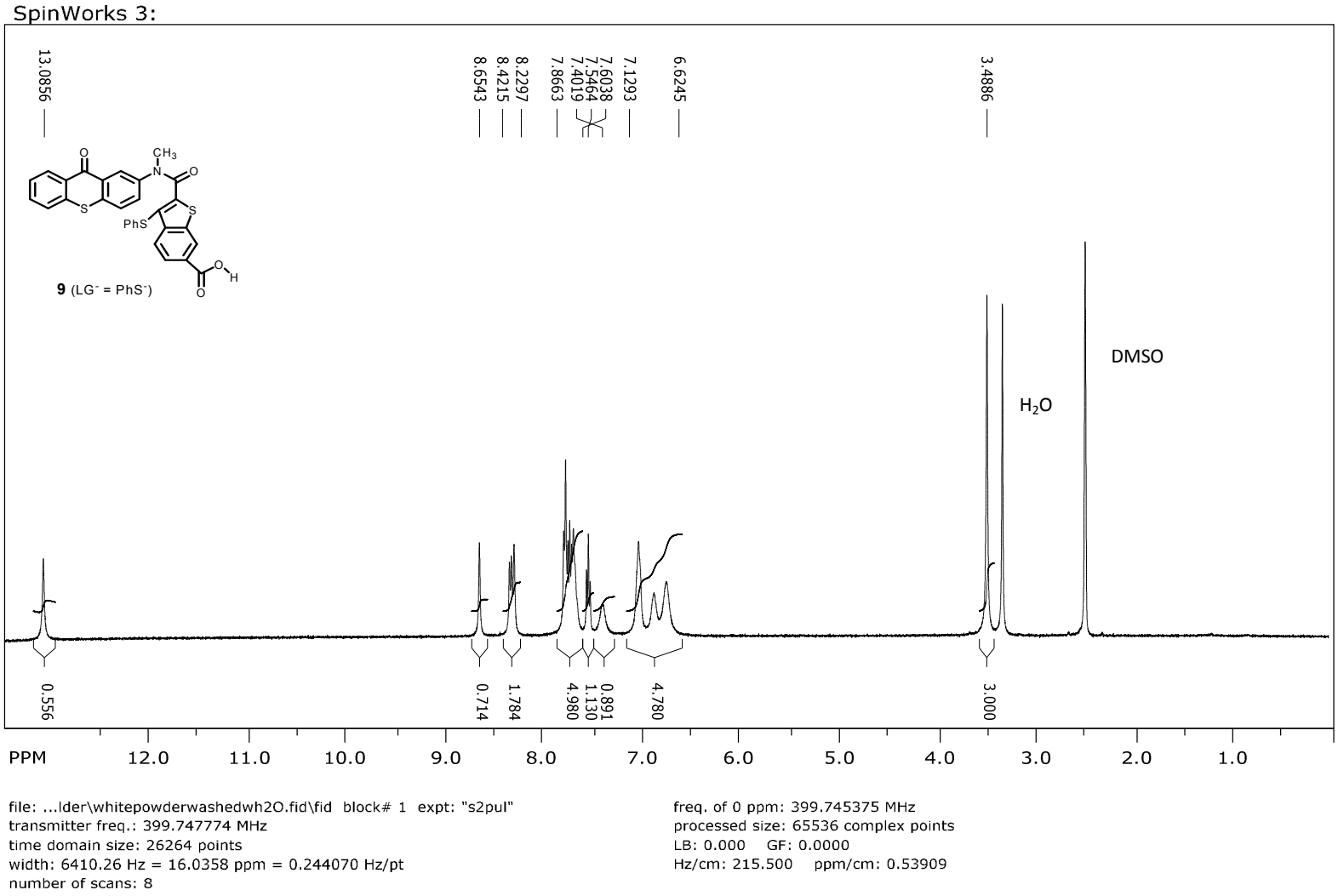

Figure 7, ^{1}H NMR spectrum of 2-[Methyl-(9-oxo-9H-thioxanthen-2-yl)-carbamoyl]-3-phenylsulfanyl-benzo[b]thiophene-6-carboxylic acid (**9**) (LG^{-} = PhS^{-}) in DMSO-d_6

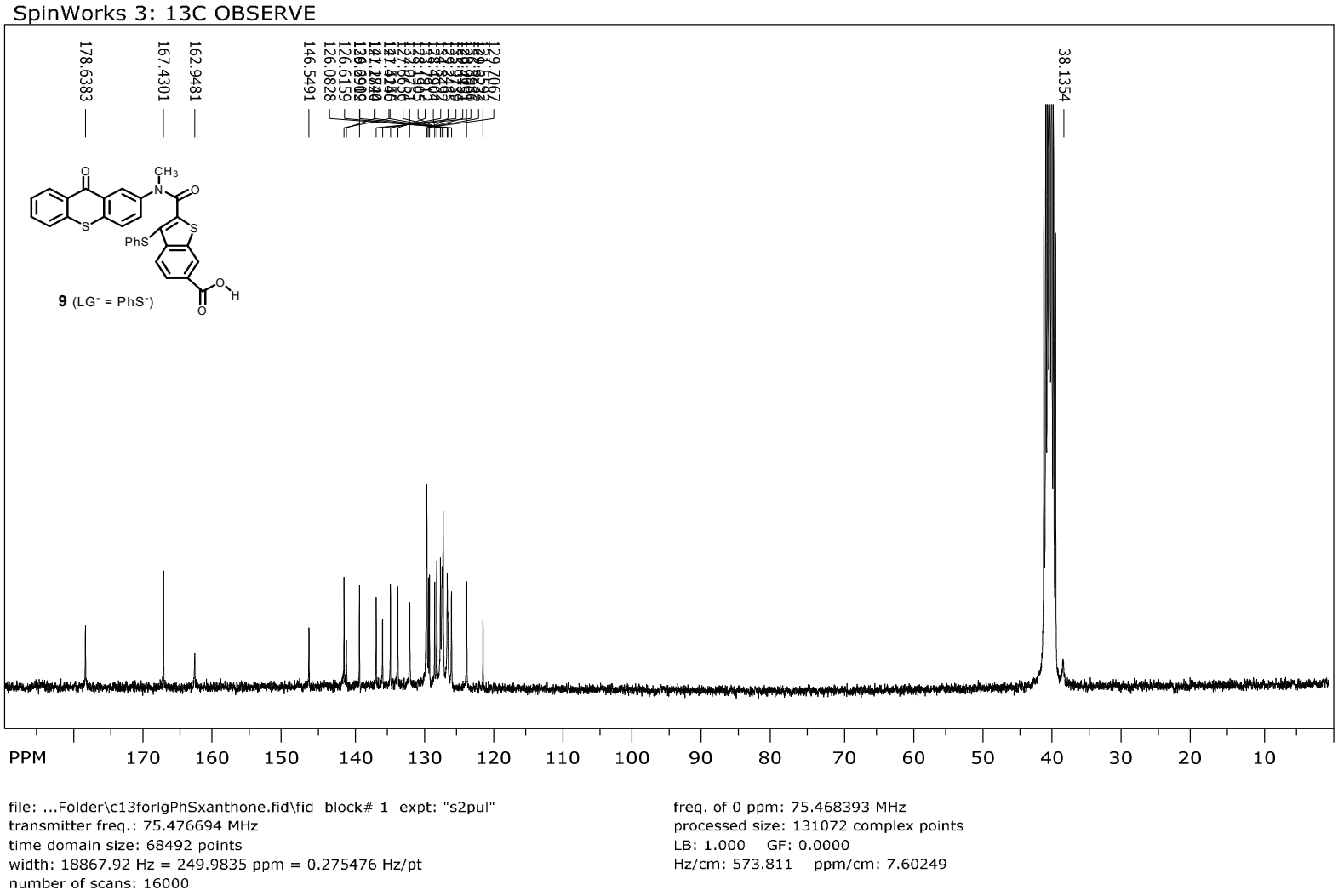

Figure 8, ^{13}C NMR spectrum of 2-[Methyl-(9-oxo-9H-thioxanthen-2-yl)-carbamoyl]-3-phenylsulfanyl-benzo[b]thiophene-6-carboxylic acid (**9**) (LG^- = PhS^-) in DMSO-d_6

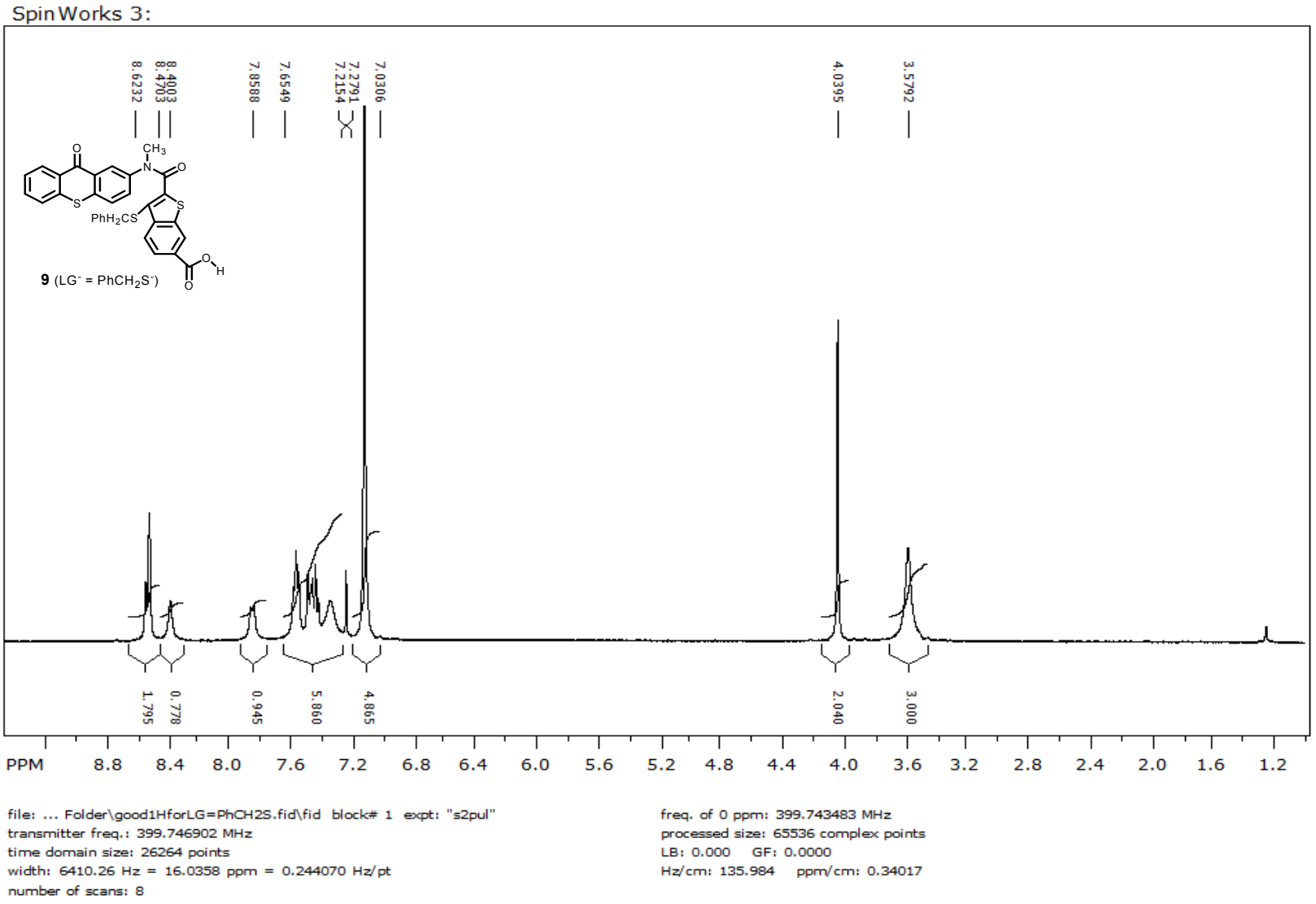

Figure 9, ^{1}H NMR spectrum of 3-Benzylsulfanyl-2-[methyl-(9-oxo-9H-thioxanthen-2-yl)-carbamoyl]-benzo[b]thiophene-6-carboxylic acid (9) (LG^{-} = $PhCH_2S^{-}$) in DMSO-d_6

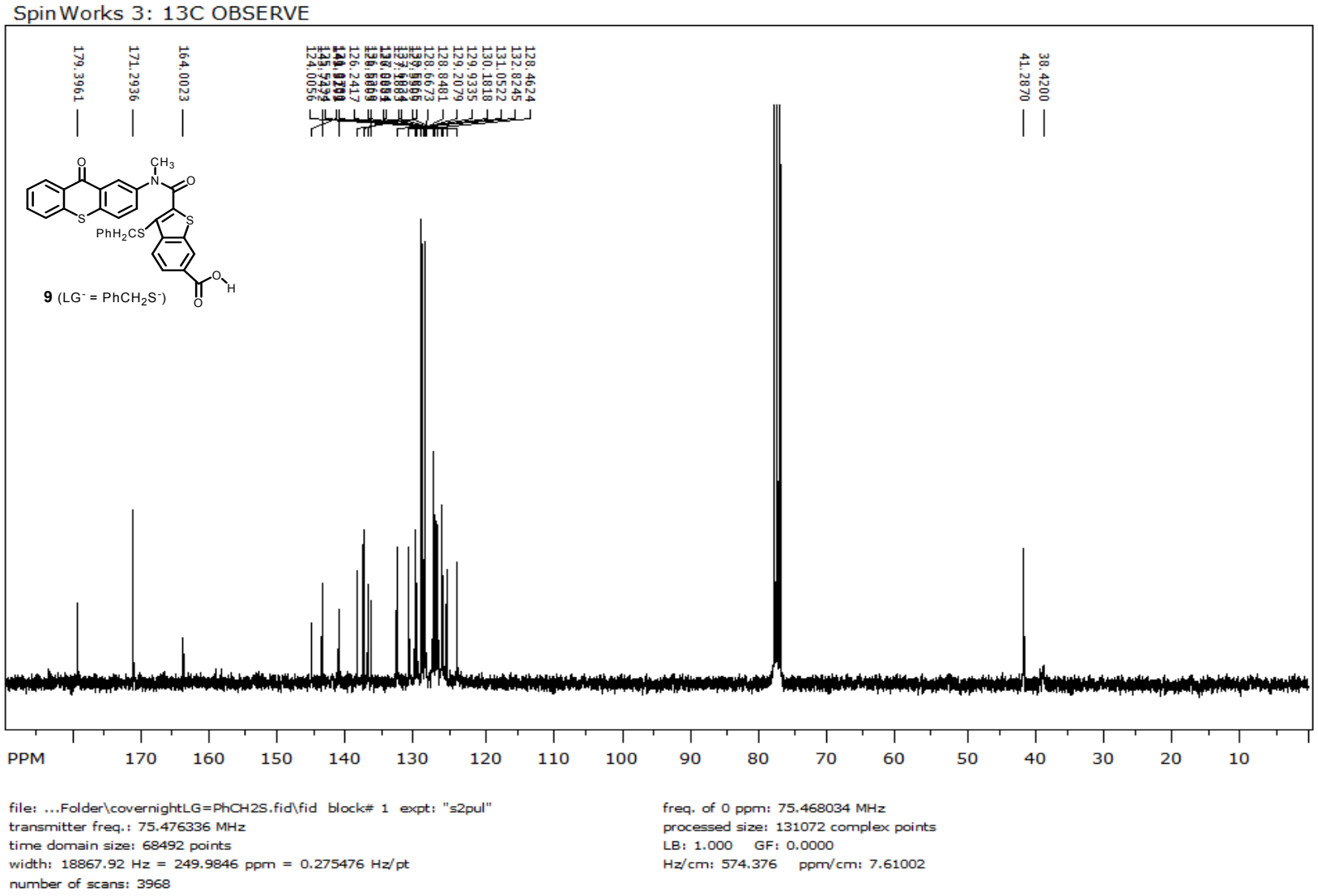

Figure 10, ^{13}C NMR spectrum of 3-Benzylsulfanyl-2-[methyl-(9-oxo-9H-thioxanthen-2-yl)-carbamoyl]-benzo[b]thiophene-6-carboxylic acid (**9**) (LG^- = $PhCH_2S^-$) in DMSO-d_6

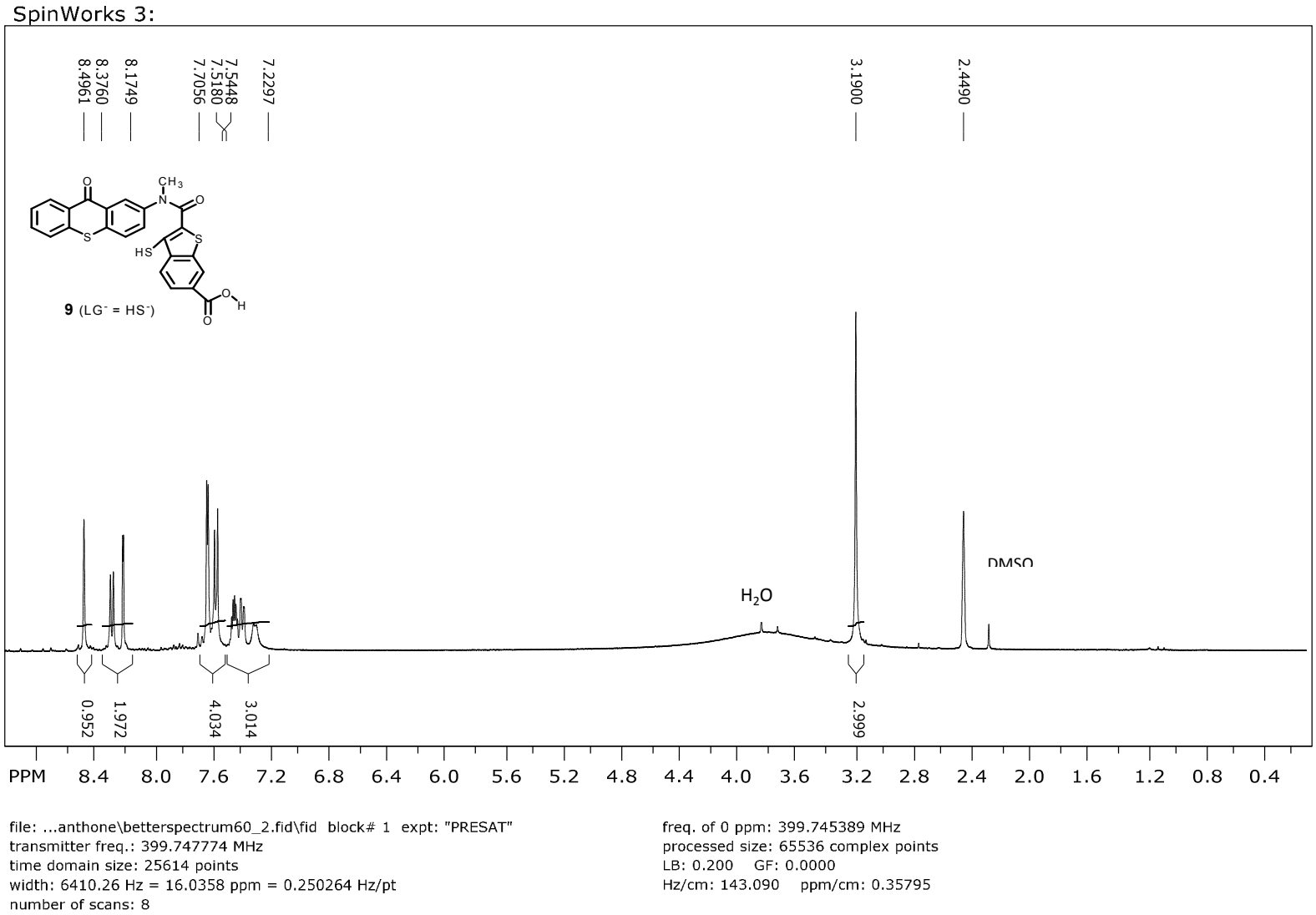

Figure 11, ^{1}H NMR spectrum of 3-Mercapto-2-[methyl-(9-oxo-9H-thioxanthen-2-yl)-carbamoyl]-benzo[b]thiophene-6-carboxylic acid (**9**) ($LG^{-} = HS^{-}$) in DMSO-d_6

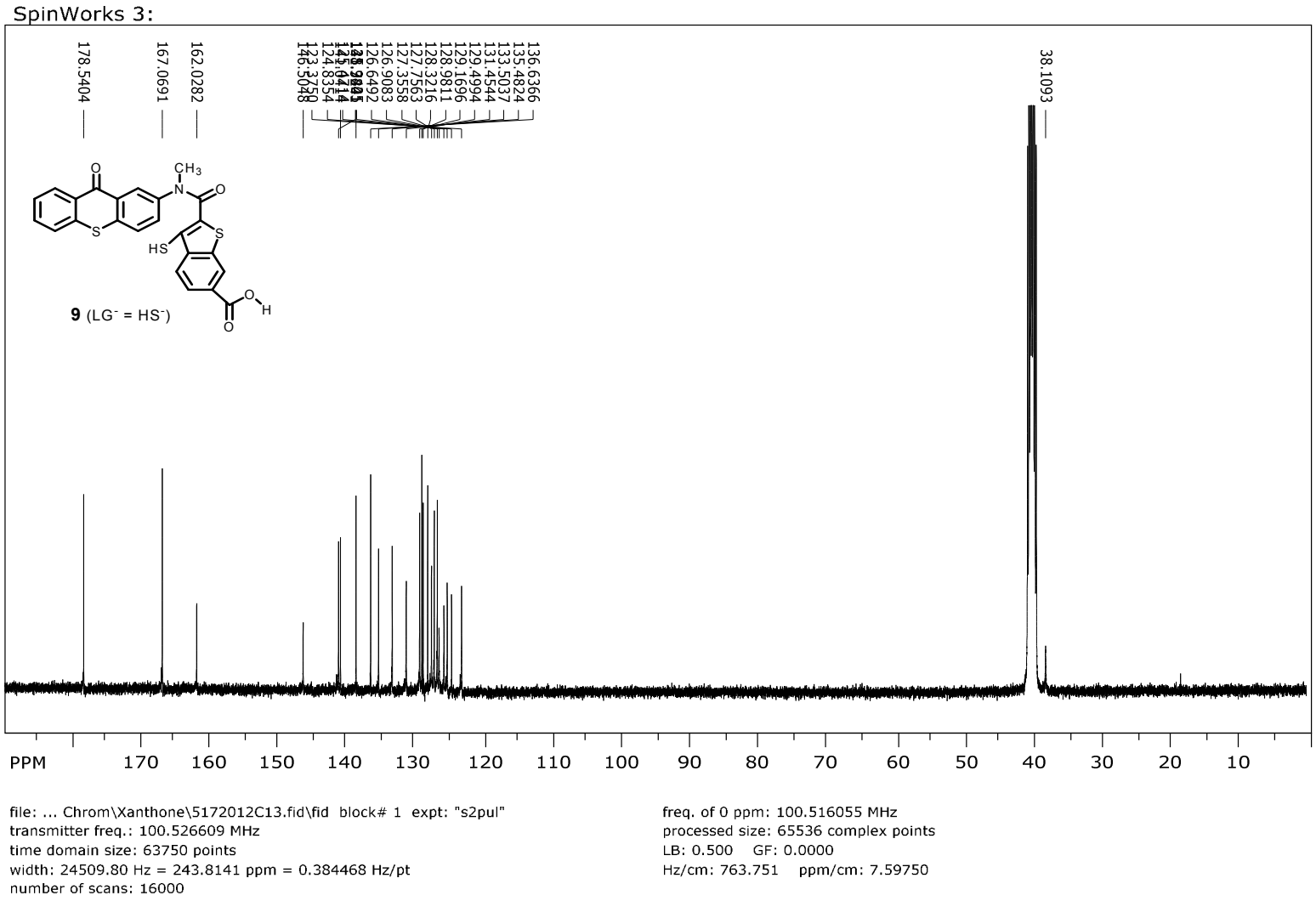

Figure 12, ^{1}3C NMR spectrum of 3-Mercapto-2-[methyl-(9-oxo-9H-thioxanthen-2-yl)-carbamoyl]-benzo[b]thiophene-6-carboxylic acid (**9**) ($LG^{-} = HS^{-}$) in DMSO-d_6

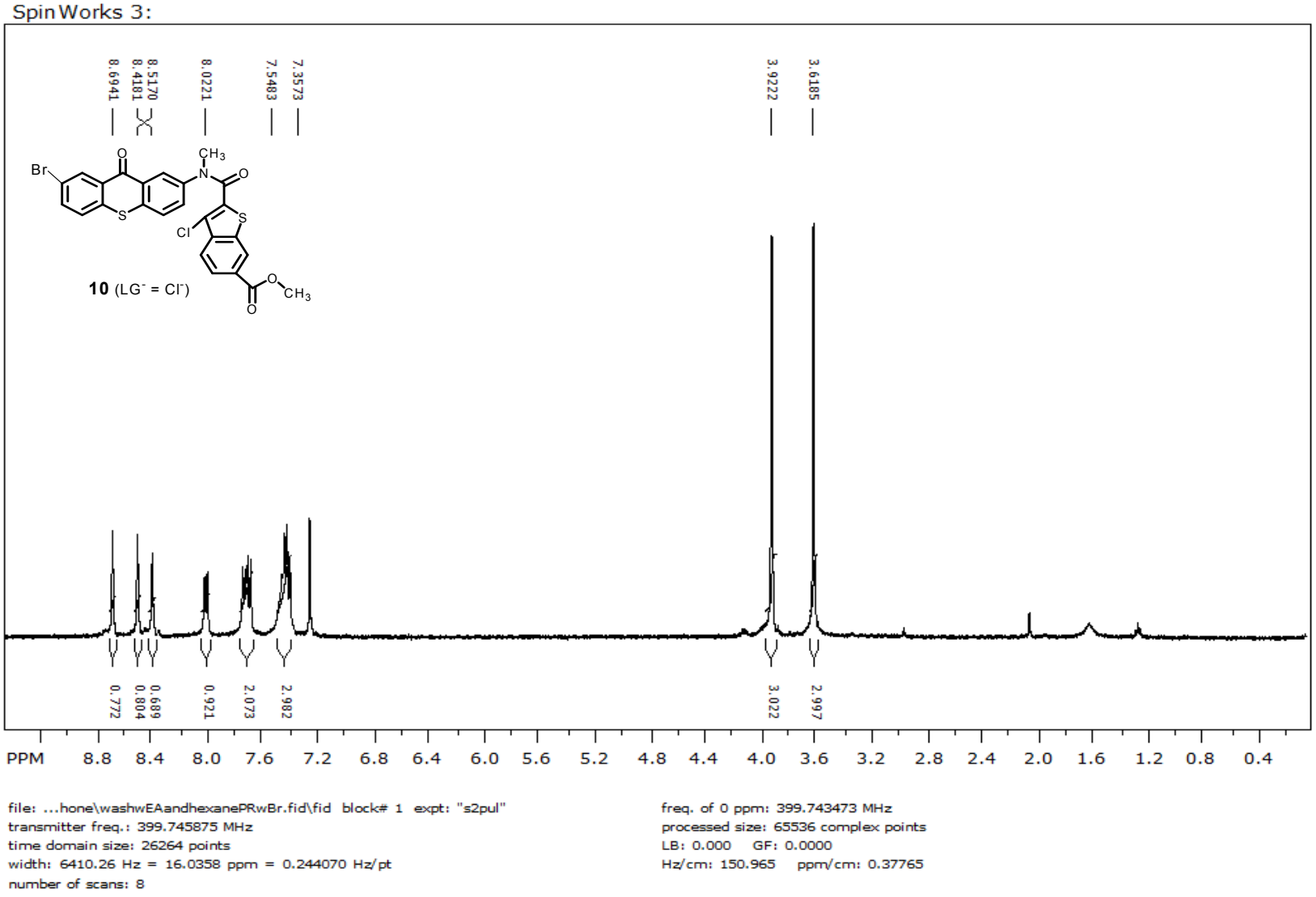

Figure 13, ^{1}H NMR spectrum of 2-[(7-Bromo-9-oxo-9H-thioxanthen-2-yl)-methyl-carbamoyl]-3-chloro-benzo[b]thiophene-6-carboxylic acid methyl ester (**10**) ($LG^{-} = Cl^{-}$) in $CDCl_3$

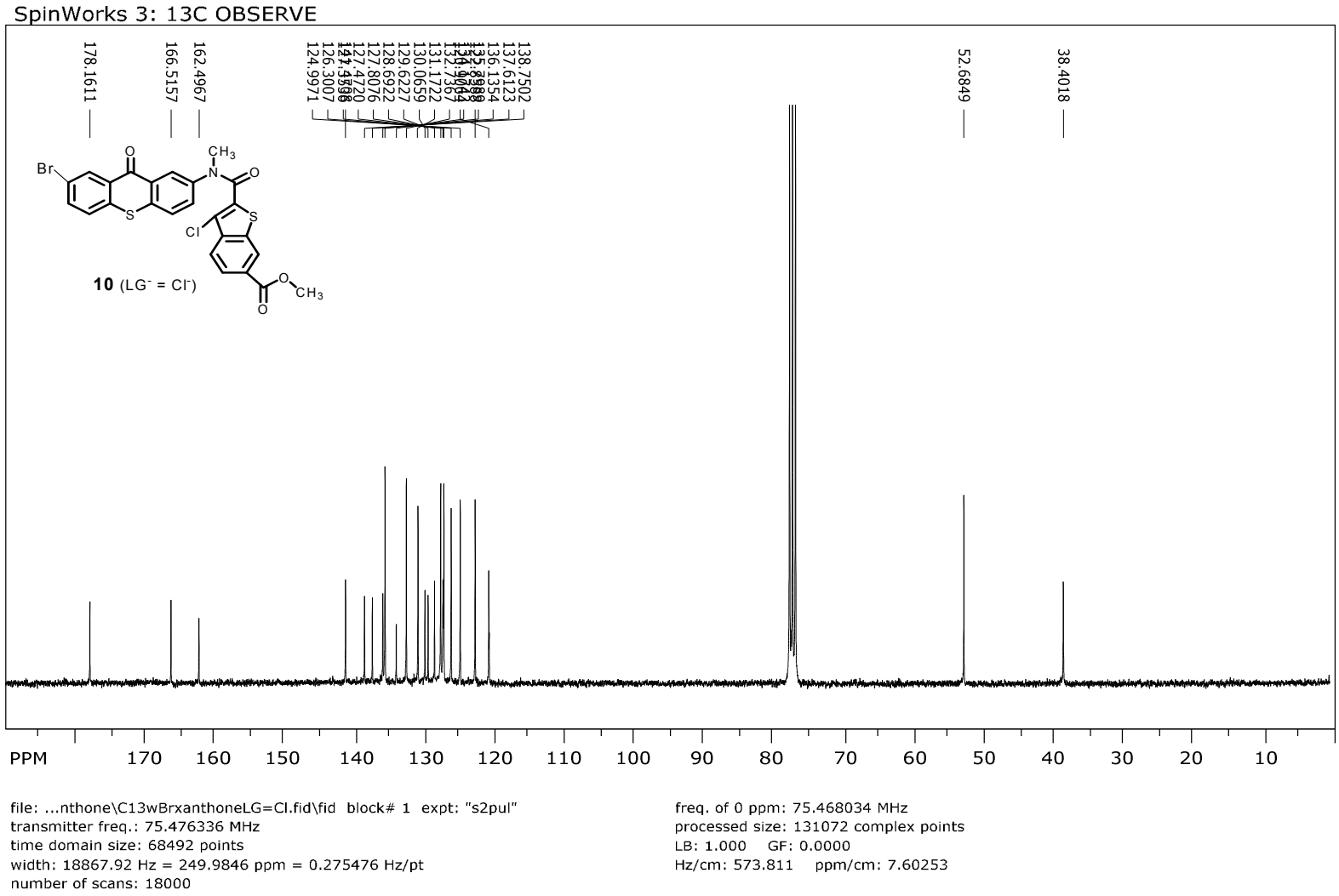

Figure 14, ^{13}C NMR spectrum of 2-[(7-Bromo-9-oxo-9H-thioxanthen-2-yl)-methyl-carbamoyl]-3-chloro-benzo[b]thiophene-6-carboxylic acid methyl ester (**10**) ($LG^- = Cl^-$) in $CDCl_3$

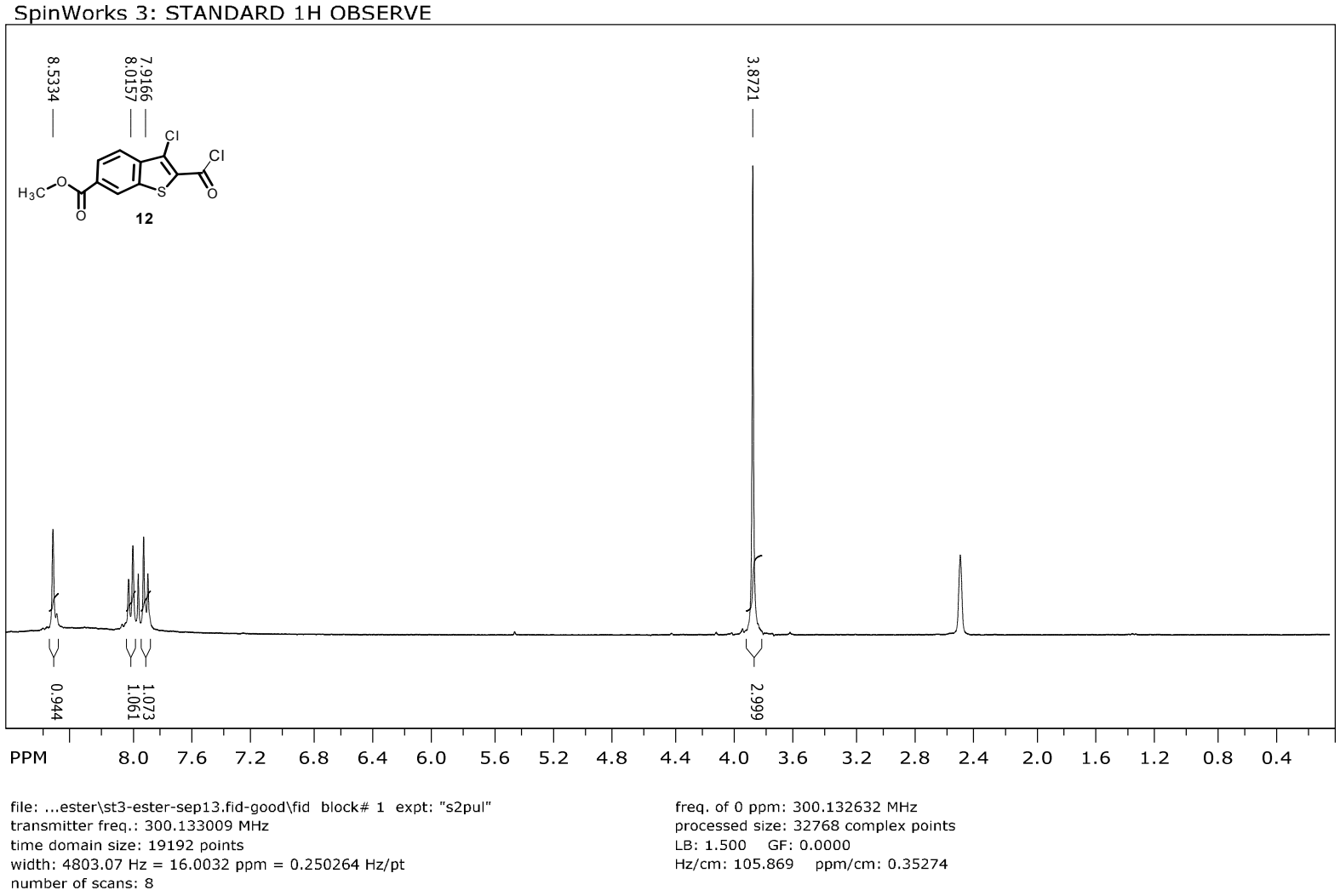

Figure 15, ^{1}H NMR spectrum of 3-Chloro-2-chlorocarbonyl-benzo[b]thiophene-6-carboxylic acid methyl ester (**12**) in DMSO-d_6

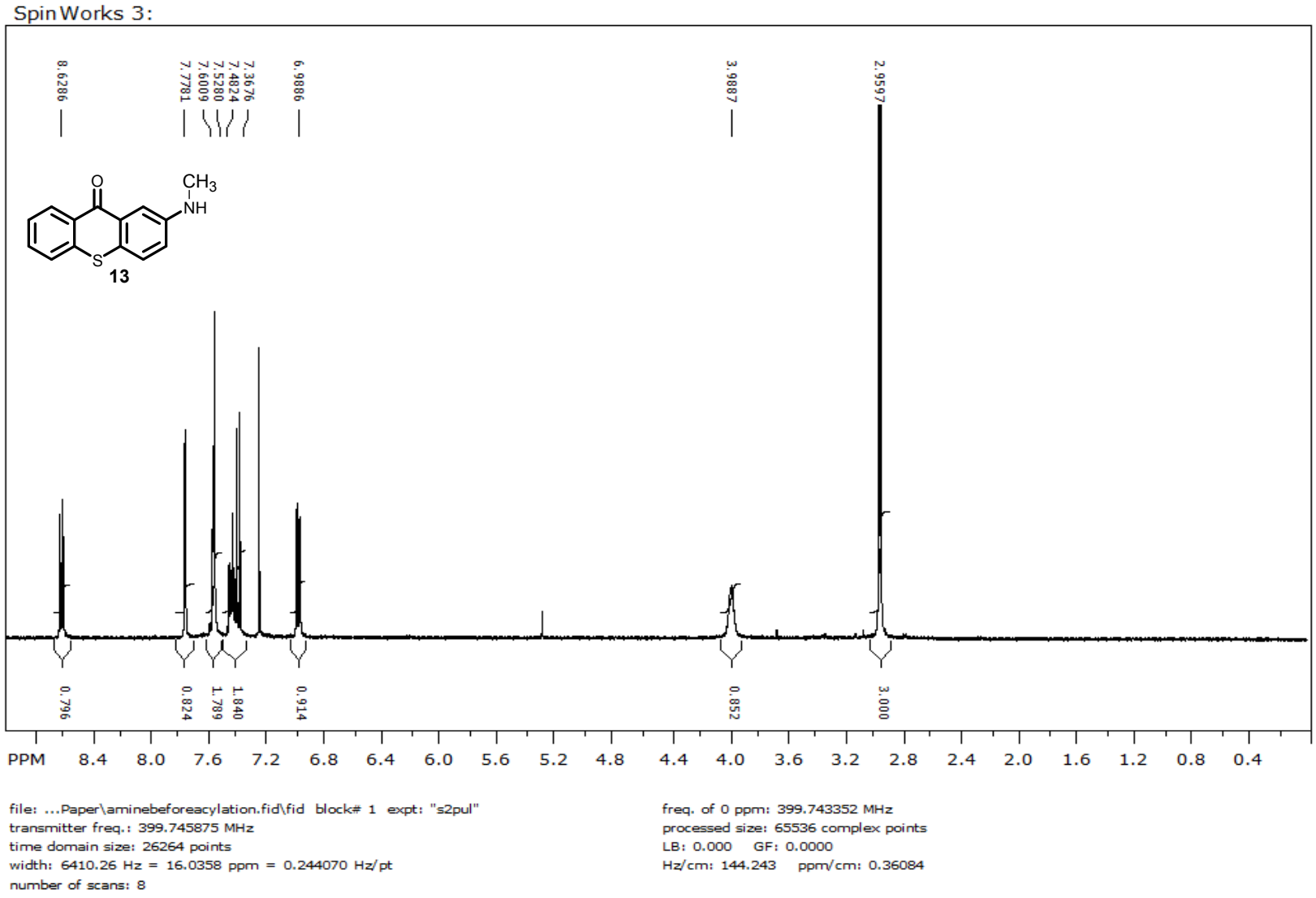

Figure 16, ^{1}H NMR spectrum of 2-Methylamino-thioxanthen-9-one (**13**) in $CDCl_3$

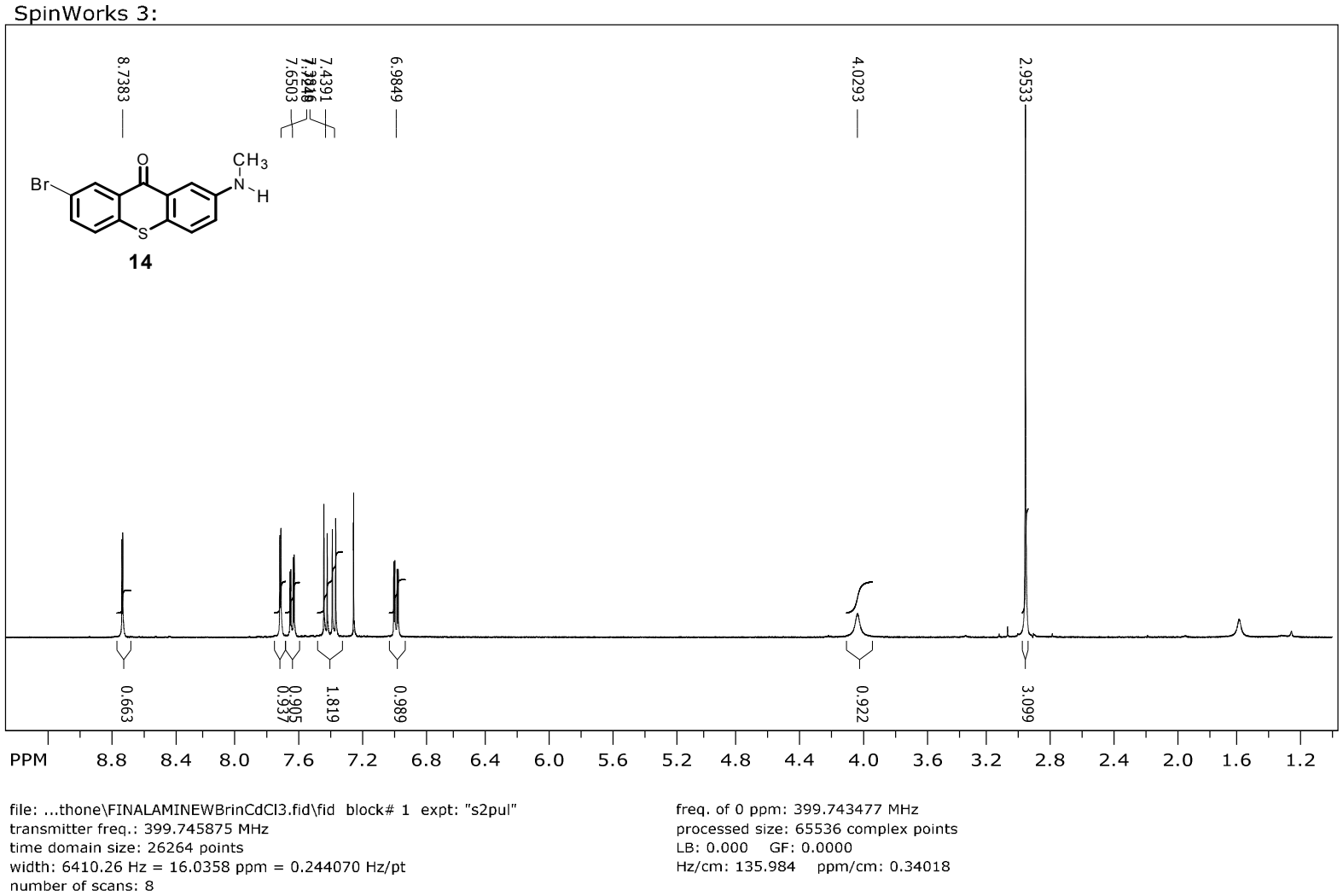

Figure 17, ^{1}H NMR spectrum of 2-Bromo-7-methylamino-thioxanthen-9-one (**14**) in $CDCl_3$

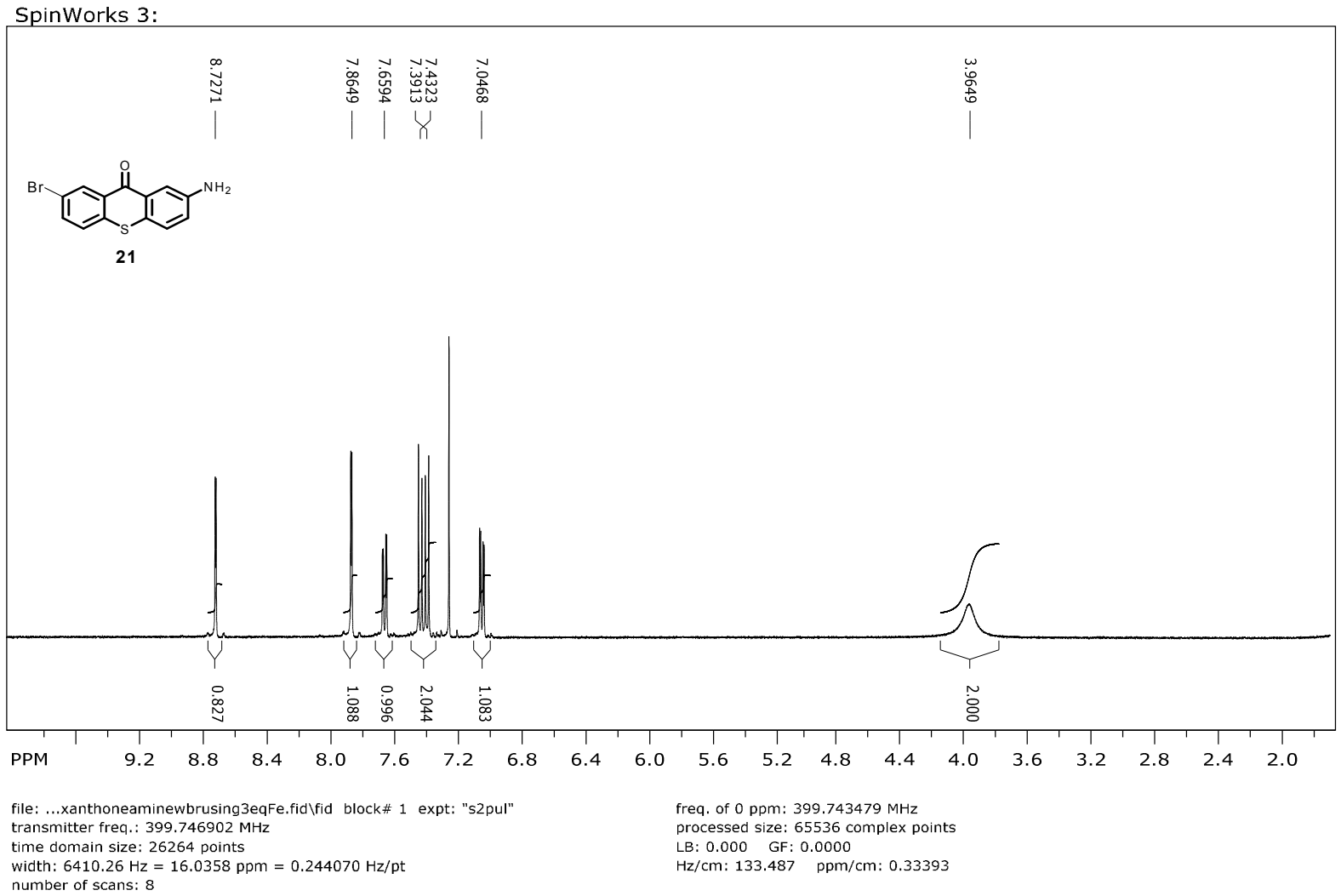

Figure 18, ^{1}H NMR spectrum of 2-Amino-7-bromo-thioxanthen-9-one (**21**) in $CDCl_3$

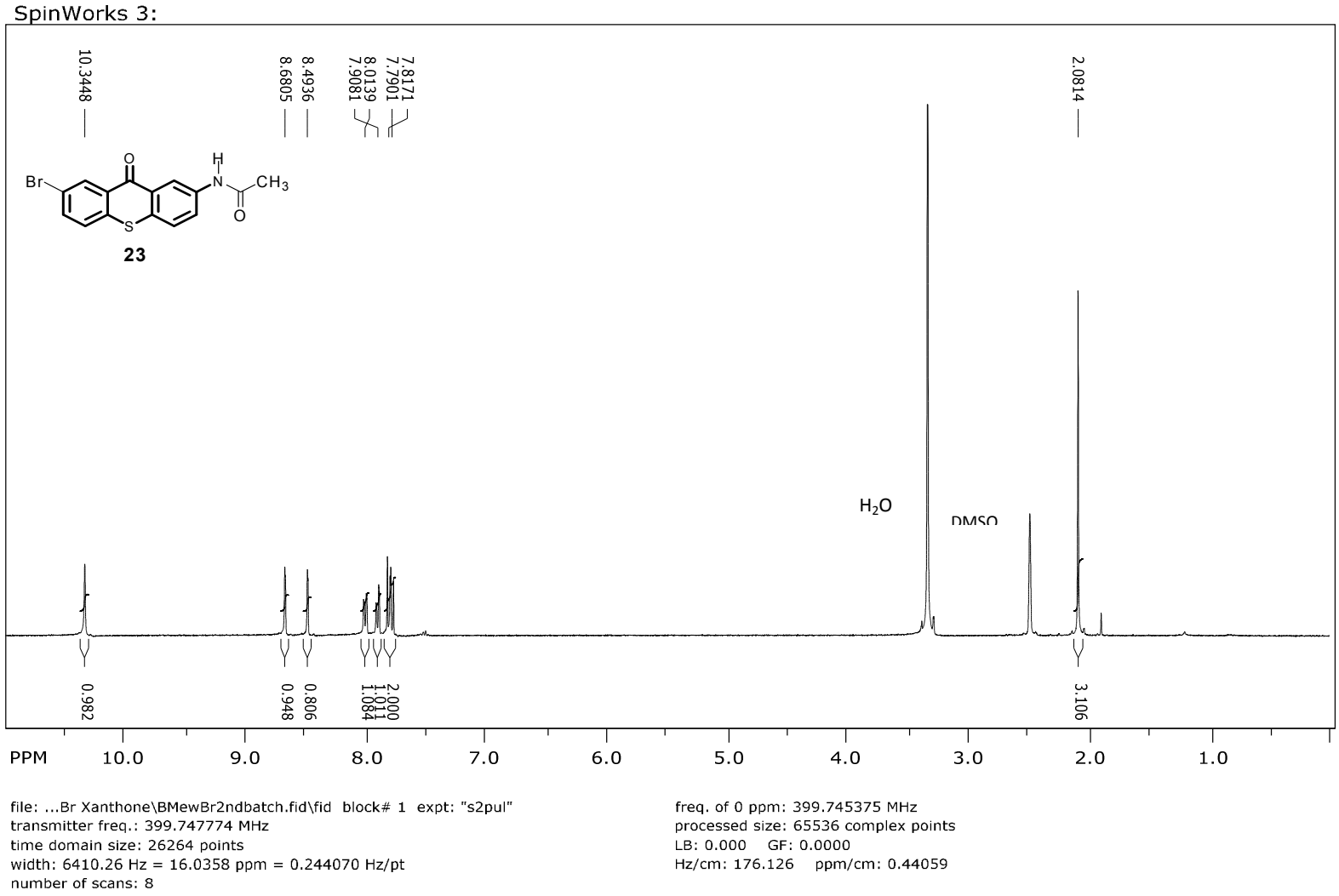

Figure 19, ^{1}H NMR spectrum of N-(7-Bromo-9-oxo-9H-thioxanthen-2-yl)-acetamide (**23**) in DMSO-d_6

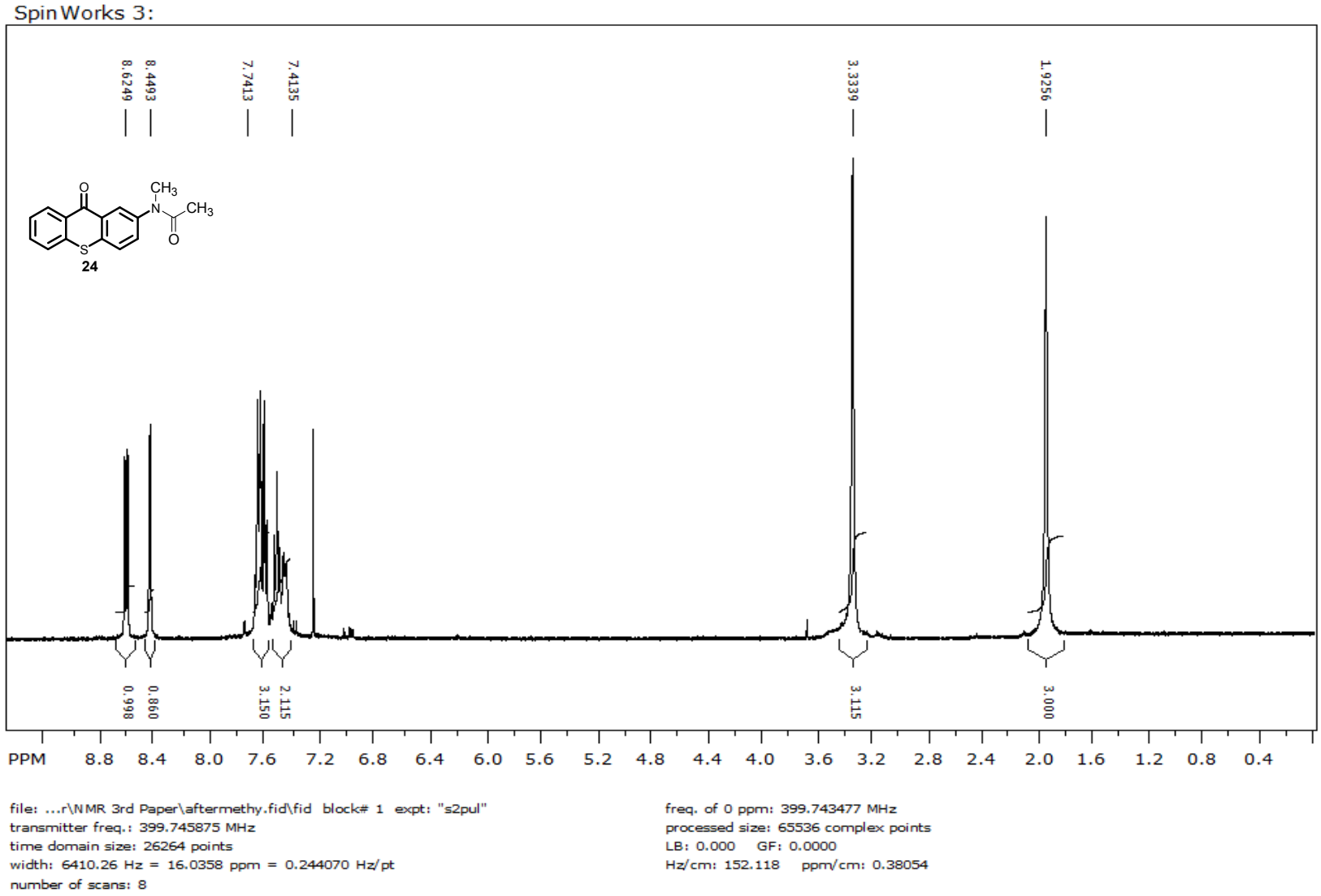

Figure 20, ^{1}H NMR spectrum of N-Methyl-N-(9-oxo-9H-thioxanthen-2-yl)-acetamide (**24**) in $CDCl_3$

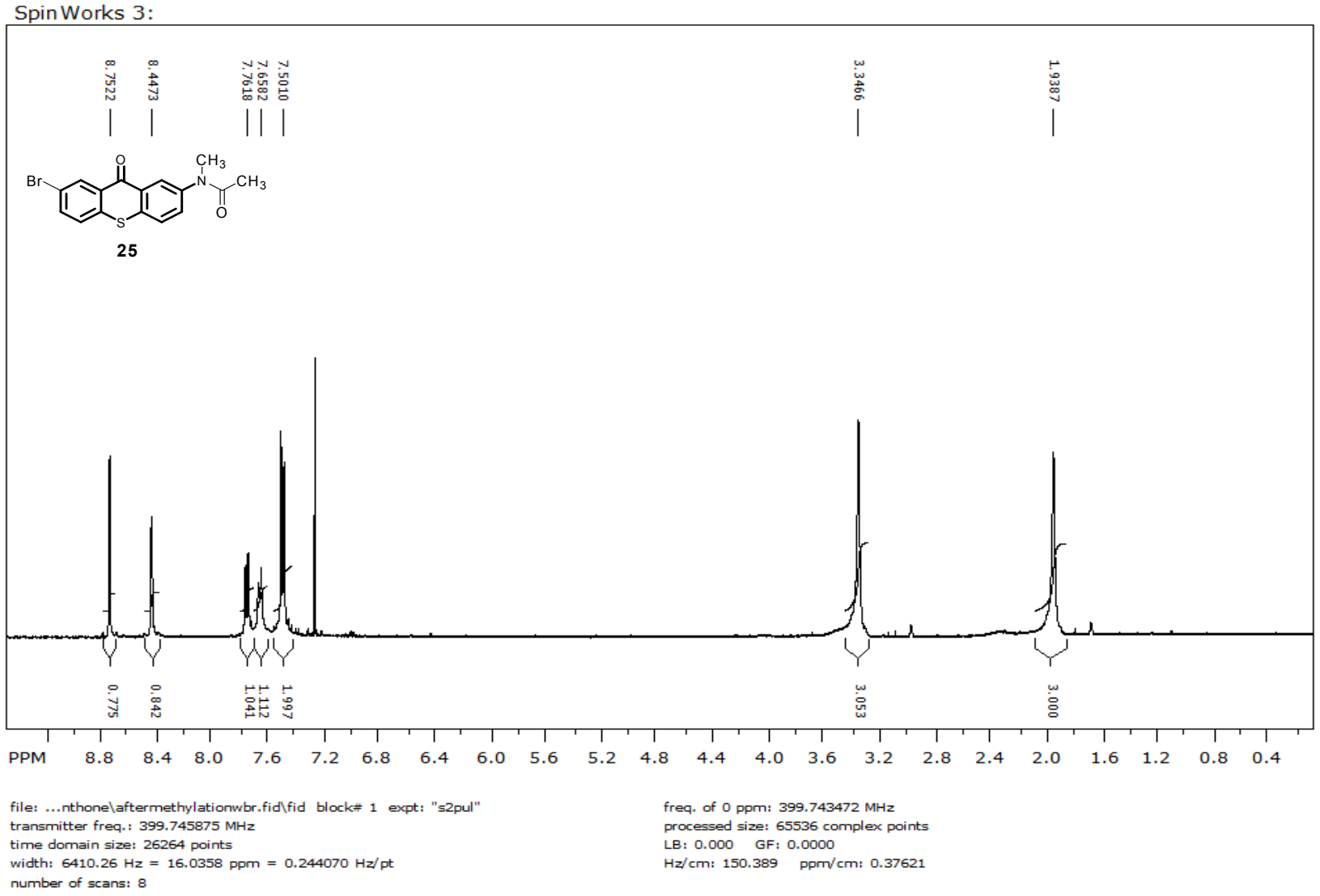

Figure 21, ^{1}H NMR spectrum of N-(7-Bromo-9-oxo-9H-thioxanthen-2-yl)-N-methyl-acetamide (**25**) in $CDCl_3$

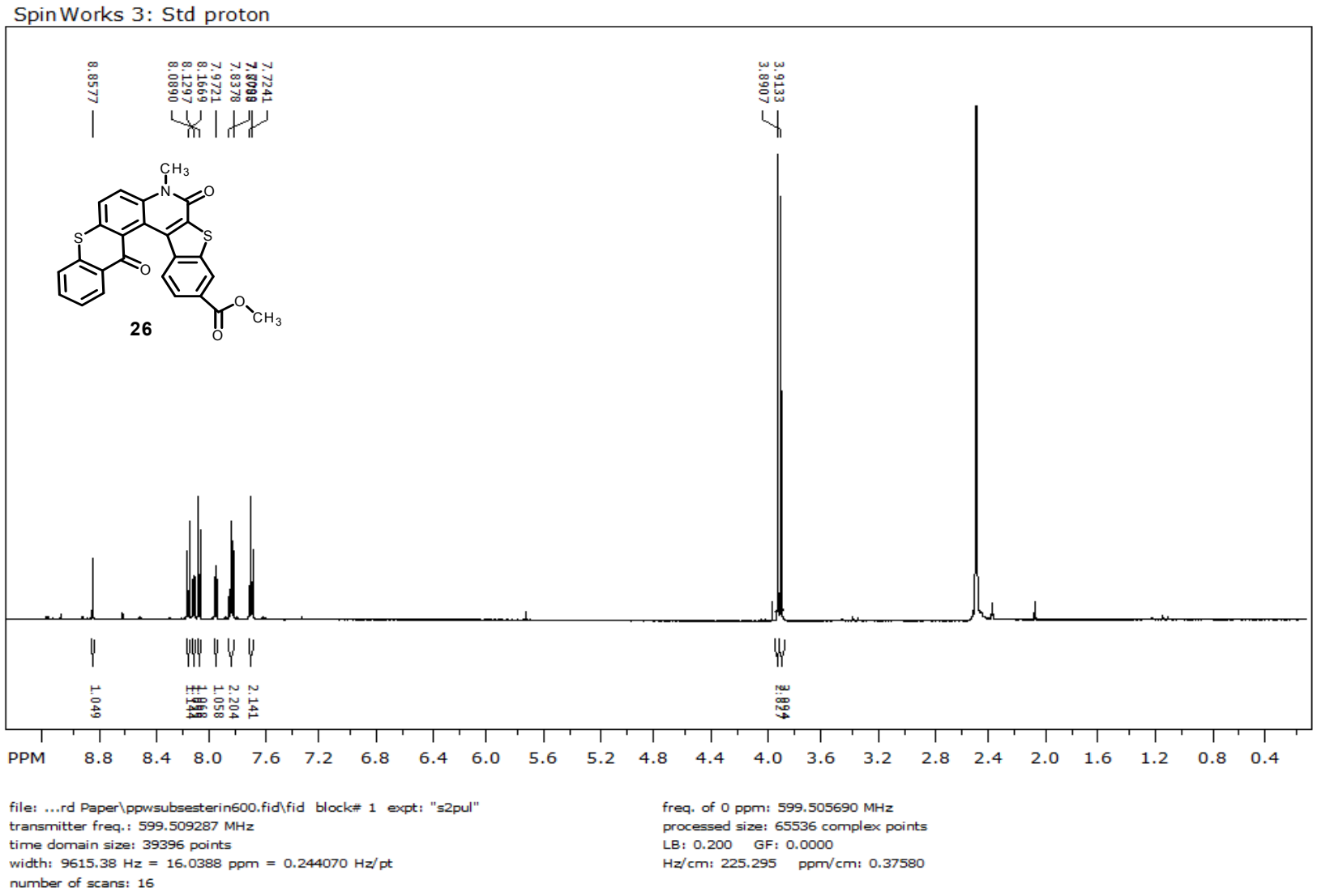

Figure 22, ^{1}H NMR spectrum of 6-methylcarboxylate-[1]benzothiopheno[2,3-c]benzo[a]anthracene-4-methyl-4*H*-7-thia-4-aza-3,12-dione **(26)** in DMSO-d_6

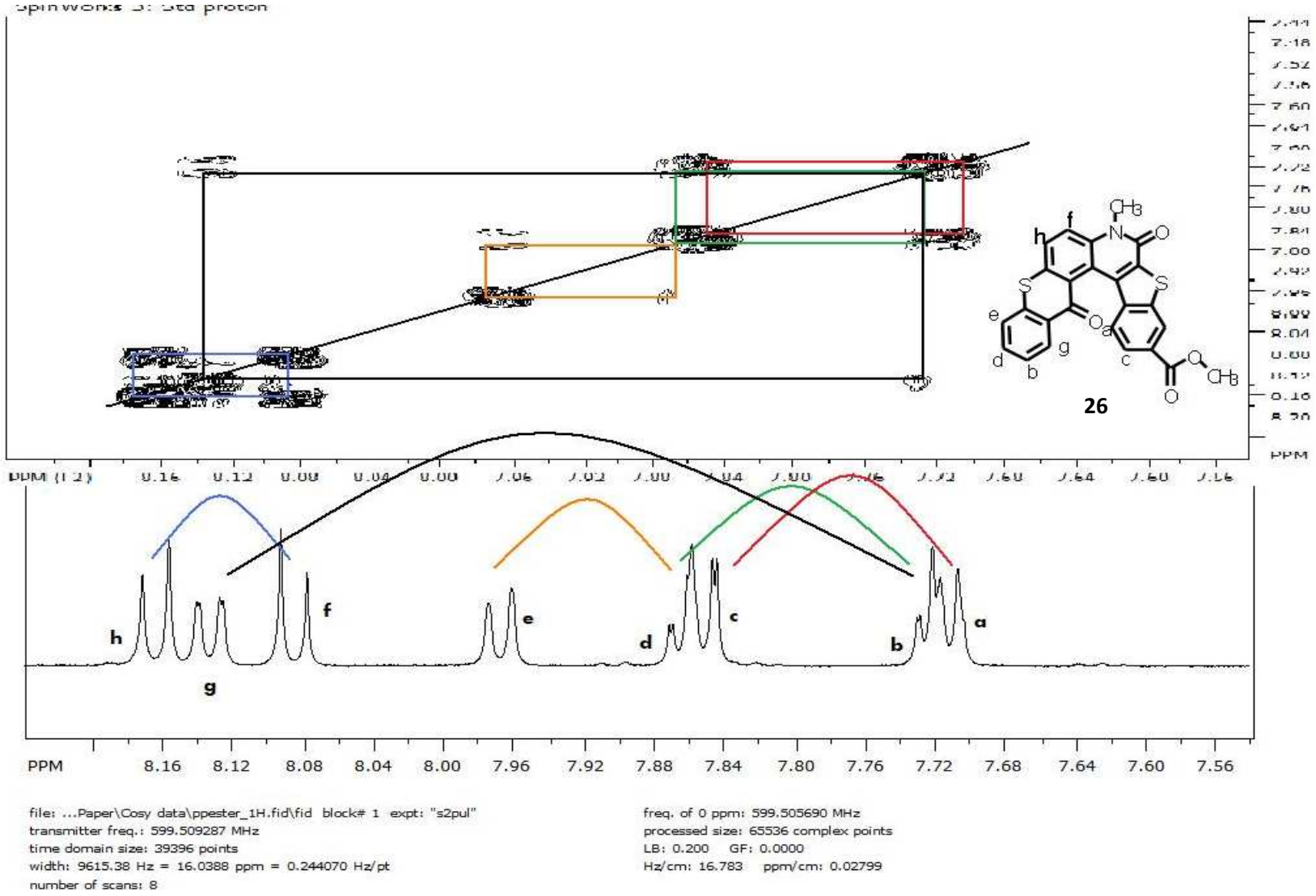

Figure 23, ^{1}H COSY NMR spectrum of 6-methylcarboxylate-[1]benzothiopheno[2,3-c]benzo[a]anthracene-4-methyl-4*H*-7-thia-4-aza-3,12-dione (**26**).

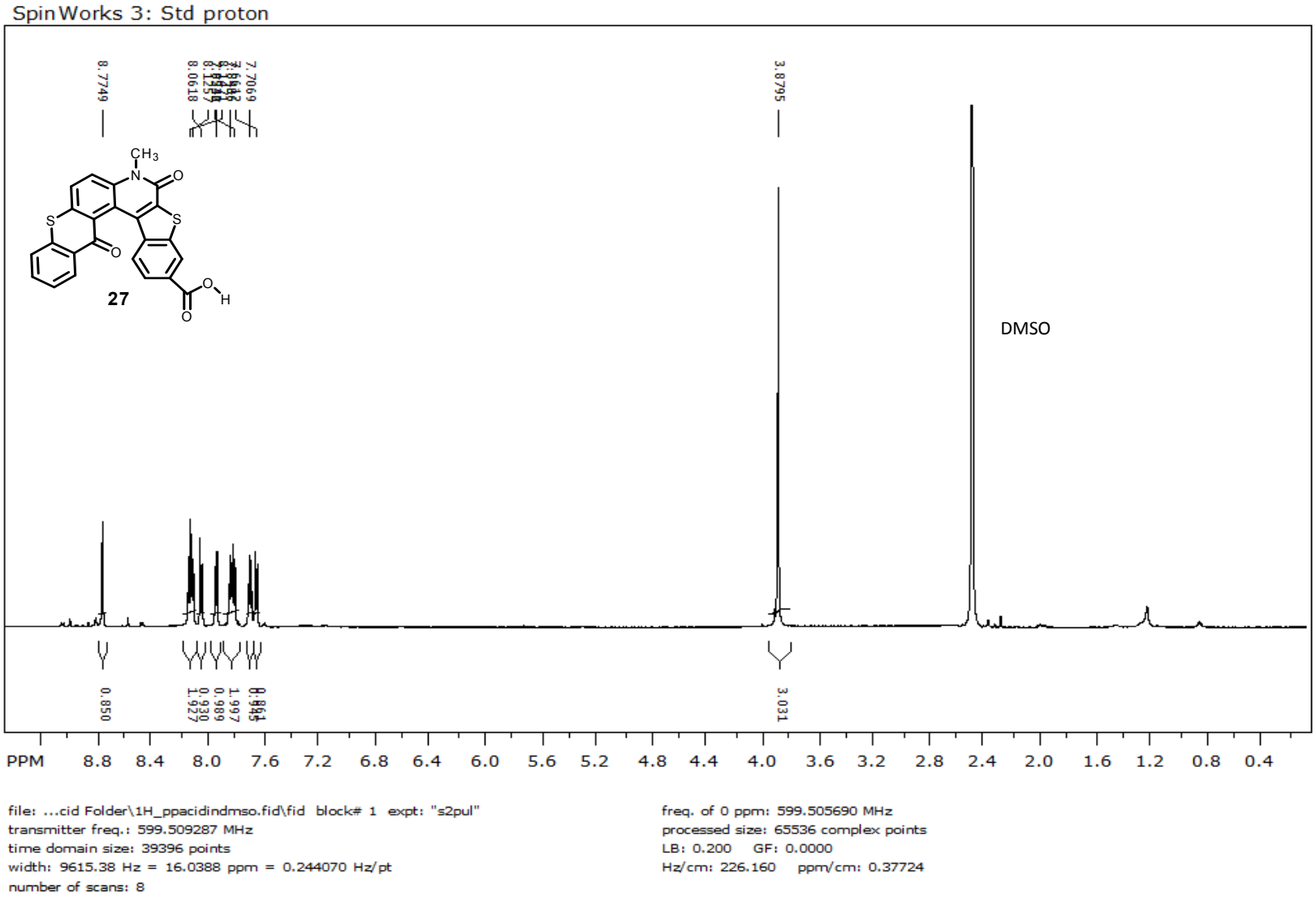

Figure 24, ^{1}H NMR spectrum of [1]benzothiopheno-6-carboxylicacid[2,3-c]benzo[a]anthracene-10-bromo-4-methyl-4*H*-7-thia-4-aza-3,12-dione (**27**) in DMSO-d_6.

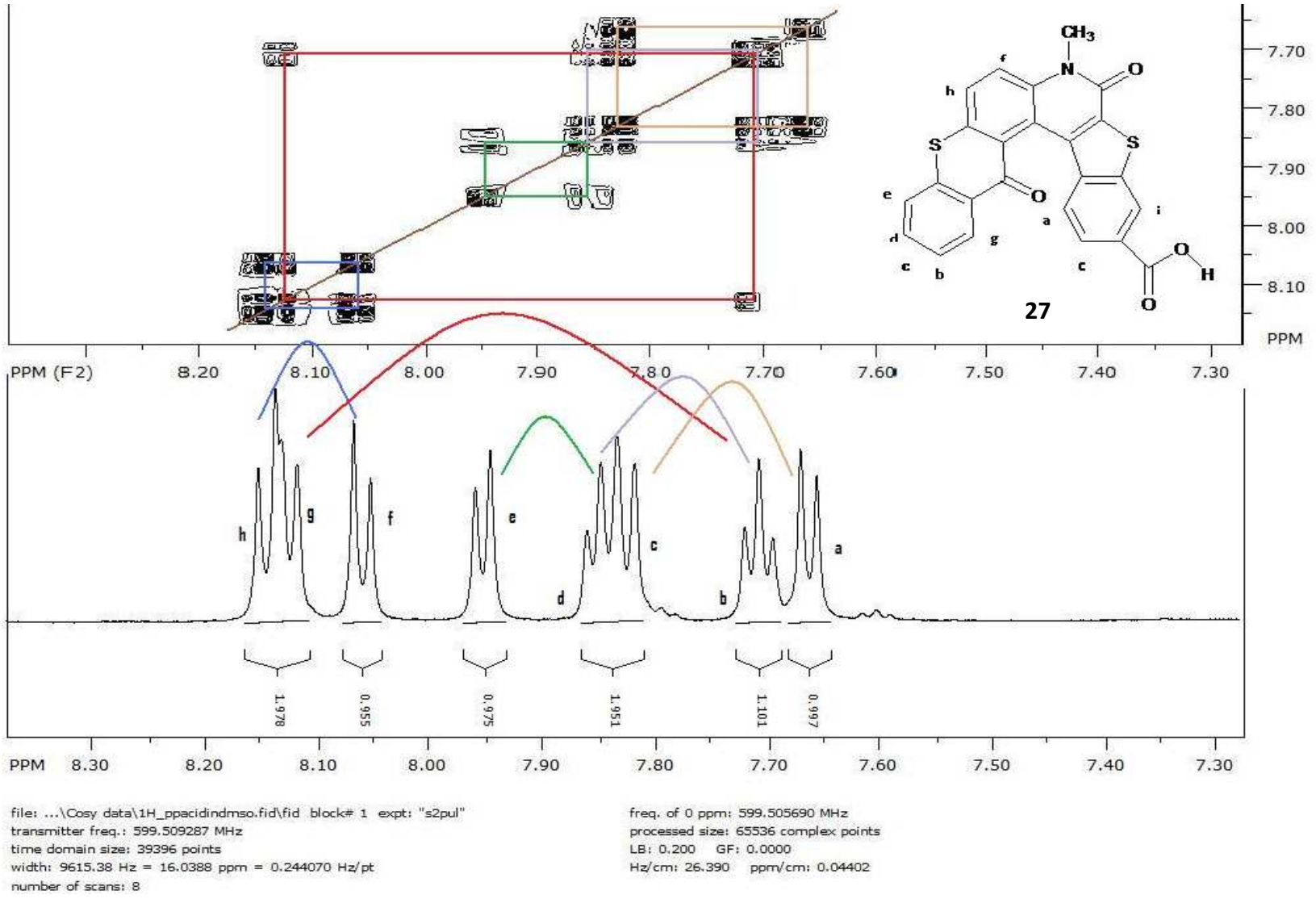

Figure 25, ^{1}H COSY NMR spectrum of [1]benzothiopheno-6-carboxylicacid[2,3-c]benzo[a]anthracene-10-bromo-4-methyl-4*H*-7-thia-4-aza-3,12-dione (**27**) in DMSO-d_6.

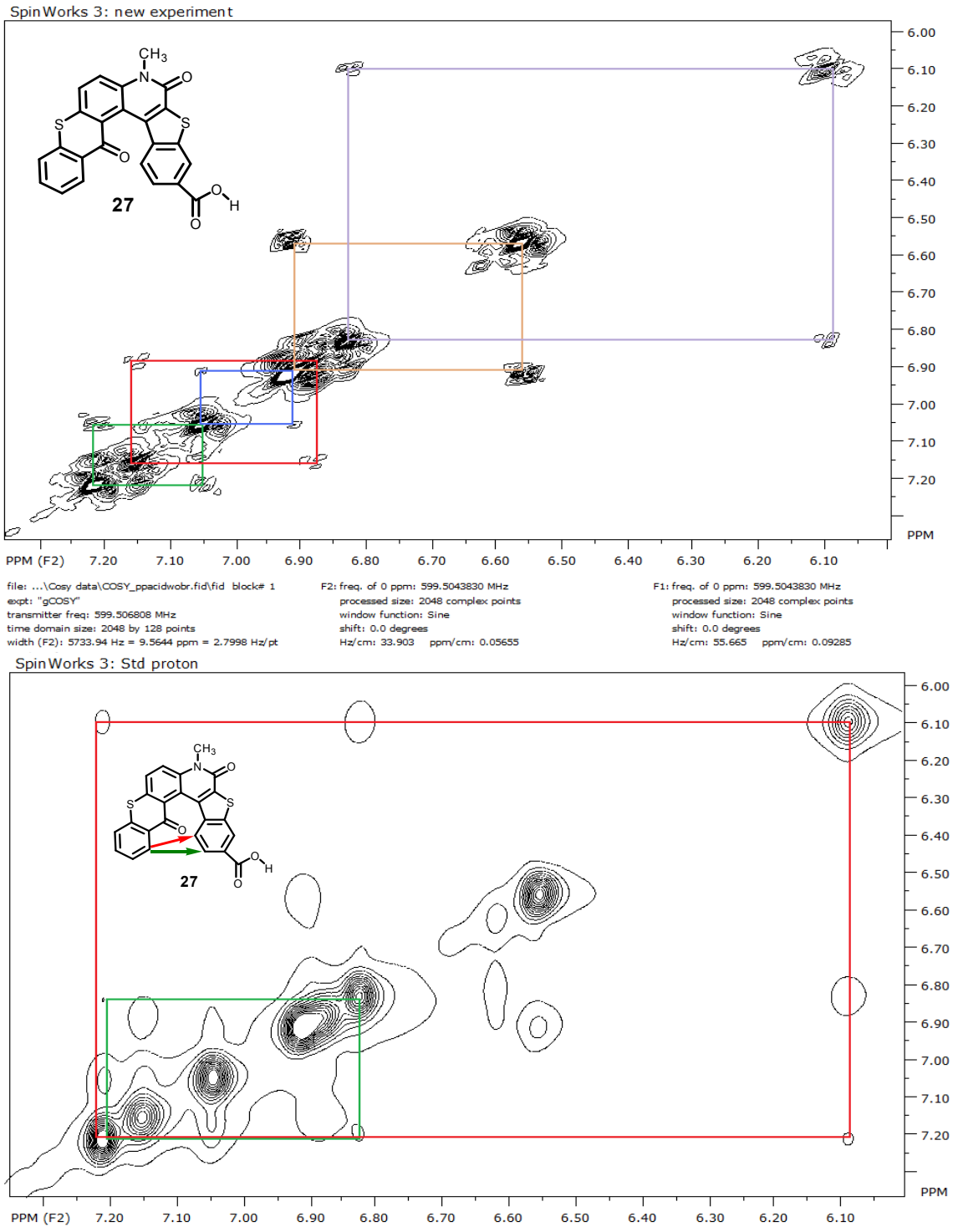

Figure 26, ^{1}H COSY and NOESY NMR spectrum of [1]benzothiopheno-6-carboxylicacid[2,3-c]benzo[a]anthracene-10-bromo-4-methyl-4*H*-7-thia-4-aza-3,12-dione (**27**) in D_2O

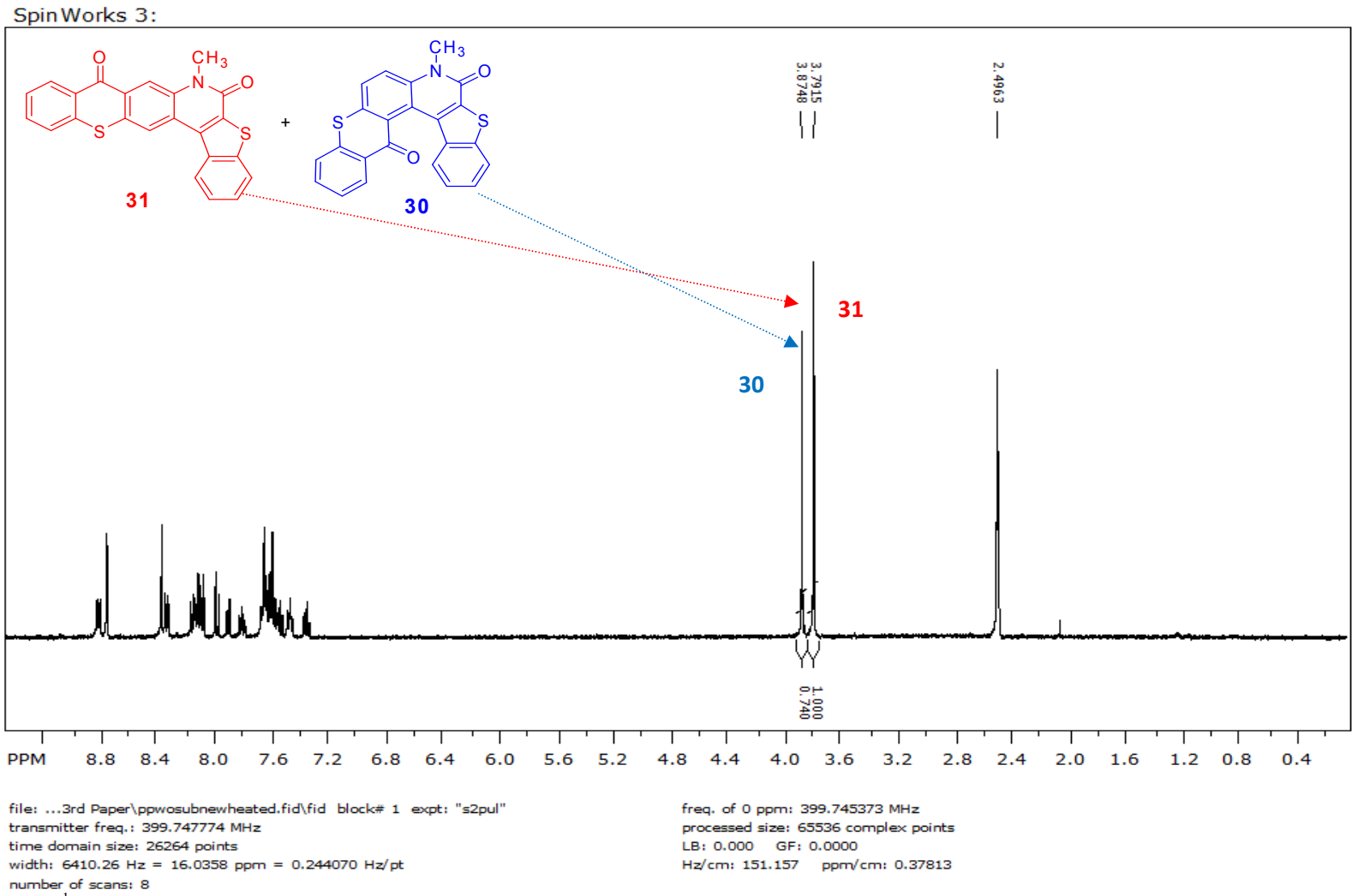

Figure 27, ^{1}H NMR spectrum of mixture of Photoproducts (**30** and **31**) by photolysis of 3-Chloro-benzo[b]thiophene-2-carboxylic acid methyl-(9-oxo-9H-thioxanthen-2-yl)-amide[1] (**7**) (LG^{-} = Cl^{-}) in DMSO-d_6

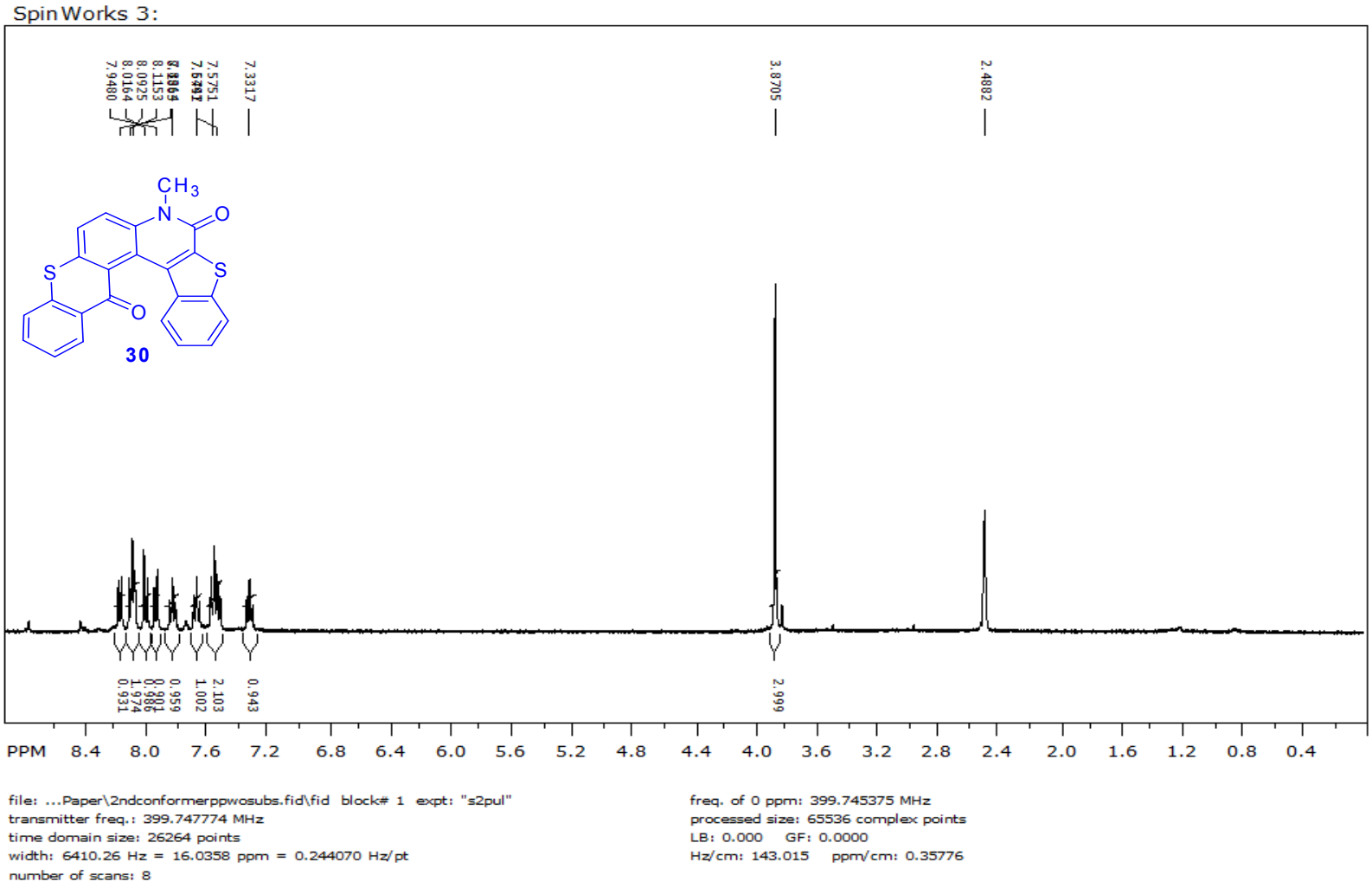

Figure 28, ^{1}H NMR spectrum of [1]benzothieno[2,3-c]benzo[a]anthracene-4-methyl-4*H*-7-thia-4-aza-3,12-dione **(30)** in DMSO-d_6.

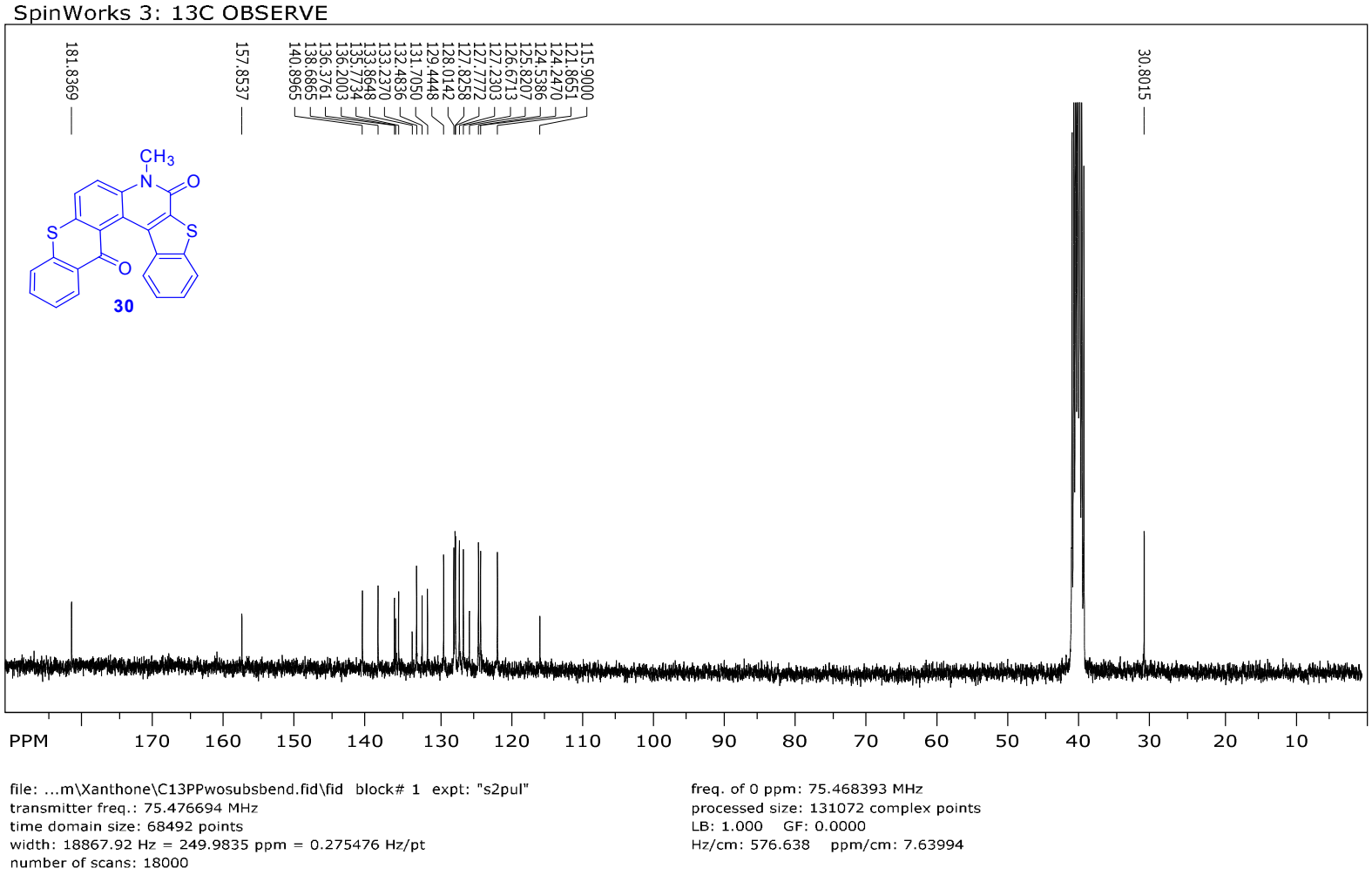

Figure 29, ^{13}C NMR spectrum of [1]benzothieno[2,3-c]benzo[a]anthracene-4-methyl-4*H*-7-thia-4-aza-3,12-dione **(30)** in DMSO-d_6.

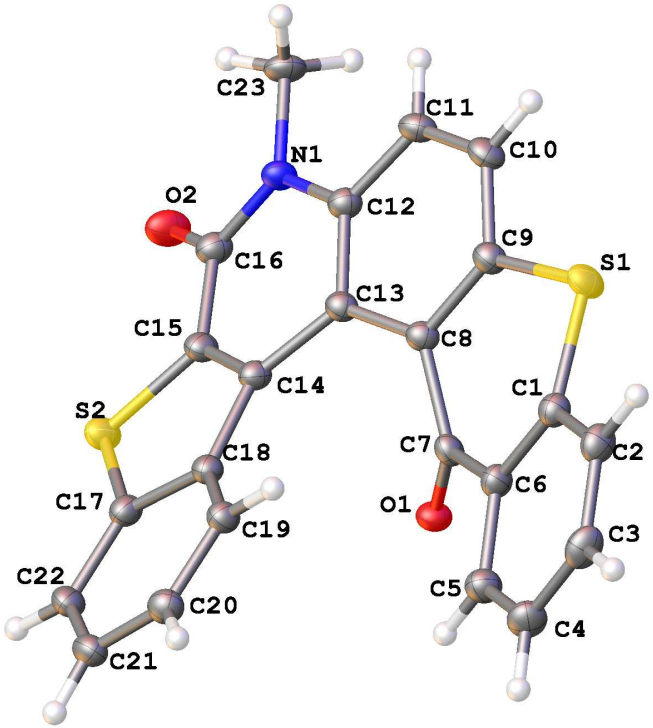

Figure 30, Crystal Structure of [1]benzothieno[2,3-c]benzo[a]anthracene-4-methyl-4*H*-7-thia-4-aza-3,12-dione **(30)**.

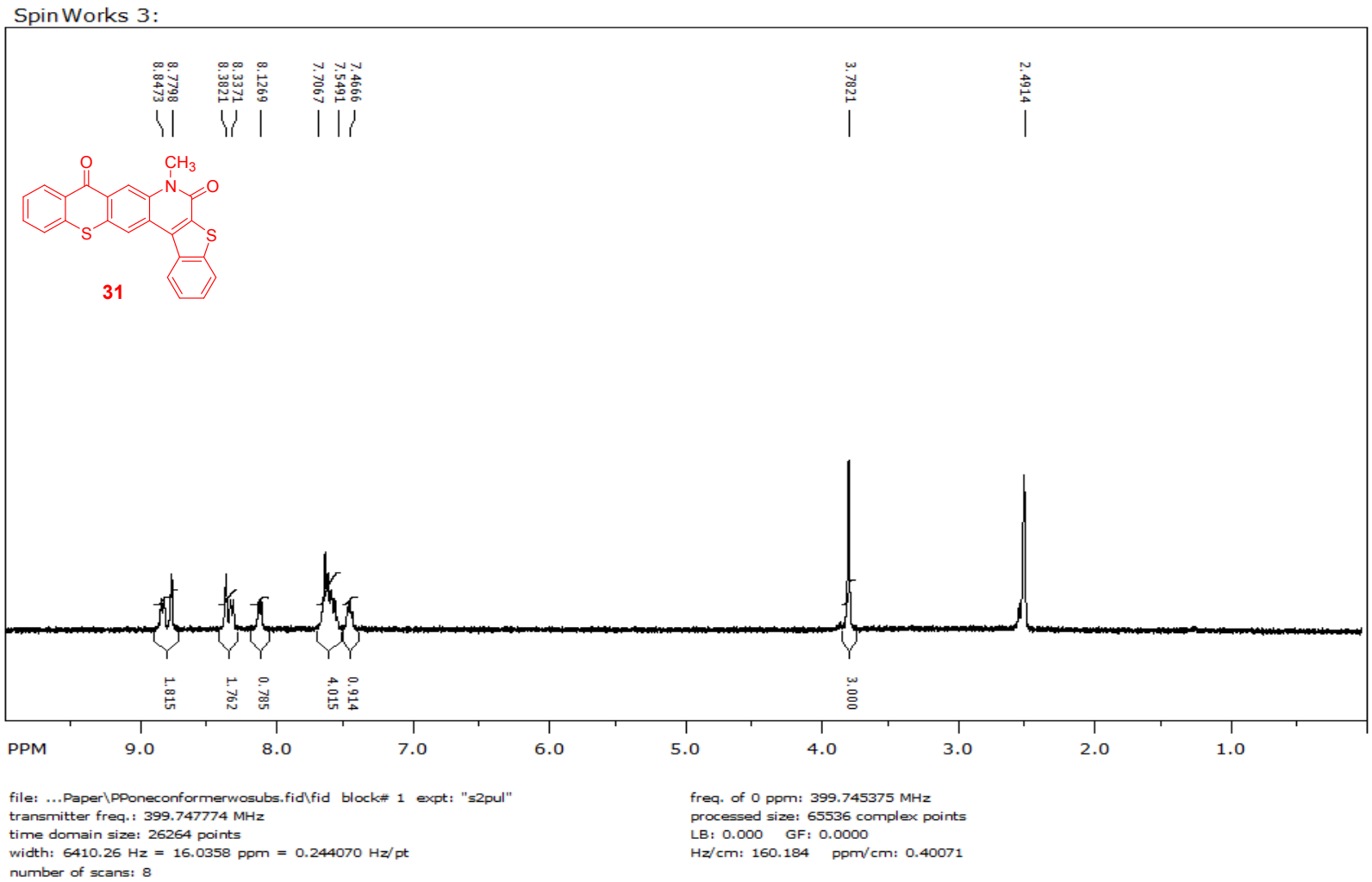

Figure 31, ^{1}H NMR spectrum of [1]benzothieno[2,3-c]naphthacene-1-methyl-1*H*-6-thia-1-aza-2,11-dione (**31**) in DMSO-d_6.

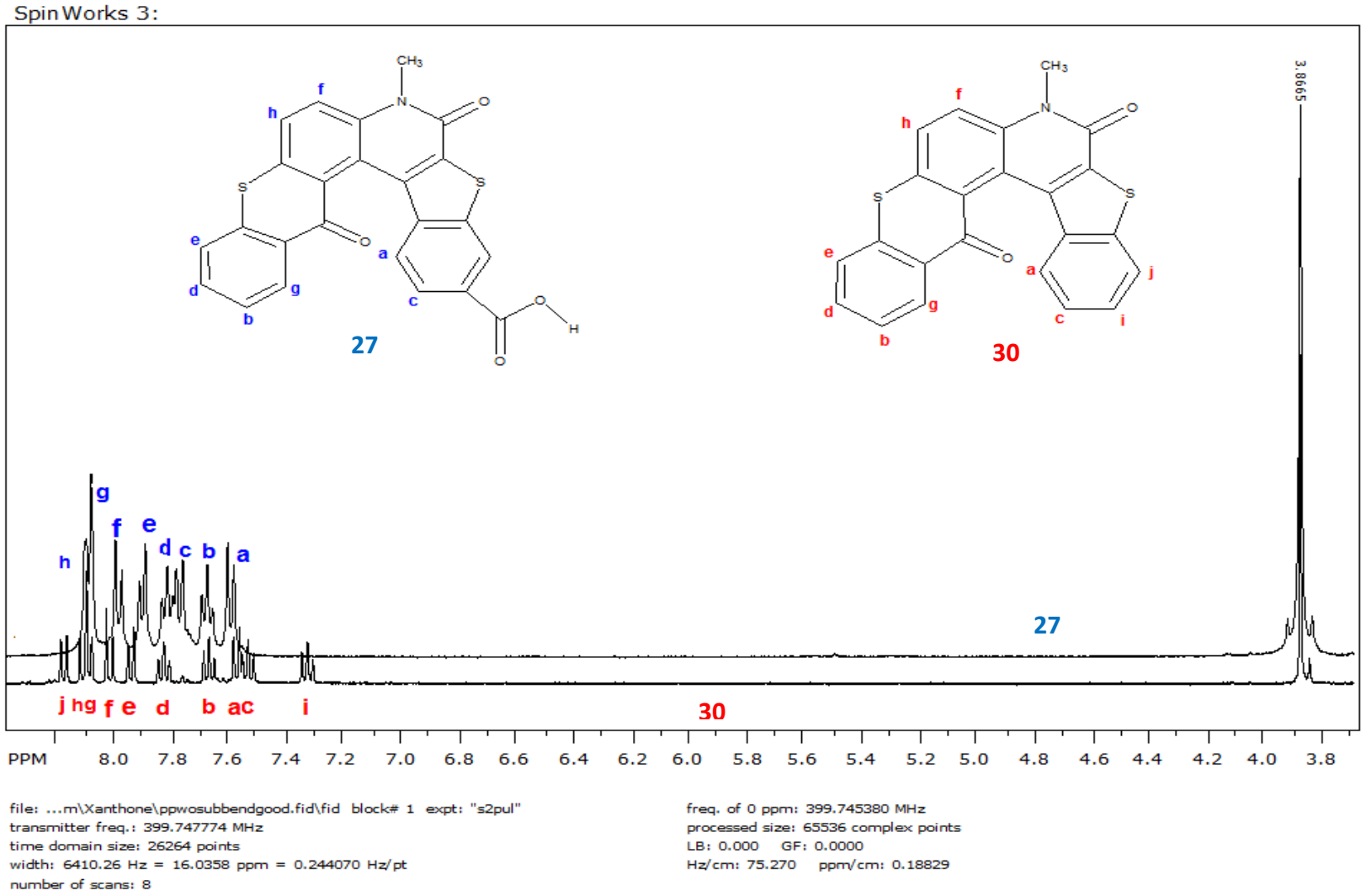

Figure 32, ^{1}H NMR spectrum comparison between Photoproduct **27** and **30** in DMSO-d_6.

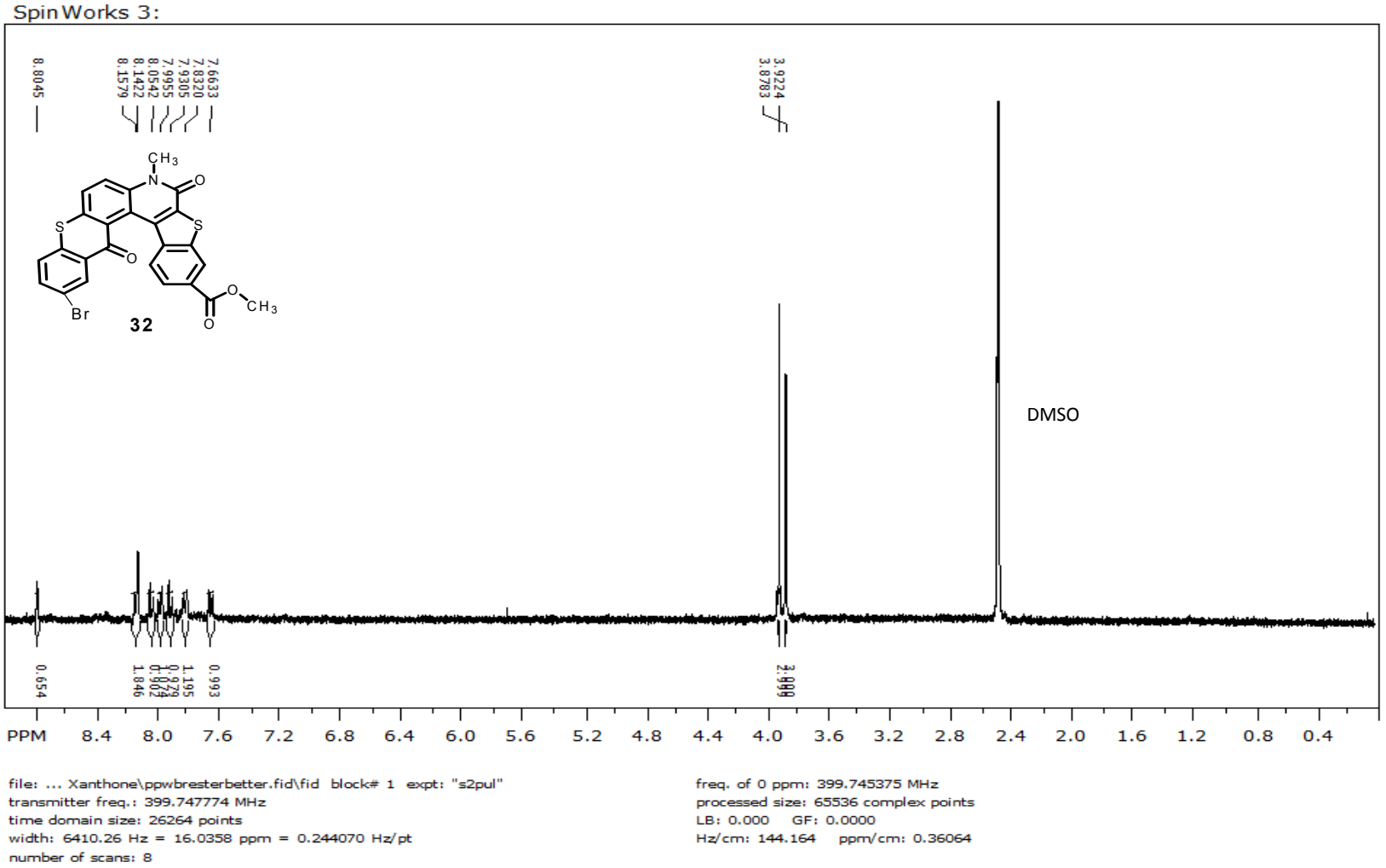

Figure 33, ^{1}H NMR spectrum of 6-methylcarboxylate-[1]benzothiopheno[2,3-c]benzo[a]anthracene-10-bromo-4-methyl-4*H*-7-thia-4-aza-3,12-dione (**32**) in DMSO-d_6.

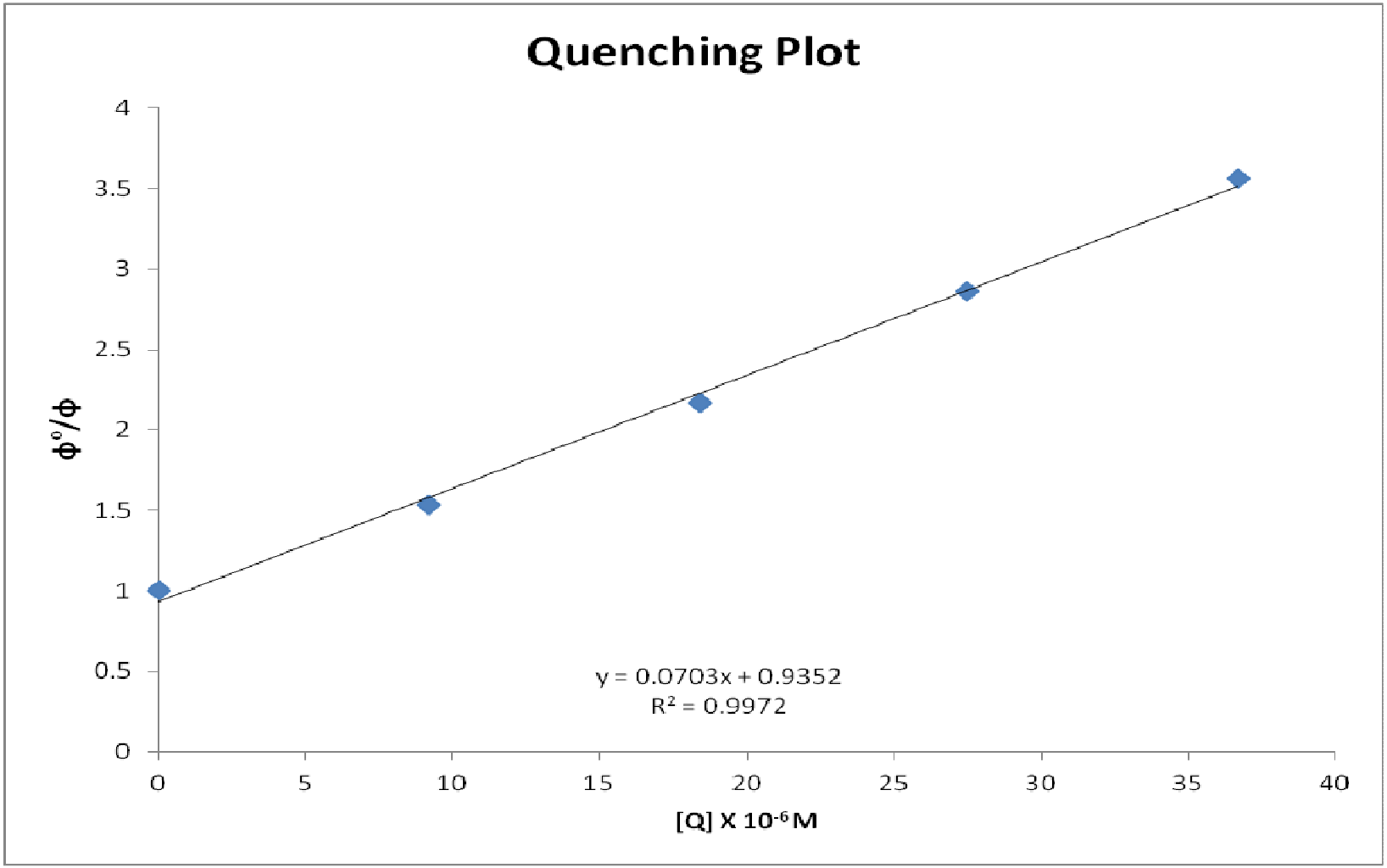

Figure 34, Stern-Volmer plot Φ^0/Φ vs [Q] of Quenching of ester **8** ($LG^- = Cl^-$) by piperylene as quencher Q

Computed Structures in Figure 3.

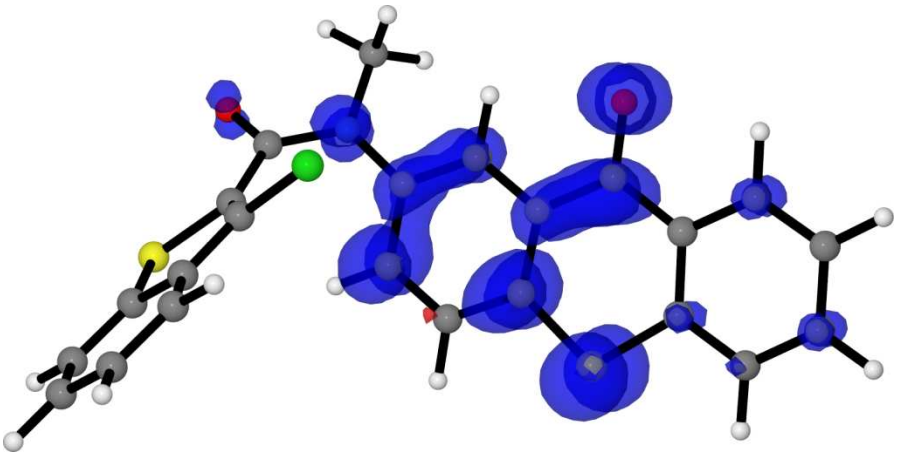

^{3}Thiox

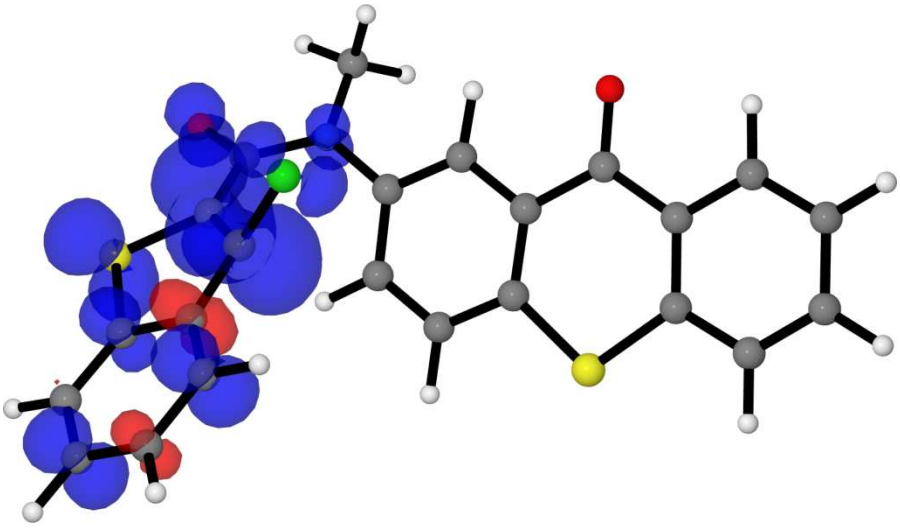

^{3}Bzt

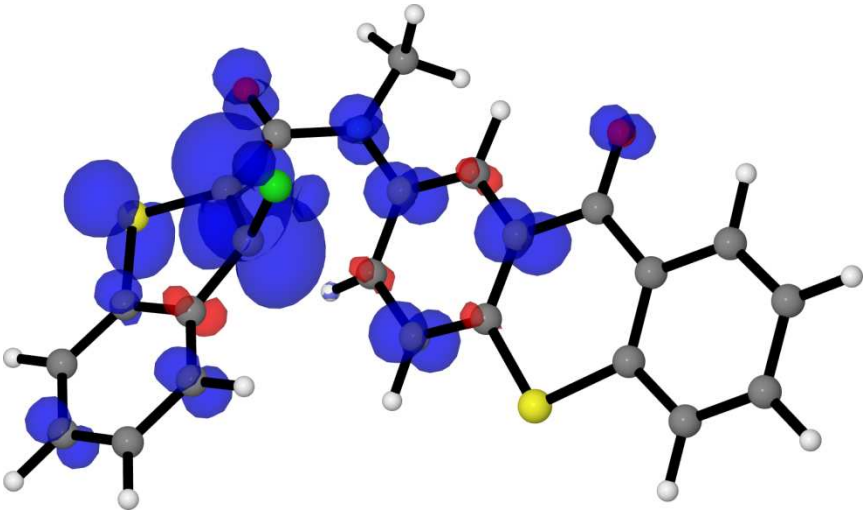

^{3}TS

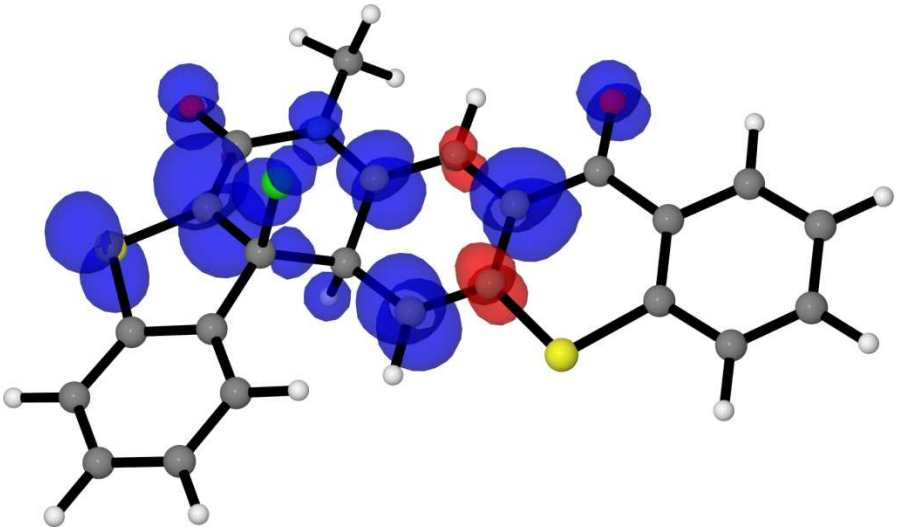

^{3}I

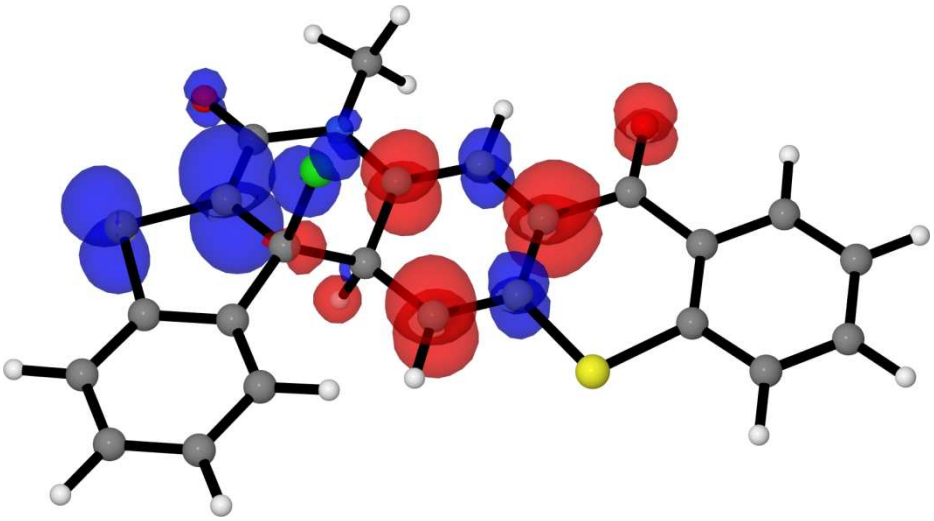

$^{1}I_{DR}$

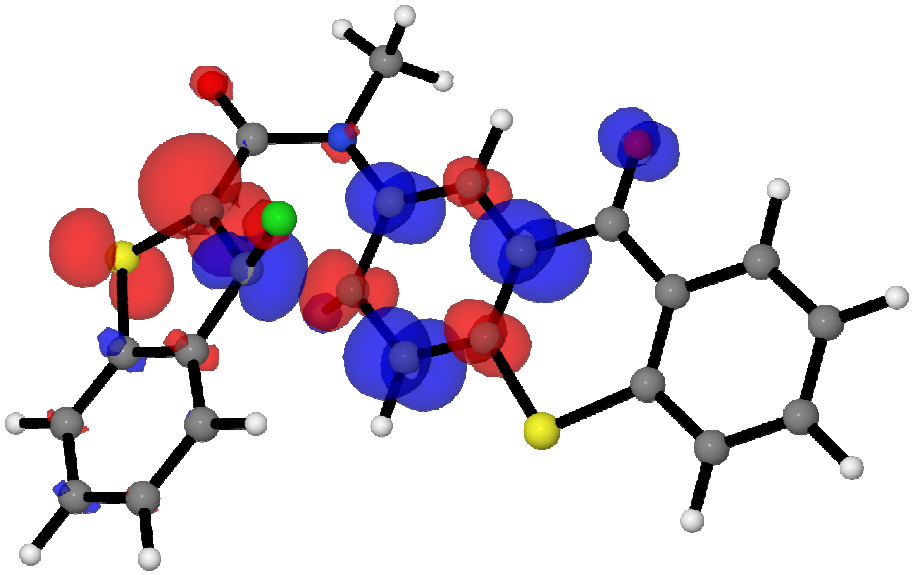

TS_{R}

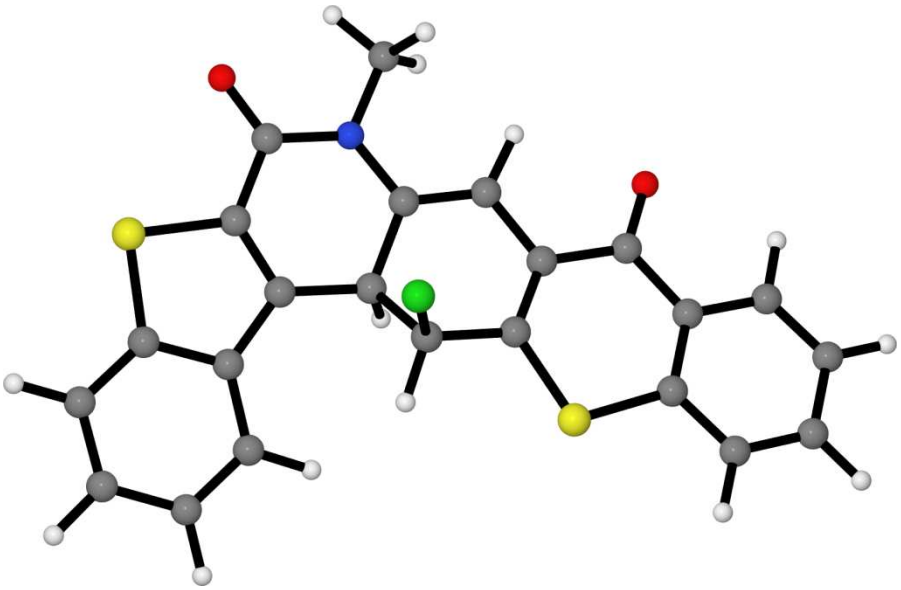

P-L

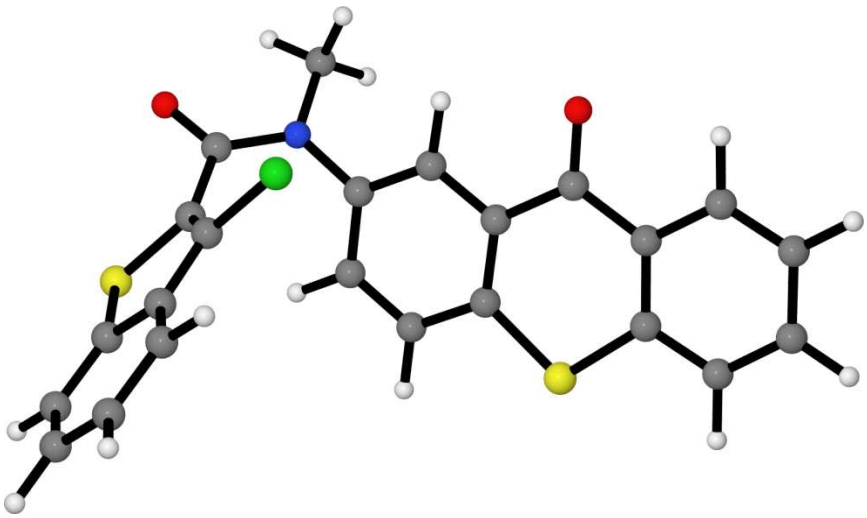

Thiox

Computed Structures in Figure 4.

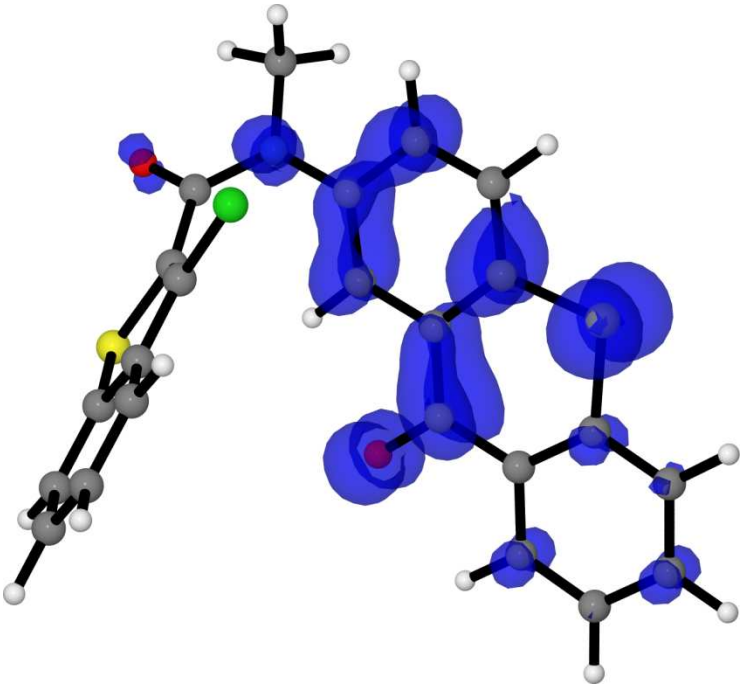

^{3}Thiox

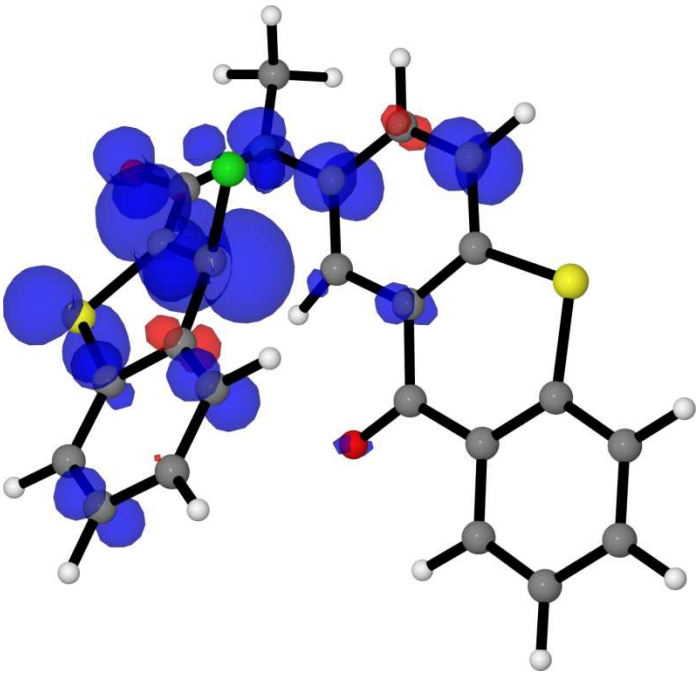

^{3}Bzt

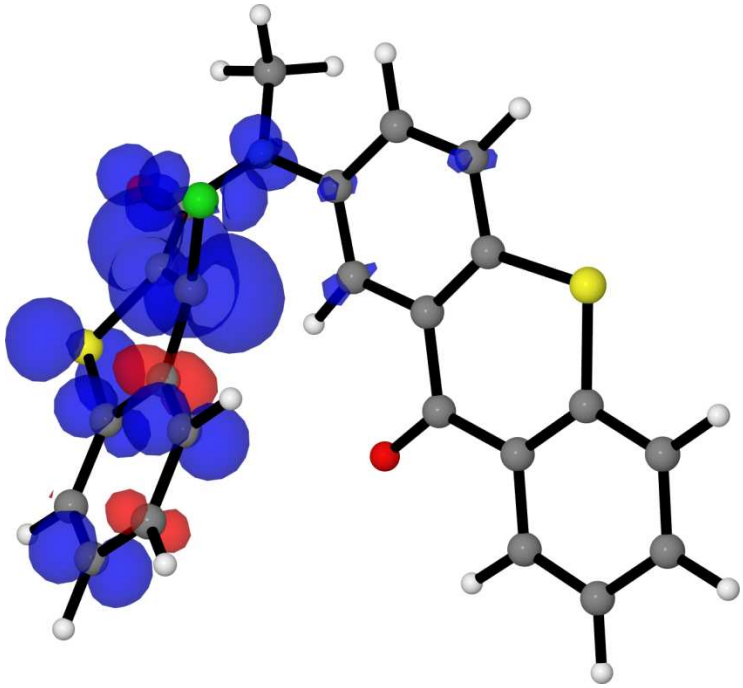

^{3}TS

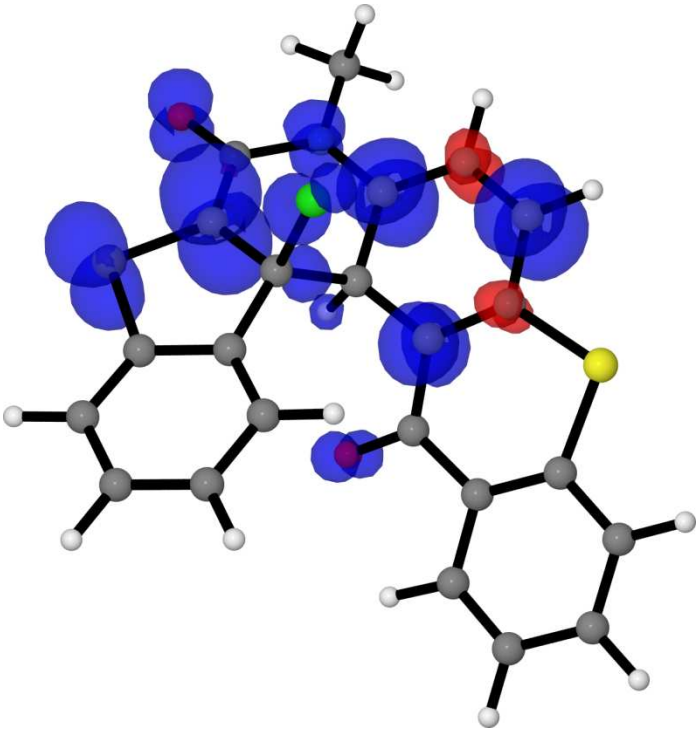

^{3}I

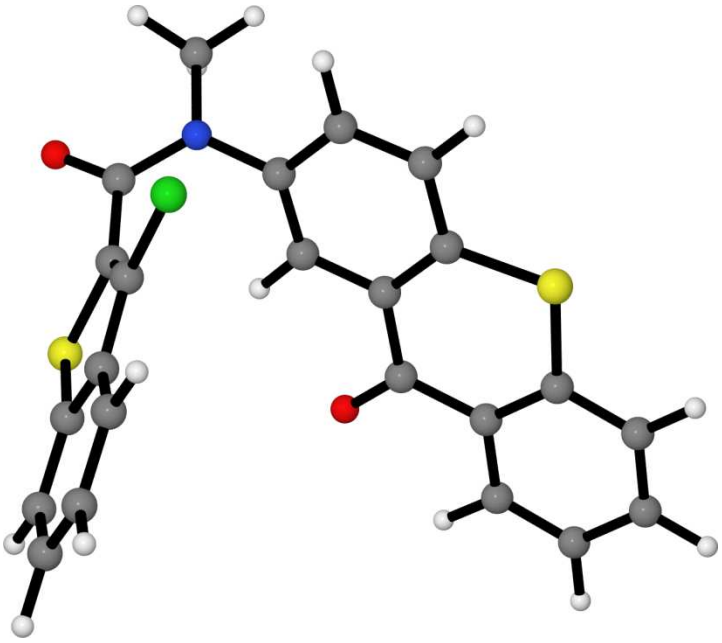

Thiox

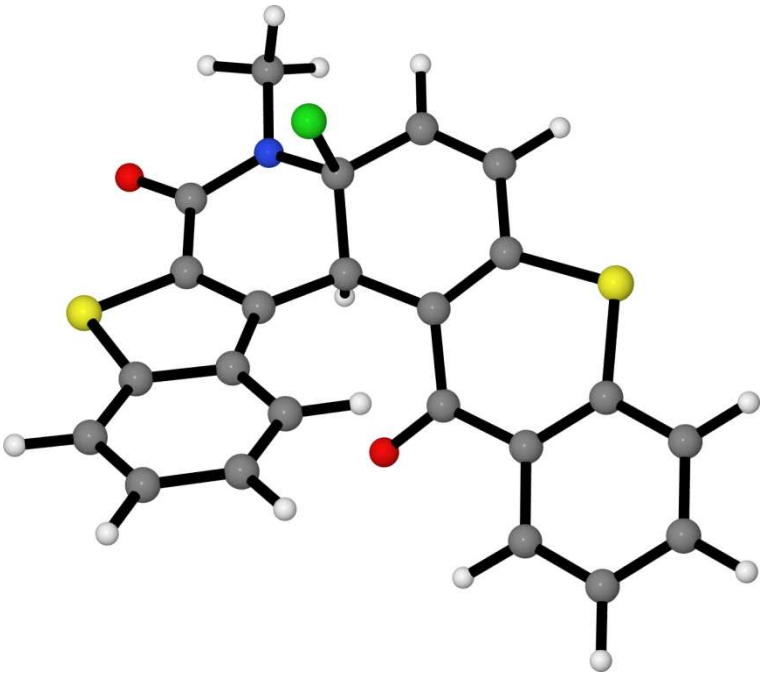

P-U